

UNIVERSIDAD DE INVESTIGACIÓN DE TECNOLOGÍA EXPERIMENTAL YACHAY TECH

Escuela de Ciencias Químicas e Ingeniería

**TÍTULO: An experimental and theoretical approach to
diaminodicyanoquinodimethanes derivatives with
luminescent and biological activities**

Trabajo de integración curricular presentado como requisito para
la obtención
del título de Químico(a)

Autor:

Jiménez Granda Edison Rafael

Tutor:

PhD – Rodríguez Cabrera Hortensia

Urququí, febrero 2020

SECRETARÍA GENERAL
(Vicerrectorado Académico/Cancillería)
ESCUELA DE CIENCIAS QUÍMICAS E INGENIERÍA
CARRERA DE QUÍMICA
ACTA DE DEFENSA No. UITEY-CHE-2020-00001-AD

En la ciudad de San Miguel de Urcuquí, Provincia de Imbabura, a los 19 días del mes de febrero de 2020, a las 09:00 horas, en el Aula CHA-01 de la Universidad de Investigación de Tecnología Experimental Yachay y ante el Tribunal Calificador, integrado por los docentes:

Presidente Tribunal de Defensa Dr. CAETANO SOUSA MANUEL , Ph.D.
Miembro No Tutor Dr. MAKOWSKI , KAMIL , Ph.D.
Tutor Dra. RODRIGUEZ CABRERA, HORTENSIA MARIA , Ph.D.

Se presenta el(la) señor(ita) estudiante **JIMENEZ GRANDA, EDISON RAFAEL**, con cédula de identidad No. 1717374860, de la **ESCUELA DE CIENCIAS QUÍMICAS E INGENIERÍA**, de la Carrera de **QUÍMICA**, aprobada por el Consejo de Educación Superior (CES), mediante Resolución **RPC-SO-39-No.456-2014**, con el objeto de rendir la sustentación de su trabajo de titulación denominado: **An experimental and theoretical approach to diaminodicyanoquinodimethanes derivatives with luminescent and biological activities**, previa a la obtención del título de **QUÍMICO/A**.

El citado trabajo de titulación, fue debidamente aprobado por el(los) docente(s):

Tutor Dra. RODRIGUEZ CABRERA, HORTENSIA MARIA , Ph.D.

Y recibió las observaciones de los otros miembros del Tribunal Calificador, las mismas que han sido incorporadas por el(la) estudiante.

Previamente cumplidos los requisitos legales y reglamentarios, el trabajo de titulación fue sustentado por el(la) estudiante y examinado por los miembros del Tribunal Calificador. Escuchada la sustentación del trabajo de titulación, que integró la exposición de el(la) estudiante sobre el contenido de la misma y las preguntas formuladas por los miembros del Tribunal, se califica la sustentación del trabajo de titulación con las siguientes calificaciones:

Tipo	Docente	Calificación
Miembro Tribunal De Defensa	Dr. MAKOWSKI , KAMIL , Ph.D.	10,0
Presidente Tribunal De Defensa	Dr. CAETANO SOUSA MANUEL , Ph.D.	10,0
Tutor	Dra. RODRIGUEZ CABRERA, HORTENSIA MARIA , Ph.D.	10,0

Lo que da un promedio de: **10 (Diez punto Cero)**, sobre 10 (diez), equivalente a: **APROBADO**

Para constancia de lo actuado, firman los miembros del Tribunal Calificador, el/la estudiante y el/la secretario ad-hoc.


JIMENEZ GRANDA, EDISON RAFAEL
Estudiante


Dr. CAETANO SOUSA MANUEL , Ph.D.
Presidente Tribunal de Defensa


Dra. RODRIGUEZ CABRERA, HORTENSIA MARIA , Ph.D.
Tutor



Kamil Makowski

Dr. MAKOWSKI , KAMIL , Ph.D.
Miembro No Tutor

Ana Maria Escobar

ESCOBAR LANDAZURI, ANA MARIA
Secretario Ad-hoc



AUTORÍA

Yo, **EDISON RAFAEL JIMENEZ GRANDA**, con cédula de identidad 1717374860, declaro que las ideas, juicios, valoraciones, interpretaciones, consultas bibliográficas, definiciones y conceptualizaciones expuestas en el presente trabajo; así como, los procedimientos y herramientas utilizadas en la investigación, son de absoluta responsabilidad de el/la autora (a) del trabajo de integración curricular. Así mismo, me acojo a los reglamentos internos de la Universidad de Investigación de Tecnología Experimental Yachay.

Urcuquí, febrero del 2020.



Edison Rafael Jiménez Granda

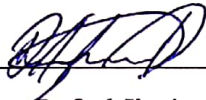
CI: 1717374860

AUTORIZACIÓN DE PUBLICACIÓN

Yo, **EDISON RAFAEL JIMENEZ GRANDA**, con cédula de identidad 1717374860, cedo a la Universidad de Tecnología Experimental Yachay, los derechos de publicación de la presente obra, sin que deba haber un reconocimiento económico por este concepto. Declaro además que el texto del presente trabajo de titulación no podrá ser cedido a ninguna empresa editorial para su publicación u otros fines, sin contar previamente con la autorización escrita de la Universidad.

Asimismo, autorizo a la Universidad que realice la digitalización y publicación de este trabajo de integración curricular en el repositorio virtual, de conformidad a lo dispuesto en el Art. 144 de la Ley Orgánica de Educación Superior

Urcuquí, febrero del 2020.



Edison Rafael Jiménez Granda

CI:1717374860

Dedicatoria

Esta investigación está dedicada para mis padres Melecio y Melida quienes han sido un pilar fundamental, no solamente durante mi formación académica, sino también a lo largo de mi vida. Les agradezco infinitamente sus esfuerzos, paciencia, pero sobretodo amor, gracias por inculcar en mí el ejemplo de perseverancia, honestidad y esfuerzo. Me enorgullece ser su hijo y poder compartir con ustedes este logro que me hace muy feliz. No tengo palabras para expresar lo enormemente agradecido que estoy de tenerlos como mis padres, es por ustedes que he logrado cumplir este sueño.

Muchas Gracias mis Suquitos

Edison Rafael Jiménez Granda

Agradecimientos

Me gustaría agradecer en estas líneas la ayuda que muchas personas me han brindado a lo largo de este proceso investigativo y sin las cuales este proyecto no se hubiera realizado.

En primer lugar, quisiera agradecer a mis padres que con su esfuerzo y dedicación me ayudaron a culminar mi carrera universitaria y quienes han sido mi apoyo incondicional a lo largo de mi vida. Quiero agradecer a mis hermanas quienes siempre han estado presentes para brindarme consejos y animarme en los momentos difíciles. A mi novia, Emilia, no solo por ayudarme a conseguir muchos de los reactivos que necesitaba para mi investigación, sino también por ser mi soporte emocional y estar siempre ahí para ayudarme y animarme en los momentos difíciles. A todos mis amigos, que más que ser mis amigos se han convertido en mi familia durante estos 5 años y siempre han estado presentes para ayudarme con mis problemas.

A mi tutora, Hortensia Rodríguez, por haberme orientado durante todo este largo proceso y también por facilitarme muchos de los materiales necesarios para este proyecto. De igual manera, quiero agradecer a mi co-tutor, “Tibo”, por enseñarme tantas cosas nuevas de química computacional y por tener la paciencia de sentarse conmigo casi todas las tardes a revisar porque no salían los cálculos computacionales.

Al profesor Manuel Caetano a quien le estoy sumamente agradecido por el apoyo incondicionalmente brindado para la culminación de este proyecto. Al profesor Juan Pablo Saucedo por ayudarme a conseguir uno de los reactivos necesarios para este proyecto y por apoyarme durante el proceso de caracterización de mis muestras.

Quiero agradecer a la Universidad San Francisco de Quito por brindarme acceso al paquete informático “Gaussian” necesario para realizar los cálculos teóricos pertinentes en este trabajo investigativo.

Finalmente quiero agradecer a la Escuela de Ciencias Químicas e Ingeniería de la Universidad Yachay Tech por ser lugar donde me formé profesionalmente, pero sobretodo donde conocí excelentes profesionales y personas.

Edison Rafael Jiménez Granda

Resumen

La emisión inducida por agregación (AIE) es un proceso foto-físico y fotoquímico inicialmente descrito en 2001. Este fenómeno describe el incremento de la emisión de luz presentada en ciertos luminóforos cuando se encuentran en estado de agregación. En este trabajo se revisarán los conceptos clave tras el efecto de AIE. También se revisarán los principales sistemas que presentan este fenómeno, enfocándonos principalmente en las moléculas que contienen grupos Ciano. Adicional a esto, se busca sintetizar sistemas capaces de presentar el fenómeno de AIE y estudiar sus actividades biológicas y luminiscentes a través de una aproximación experimental y teórica. Estos dos sistemas derivados de los diaminodicianoquinodimetanos (DADQs) serán sintetizados utilizando TCNQ como el principal reactivo de partida. Para el cálculo del rendimiento cuántico se ha utilizado el método comparativo de Williams en el cual se ha utilizado al 2-(4-(imidazolidin-2-yl)phenyl)malononitrilo como la muestra de referencia. Adicionalmente, se ha realizado cálculos de DFT para obtener mayor información acerca de las capacidades luminiscentes de las moléculas sintetizadas. Finalmente, la actividad biológica de los derivados de DADQs fueron estudiados por el método de difusión en agar y mediante medidas de densidad óptica OD_{600} usando *Escherichia coli* (DH5-alpha) como la cepa principal para este estudio.

Palabras clave

Agregación-inducida por emisión, AIEenos, Ciano, quinonas, DADQs, fluorescencia, luminiscencia, actividad antimicrobiana, rendimiento cuántico, teoría de densidad funcional.

Abstract

The aggregation-induced emission (AIE) is a photophysical and photochemical process initially described in 2001. This phenomenon describes the light emission enhancement presented in specific types of luminophores when they get aggregated. In this work, the key mechanistic concepts behind the AIE effect will be reviewed. The main AIE systems will be discussed mostly focusing in the cyano-containing molecules. Additionally, the goal of the work is to synthesize a system capable to present AIE characteristics and study its biological and luminescent activities through an experimental and theoretical approach. To tackle it, two diaminodicyanoquinodimethane (DADQ) derivatives were synthesized using TCNQ as the initial reagent. For the quantum yield calculations, a comparative approach using 2-(4-(imidazolidin-2-yl)phenyl)malononitrile as the reference sample was used. Additionally, DFT were performed to approach all the quantum chemical calculations to obtain a further insight to the possible reasons of fluorescence enhancement produced in these molecules. Finally, the biological activity of DADQ derivatives were studied by the agar diffusion and the optical density measurements using *Escherichia coli* (DH5-alpha) as the main bacterial strain.

Keywords

Aggregation-induced emission, AIEgens, cyano, quinones, DADQs, fluorescence, luminescence, antimicrobial activity, Quantum yield, Density Functional Theory

Index

<i>Introduction – justification</i>	1
General introduction	1
Problem Statement	2
General and specific objectives	3
General objective.....	3
Specific objectives	3
Chapter 1	4
1. Justification	4
Chapter 2	27
2. Methodology	27
2.1. General information	28
2.1.1. Reagents	28
2.1.2. Equipment	28
2.2. Chemical section – Synthesis	29
2.2.1. Synthesis of 1-chloro-4-nitrobenzene (1).....	29
2.2.2. Synthesis of 7-pyrrolidino-7,8,8-tricyanoquinodimethane (2)	29
2.2.3. Synthesis of N-(4-nitrophenyl)ethylenediamine (3).....	30
2.2.4. Synthesis of N-(2-nitrophenyl)ethylenediamine (4).....	30
2.2.5. Synthesis of 2-(4-(imidazolidin-2-yl)phenyl)malononitrile (a).....	31
2.2.6. Synthesis of 2-(4-(1-(4-nitrophenyl)imidazolidin-2-yl)phenyl)malononitrile (b).....	31
2.2.7. Synthesis of 2-(4-(1-(2-nitrophenyl)imidazolidin-2-yl)phenyl)malononitrile (c)	32
2.3. AIE studies	32
2.3.1. Quantum yield (QY) measurements.....	32
2.3.2. Theoretical approach	33
2.4. Antibacterial Activity	33
2.4.1. Preparation of inoculums	33
2.4.1.1. Culture media.....	33
2.4.1.2. Bacteria strains.....	34
2.4.2. Antibacterial tests.....	34
2.4.2.1. Agar diffusion	34
2.4.2.2. Optical density measurements (OD)	34
Chapter 3	36
3. Results and Discussion	36
3.1. Synthesis	38
3.1.1. Synthesis of 2-(4-(imidazolidin-2-yl)phenyl)malononitrile (a).....	38
3.1.1.1. Characterization of 2-(4-(imidazolidin-2-yl)phenyl)malononitrile (a)	38
3.1.2. Synthesis of 2-(4-(1-(4-nitrophenyl)imidazolidin-2-yl)phenyl)malononitrile (b)	41
3.1.2.1. Characterization of 2-(4-(1-(4-nitrophenyl)imidazolidin-2-yl)phenyl)malononitrile (b). ...	43
3.1.3. Synthesis of 2-(4-(1-(2-nitrophenyl)imidazolidin-2-yl)phenyl)malononitrile (c)	45
4.1.1.1. Theoretical approach for the synthesis of 2-(4-(1-(2-nitrophenyl)imidazolidin-2-yl)phenyl)malononitrile (c).	47

4.2. AIE studies.....	48
4.2.1. Quantum yield (QY) measurement	48
4.2.2. Theoretical Research	51
4.2.2.1. Geometry in Ground & Excited states	52
4.2.2.2. Oscillator strength and dipole moments.....	55
4.2.2.3. Energies associated with the optimized geometries	57
4.2.2.4. Mulliken Charges.....	58
4.3. Antibacterial Activity	59
4.3.1. Agar diffusion method	59
4.3.2. Optical density measurements (OD ₆₀₀).....	61
<i>Conclusions</i>.....	64
<i>Recommendations</i>.....	64
<i>References</i>	65
<i>Annexes</i>.....	68

Introduction – justification

General introduction

Nowadays, light is so important that it is completely unthinkable to live in a world or society without it. Also, it is of essential importance to the universe and has always been since the beginning of the time. In these regards, during the history of civilization, men have worked assiduously to obtain more information and knowledge about it. Albeit, great advances have been made and a lot of information has been gained, there is still so much work to do and many things to explore related to this topic.

In general, luminophores are responsible for the emission of light, and their development into luminescent materials that could be used at will, has contributed to high technology applications. These breakthroughs on luminescent materials and the light emitting processes behind them, have led to new scientific and social advancements. Which have been the principal focus of research within the scientific community.

Luminophores should be capable to emit electromagnetic radiation at any physical state. However, most of the practical applications requires to have luminophores as solid-films, aggregates or crystals.^{1,2} For example, in optoelectronic applications as in electroluminescent devices like organic light-emitting diodes (OLEDs) and organic field-effect transistors (OFETs)^{1,3} or as in sensing applications for ecosystem monitoring and biomedical research,⁴⁻⁶ it is necessary to have the luminophores in solid films or as aggregates.

When the aggregate state is induced in a conventional luminophoric system like in TPE, it is expected to obtain a self-luminescence quenching effect. Once the system is in a state of aggregation or at high concentration in a solution, the molecules are located very close between each other, allowing the aromatic rings to experience strong π - π stacking interactions. The excited states in such aggregates are lost via non-radiative channels, causing an emission reduction or quenching. This phenomenon is known as aggregation-caused quenching (ACQ).^{7,8}

The problems soon arose with the necessity to give an application to these luminophores, which requires the molecules to be in a solid or aggregate state. Furthermore, luminophores are mainly used as clusters where they are arranged as molecular assembly,

nano-aggregates or solid phase in which is mandatory the aggregation of the molecules,^{9–11} being the problem that a lot of scientists tried to solve. As expected, this was a difficult task and an intense investigation came across, considering a variety of physical and chemical approaches to avoid the aggregate formation and offset the fluorescence quenching disadvantage.⁸ However, the efforts were worthless due to, most of these approaches tried to counteract a natural process of aggregation.

Due to the failed attempts and the necessity to have high luminescent molecules under the aggregate state, in 2001 Yuning Hong and its research group found a new kind of organic luminogen, in which the aggregation of the molecules increased the radiative emission rather than decreasing it.¹² They also found that there are a series of silole derivative molecules that do not present emission when are diluted, but once they get aggregated a high luminescent behavior is observed. Since the light emission is induced by the formation of aggregates, this process was perfect to offset the previously mentioned problem and it was called as “aggregation-induced emission” (AIE).¹³ The AIE effect has an opposite behavior to the one exposed by the ACQ phenomenon, defying the conventional perspective of “useless” materials, that the non-luminescent molecules in dilution had, into a potentially high luminescent species under the aggregate conditions. During the last years, major progress has been made in this field leaving a great variety of luminogens with AIE characteristics (AIEgens), which are capable to emit at different wavelengths, have different applications and have opened a brought new insight into the light-emission processes. Besides, the processes behind the AIE are not yet fully understood as well as the different AIEgen systems. For all the above, more research is needed in this field.

Problem Statement

The aggregation induced emission effect is a relatively recent discovered phenomenon, which has raised a lot of interest, especially in the material science field, because of its great potential in high technology applications. Since its first description in 2001 numerous of different systems that presented this effect were discovered including hydrocarbon containing systems, hexaphenylsiloles, cruciform, diaminodicyanoquinone derivatives (DADQs) and others. From this great variety of systems, the diaminodicyanoquinones are molecules that despite of possessing high dipole moments generally are not considered as fluorescent dyes due to their low quantum yields in

solution, commonly below 0.5%, and the moderate increase of the quantum yield to 45% in the solid state. However, in the last years it has been found that some DADQs are capable to present an enhancement of their emission to around 90% in the solid state, opening the possibility to research the application of such DADQs systems in solar cells, light emitting devices, bio-imaging studies, as well as, their use in nonlinear optics and polarity sensitive. Furthermore, the search of new DADQs with high emission quantum yields are of great importance to obtain further insight in the mechanisms behind the AIE phenomenon and its relationship with their molecular structure. In addition, due to its structural conformation it has been hypothesized that the DADQs could have a potential use in biological systems

Hereof, as hypothesis, it is going to be investigated the fluorescent properties of two diaminodicyanoquinone systems which derive only in the position of one substituent, using together an experimental and theoretical approach. In addition to that biological tests will be performed in these systems because their molecular structures suggest a possible biological activity.

General and specific objectives

General objective

- To develop two DADQs systems with potential aggregation-induced emission (AIE) characteristics and biological activities.

Specific objectives

- To synthesize two different AIEgens, using as starting material the 7-pyrrolidino-7,8,8-tricyanoquinodimethan.
- To characterize the synthesized AIEgens using UV spectroscopy, mass spectroscopy and FTIR.
- To calculate the quantum yield of the synthesized AIEgen systems
- To perform computational studies in the different systems to compare these approaches with the experimental data.
- To perform antimicrobial activity tests to the DADQ derivatives.



Chapter 1.

Justification

Aggregation-induced emission: a review of promising
cyano-functionalized AIEgens

Jimenez, E.R. & Rodríguez, H. *J Mater Sci* (2020) 55: 1366. <https://doi.org/10.1007/s10853-019-04157-5>



Aggregation-induced emission: a review of promising cyano-functionalized AIEgens

Edison Rafael Jimenez¹ and Hortensia Rodríguez^{1,*}

¹School of Chemical Sciences and Engineering, Yachay City of Knowledge, Yachay Tech University, 100650 Urcuqui, Ecuador

Received: 1 September 2019

Accepted: 23 October 2019

© Springer Science+Business Media, LLC, part of Springer Nature 2019

ABSTRACT

The aggregation-induced emission (AIE) is a photochemical process described in 2001, where the aggregation of specific kinds of organic compounds enhances the emission of light performed by these organic compounds. Since then, this phenomenon had attracted much interest because of its potential application in optics, electronics, energy and bioscience. In this review, the main concepts of AIE are going to be explained through the mechanistic decipherment of these photophysical processes. Additionally, some AIE systems will be discussed, describing the phosphorescence enhancement induced in organic molecules by this effect, but we will be focusing on the cyano-containing AIEgens, its recent advances and the driving forces that lead to the AIE effect in these cyano-containing molecules.

Introduction

Molecules with luminophore characteristics are of great interest in the field of material science. Furthermore, if there are molecules capable of presenting fluorescence or phosphorescence under the aggregate or solid state, the possible technological applications are enormous, in comparison with molecules that exhibit this behavior in others state of matter. These luminophores can be used in OLEDs, liquid crystals, DNA visualization, bioimaging, explosives detection, among others. However, in most of the conventional luminophoric systems, the induction of the aggregate state produces an adverse effect in luminescence; this effect is known as the "Aggregation-caused quenching" (ACQ) [1]. One of the most common examples of

the ACQ effect is present in the molecules of perylene (Fig. 1).

Perylene molecules have a strong luminescence when it is in solution with THF. However, as soon as the fraction of a poor solvent is increased in solution, the emission in these molecules gets significantly reduced. Thus, once the perylene molecules get aggregated, they present a π - π stacking interaction, due to its planar aromatic structure. The result of these interactions gives rise to very short lifetime dimeric or heterodimeric species known as excimers. The formation of the excimers is harmful to the emission in the aggregated state and gives rise to the well-known ACQ phenomena [2]. It is essential to remark that the presence of the ACQ effect is attributed to most of the aromatic molecules and its derivatives because of its intrinsic planarity, as Bricks

Address correspondence to E-mail: hmrodriguez@yachaytech.edu.ec

<https://doi.org/10.1007/s10853-019-04157-5>

Published online: 31 October 2019

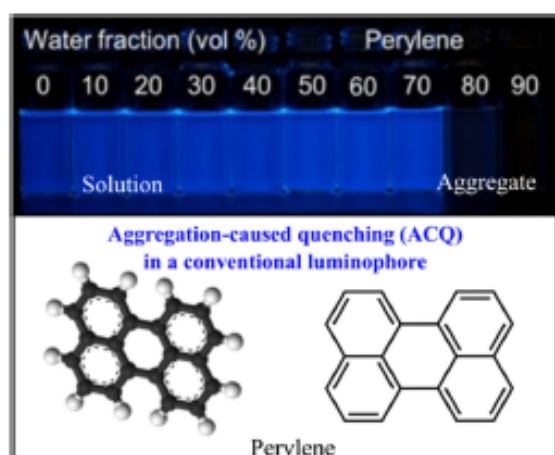


Figure 1 ACQ effect in perylene induced by the increase in water fraction. Reprinted (adapted) with permission from Ref. [1]. Copyright (2015) American Chemical Society.

state it in his book "Photophysics of aromatic molecules" [3].

In addition to that, conventional organic luminophores usually present strong luminescent characteristics as isolated molecules, but they lose this characteristic as the degree of aggregation increases. In this scenario, a lot of aromatic molecules are very close between each other, leading to intense intermolecular π - π stacking interactions, especially to those molecules with disk or rod-like shapes. These stacking interactions produce a non-radiative decay in molecules that present excited states before the stacking, resulting in the emission quenching of the luminophores [1]. Another closely related process in regard to the non-radiative relaxation pathways is produced by a conformational change that leads to cis-trans isomerization's, which are directly related with the solvent viscosity, the size and mobility of the freely movable moieties in the molecules [4-11].

In these regards, we can say that the ACQ effect is generally unfavorable for the vast majority of applications on luminophoric materials; unfortunately, it is present in most of the conventional organic molecules. Because of this, many research groups made a lot of efforts trying to tackle down the ACQ effect, without any significant success. The main problem with these attempts was the approach that the

researchers took, in which they tried to alter or modify a natural process that is related to the intrinsic tendency of the aromatic molecules to form aggregates in concentrated solutions [12].

Due to the failed attempts and the necessity to have high luminescent molecules under the aggregate state, in 2001, Yuning Hong and its research group found a type of organic luminogen, in which the aggregation of molecules increased the radiative emission rather than decreasing it [2]. They found that there are a series of silole derivative molecules that do not present emission when they are diluted, but once they get aggregated, a high luminescent behavior is observed. Since the formation of aggregates induces the light emission, this process was termed as "aggregation-induced emission" (AIE) [13]. In this scenario, the AIE effect has an opposite behavior to the one exposed by the ACQ phenomena, defying the conventional perspective of "useless" materials, that non-luminescent molecules in dilution had, into a potentially high luminescent species under aggregate conditions.

From Yuning's breakthrough, a new path to study the radiative emission of molecules under the aggregate state was opened, leading to the acquirement of structure-property relationships and some insight into the working mechanisms of the effect. Thus, many research groups synthesized and studied different molecules that could potentially present the AIE effect, changing the preparations and modulating how the aggregation conditions of these compounds are. As a result of the performed investigation, a lot of information was obtained, a variety of new AIE systems were discovered, and the operating mechanisms behind the effect and many practical applications started to being explored [2]. Some of the systems that present the AIE effect are: cruciforms [14], hexaphenylsilole [15], diaminodicyanoquinodimethanes (DADQs) [16], diphenylbutadienes [17] and tetraphenylethenes [18].

To ensure a complete understanding of this phenomenon, there is a brief explanation of those to the date known and accepted operating principles that govern the aggregation-induced emission effect as well as an introduction to the two main classifications for the systems that have this effect and a view in the cyano-containing AIEgens.

Operating principles of the AIE systems

To understand the principles behind the AIE effect, it is necessary to recall that luminogenic molecules that suffered an excitation of their electrons are capable of releasing this excess of energy, obtained during the excitation process, via photophysical and/or photochemical pathways [19]. As it is expected in the non-radiative relaxation, the excess of energy present in the molecule is released by the emission of phonons, which are commonly known as heat. On the other hand, the radiative relaxation process is entirely the opposite, and here, we are talking about an energy release pathway in which the emission of photons frees the energy.

In the case of the AIE systems, the relaxation of the excited state by a photophysical pathway could be accomplished in two ways: the non-radiative and radiative processes, while the photochemical one refers to the loss of energy through a chemical reaction. Therefore, in solution, the excited AIEgens should decay mainly through non-radiative photophysical or photochemical processes and in the aggregated state, they should decline mostly through the radiative photophysical process. The collective effects of these radiative and non-radiative ways of releasing energy give rise to an increase or quench in the luminescence of each different luminogen [20].

Thus, there exist three main hypotheses that explain the mechanical causes of the non-radiative relaxations or the enhancement of the radiative ones. These mechanisms are known as RIR, RIV and RIM.

Restriction of intermolecular rotation (RIR)

This mechanism was firstly proposed by Zikai and coworkers, to understand its principle; we initially should imagine a "propeller-shaped" molecule (PSM), as it is shown in Fig. 2. Thus, once the PSM is taken to its excited state it has two options for the relaxation process: the radiative and non-radiative pathways. Hence, when a propeller-shaped molecule is taken to its excited state and it is in solution the free mobile parts of the molecule that are attached, generally by a single bond, to the main core of the molecule can freely rotate, releasing the energy from the molecules by the realization of intermolecular movements [21]. This is a non-radiative way that is harmful for the effect that we are looking for.

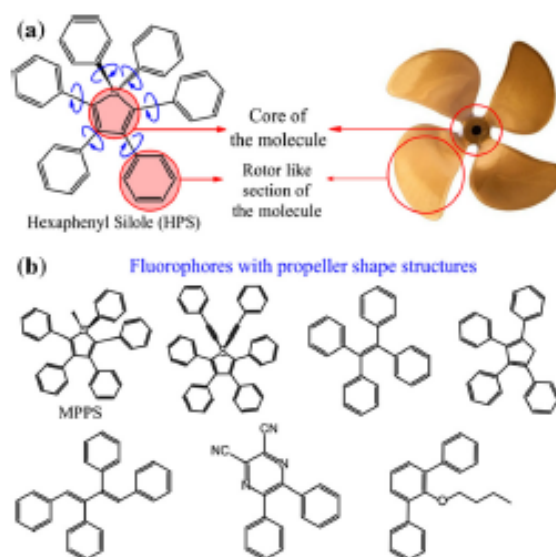


Figure 2 a Comparison between the chemical structure of the non-planar hexaphenyl silole and the shape of a conventional propeller. b Examples of silole, hydrocarbon and heteroatom-containing fluorophores that have the propeller shape.

Furthermore, this effect is responsible of the luminescence quenching ACQ in the AIEgen species [22, 23].

On the other hand, at the aggregate state, these propeller-shaped molecules are not able to pack tight together, avoiding the π - π stacking process, which is responsible for the ACQ effect in conventional luminophores, due to the free rotating groups that confer the propeller shape of these compounds. Even more, in the aggregate state the molecules cannot pack tightly together because of the free rotating groups that do not adopt a planar conformation, producing intrinsic steric restriction. Instead, the "rotor" moieties attached to the core section of the molecule are greatly restricted owing to the physical constraints provided by the neighboring moieties and molecules that are very close between each other. This restriction of the intramolecular rotation blocks the photophysical non-radiative pathway and opens up the photophysical radiative way. As a result, the PSMs become highly emissive in the aggregate state.

As a general idea of what should be the main structure of the propeller-shaped molecules mentioned before, some examples of AIEgens that have the specified shape are shown in Fig. 2 [15].

To illustrate the RIR mechanism, we can use a fairly known AIEgen that presents aggregation-

induced emission due to the RIR mechanism; this molecule is the tetraphenylethene (TPE) Fig. 3 [21].

In Fig. 3, we can see that the TPE molecule is non-emissive in solution as the excited state of the TPE can decay quickly in a non-radiative way, mostly by the free rotation of the pendant phenyl groups of TPE, which are shown in blue arrows. Once the TPE gets aggregated, these intermolecular rotations are restricted due to multiple intermolecular interactions that block non-radiative decay pathways and leave the radiative channel open as the only method to release the energy in the molecule [18].

The restriction of intermolecular vibrations (RIV)

As the AIE study advances, the family of AIE molecules continues growing, leading to some peculiar systems that exhibit the AIE phenomenon, but the molecules forming these systems are lacking any rotor-like moiety in its molecular structure, and this is the case of molecules like THBDBA and BDBA (Fig. 4) among other molecules [24]. For these systems, the AIE effect cannot be explained using the RIR mechanism, and therefore, other parameters need to be taken into account. As the concept of RIR focuses on the restriction of intramolecular rotations, perhaps these new systems perform the AIE effect under the limitation of another intramolecular motion. The other motion proposed is the intramolecular vibration (RIV) [24]. Thus, the RIV should work similarly as the RIR mechanism; the different conformation that the molecules can adopt in the solvated state will consume the energy of the excited molecule in a non-radiative manner which produces the lack of emission when the system is in solution.

In, contrast, when the system is in a cluster it experiences conformational vibration hindrances, because of the neighbor molecules as shown in Fig. 4. This is reflected in the restriction of the molecule

motions (vibrations) blocking the non-radiative pathways and inducing the release of energy under a radiative way to finally produce the observed AIE effect [1]. Some examples of AIEgens capable to produce an excited-state decay by intermolecular vibrations are shown in Fig. 5.

Finally, an essential aspect of this mechanism is that AIE molecules that get activation through RIV may not have as many and efficient non-radiative vibrational decay pathways as in the RIR mechanism. Therefore, the restriction of these channels will result in a less pronounced AIE effect [24].

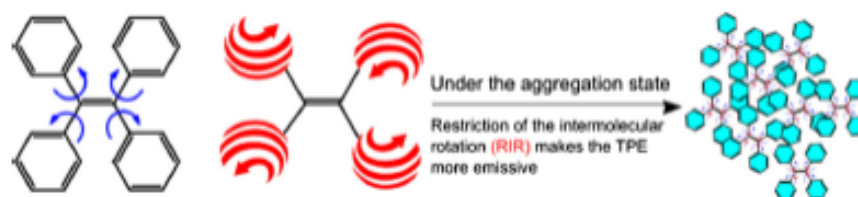
The restriction of intermolecular motions (RIM)

This new mechanism gives a broader idea of the fundamental principles that govern the AIE effect. In general, it is an integration of the RIR and the RIV mechanisms in which the motion of a molecule is described as the rotation and vibration that its structure presents. Generally, in AIE systems, the flexibility of a structure promotes intramolecular motions which increase the non-radiative decay channels. The aggregation induces some structure hardening, and in that way, it blocks the non-radiative decay pathways, increasing the emission of photons in the relaxation process [21].

AIEgens that can present this new RIM principle need to have a vibratory core and rotatable sections in its conformation. An example of a molecule that fulfills these requirements is shown in (Fig. 6).

The main idea of RIM is that the RIR and RIV mechanisms are not mutually exclusive, instead they can work together to increase the AIE phenomenon. It seeks to explain and create a much more diverse family of AIEgens where intramolecular motions can enhance non-radiative decay rates of isolated single molecules, whereas structural stiffen blocks the non-radiative pathways, directing relaxation of the excited species through radiative channels [1].

Figure 3 Chemical structure of tetraphenylethene (TPE), which emission is due to the RIR mechanism.



Author's personal copy

J Mater Sci

Figure 4 Chemical structure of THTBDA, which emission is due the RIV mechanism.

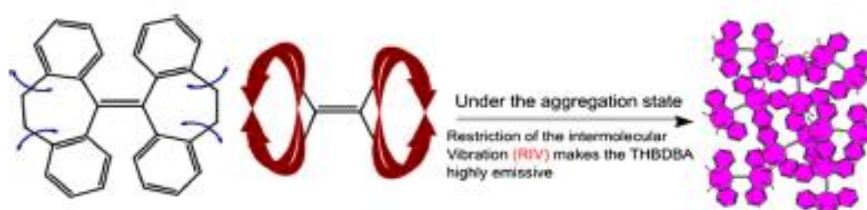
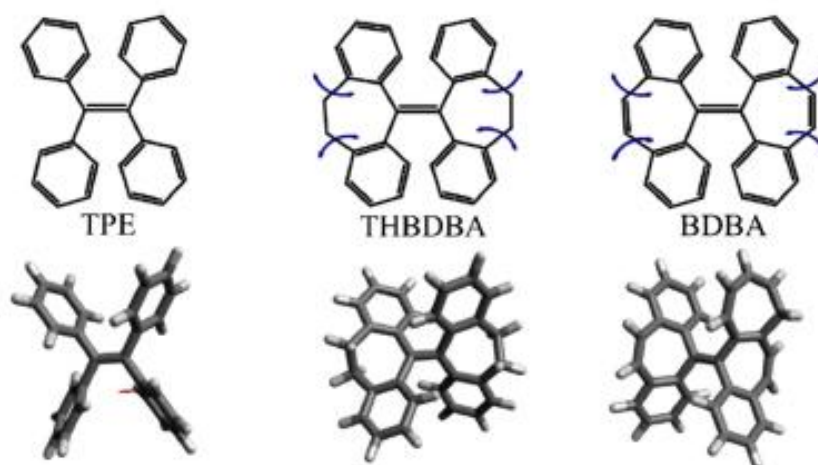


Figure 5 Molecular structures of tetraphenylethene (TPE), 10,10',11,11'-tetrahydro-5,5'-idibenzo[a,d][7]annulenyliene (THBDBA), and 5,5'-bidibenzo[a,d][7]annulenyliene (BDDBA) with its single-crystal structures and its possible conformational movements (vibrations) indicated by the blue curved arrows.



Macrocyclic molecules showing RIM mechanism

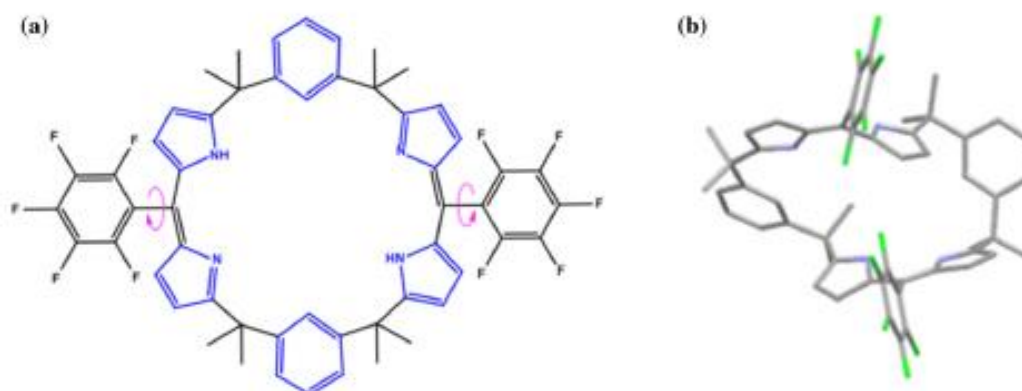


Figure 6 Macrocyclic luminogenic molecules whose AIE activity is produced by the RIM process. **a** The pink arrows show the sections of the molecule capable to rotate, and the blue parts of the molecule can vibrate. **b** The optimized crystal structure of the

molecule (MMFF94) is obtained from Chem 3D. Reprinted (adapted) with permission from Ref. [1]. Copyright (2015) American Chemical Society.

Enhancement of phosphorescence lifetime

Usually, organic molecules exhibit weak or non-phosphorescent radiation because of the tight binding of valence electrons that contains the emission caused by the transition from triplet excited states to

the ground state. Besides of that, long-lived phosphorescence of certain organic molecules is under study, and a long-life phosphorescence could be achieved in organic molecules if the system is capable of producing an intersystem crossing (ISC) and also

has the capability of tuning the phosphorescence radiative decay [25].

Thus, the ISC effect between a singlet and a triplet excited states of the organic system is absolutely necessary [26, 27]. A considerable strategy to favor the ISC rate is to reduce the energy difference between the singlet (S_m) and the triplet (T_m) excited states; this means that it is necessary to reduce the energy gap between excited states. An interesting approach to achieve this is to induce the aggregation of molecules Fig. 7, which may be useful in the reduction in the mentioned energy gap between the excited states. Thus, the AIE effect could be responsible for the phosphorescence rise in organic molecules.

Recently, research revealed that ISC and the internal conversion (IC) could have a comparable time-scale and ISC can occur in high-lying excited states [27]. Consequently, it is considered to compare the use of the aggregation as a method to reduce the ISC energy gap to increase the conjugation of different polymeric compounds, which enhance their conductivity by reducing the band gap. In both cases, if there is just one molecule of the compound "monomer," the energy levels are quite distant from each other, and the ISC is mainly negligible. But, when the number of molecules is increased to two "dimer," the excited states will go under a splitting of the energy levels resulting in the reduction in the energy gap. Even more, if the aggregation proceeds, the behavior will be the same than the increase in conjugation in a semiconductor "polymer," the excited states go under

splitting, and the energy gap of the singlet and triplet excited states will be smaller.

This concept of aggregated induced intersystem crossing, AI-ISC, allows the suppression of the lowest singlet state. This means that the fluorescence of the molecule will also be suppressed to allow for the appearance of phosphorescence, which can be considered as complementary to AIE. However, the influence of AI-ISC on phosphorescence lifetime remains unexplored [28].

AIEgens systems

The high level of interest in the AIE phenomena and the further understanding of the mechanisms behind this effect lead to the discovery of a high number of systems with these qualities. Thus, the development of different molecules capable of showing luminescence under the aggregate conditions obtained significant progress. In this regard, different families of these compounds appeared, being the most representative those composed by pure hydrocarbon molecules, compounds containing heteroatoms, polymeric, inorganic and organometallic. This shows that the variety of AIE systems has maintained a continual or even an exponential growth since it was discovered [2].

In this section, we are going to briefly discuss the general characteristics and showcase some examples of the two first-mentioned systems to later completely focus in the cyano-containing AIEgens and their characteristics.

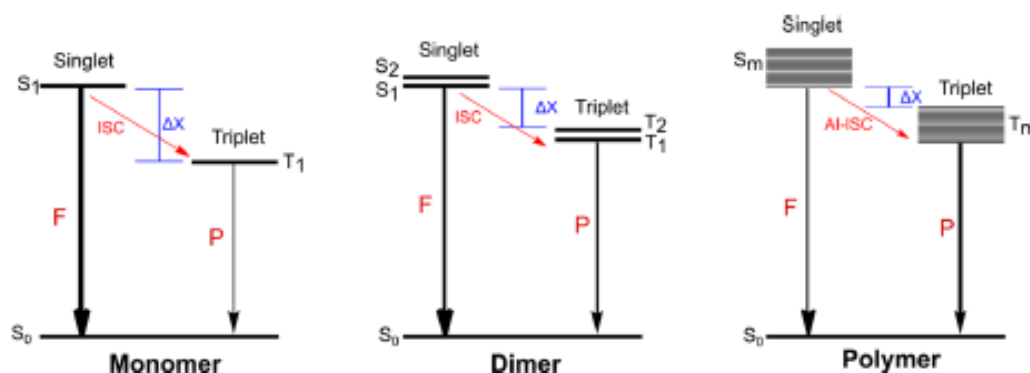


Figure 7 Schematic diagram of intersystem crossing (ISC). The diagram displays the energy splitting during the aggregation process. F: fluorescence, P: phosphorescence. The thickness of the straight arrows shows the emission intensity of both fluorescence

and phosphorescence. The red arrows denote the process of Intersystem crossing, and the blue bar indicates the distances between the single and triplet excited states.

Hydrocarbon AIEgens

These systems are composed of molecules with just carbons and hydrogens atoms in its chemical structure; they comprise a fundamental role in all the types of AIEgen systems. Because, by not having any heteroatom in their structure, the analysis of the interactions between molecules, polarity, electronic, photophysical and other properties of the molecule is much simpler and straight forward, leading to a quite accurate structure to property relationship. That provides insight into the driving mechanisms behind the AIE effect. Additionally, the hydrocarbon systems could work as building blocks or models for the development of different functional AIEgens, taking into account the moieties capable to freely rotate or vibrate and the structural non-planarity of the molecules when they are in the aggregate state [12].

Some of the simplest and more representative structures of the hydrocarbon AIEgens are the ones reported by Shimizu et al. [29], which are based on cores of hexa-1,3,5-trienes decorated with different aromatic moieties (Fig. 8).

In molecules (a) and (b), shown in Fig. 8, the phenyl groups attached to the triene core are capable of rotating freely. But the phenyl located in the equatorial zone of both compounds almost does not rotate, showing dihedral angles of less than 2° for (a) and 15° for (b). This is not enough to avoid the formation of π - π stacking interactions under the aggregate state, due to tight packing between same species molecules. Besides of that, this molecule

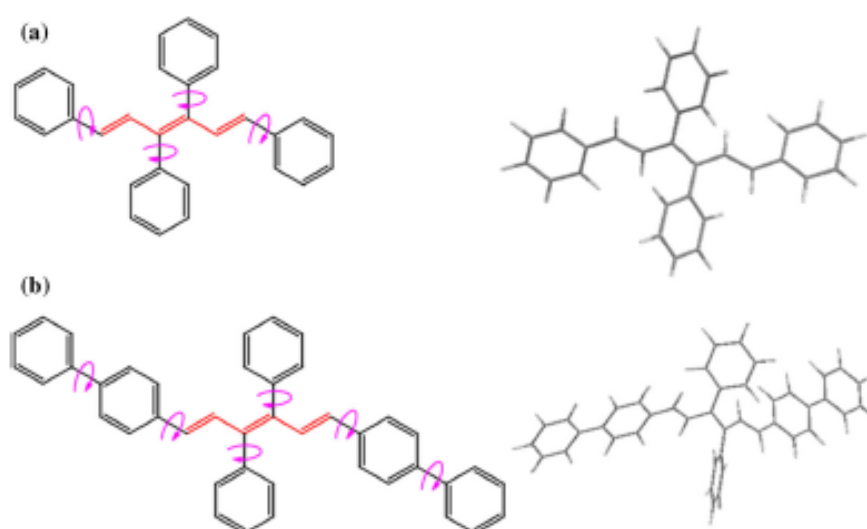
presents an AIE behavior due to the two phenyl groups located in the vertical axis that shows a dihedral angle of almost 80° . This angle is produced in response to the hindrance generated by the hydrogen atoms of the triene core and the meta hydrogen in the phenyl group [30]. Now, the molecules are unable to pack tightly in the aggregate state and also are limited to perform intermolecular motions, reducing the non-radiative relaxation pathway and induce the AIE effect.

Heteroatom AIEgens

As mentioned before, the hydrocarbon systems are quite simple and their AIE effect is not as complicated as the heteroatom-containing molecules. Hence, the emissions related to these molecules are also quite simple, producing for most of the pure hydrocarbon systems emissions at the blue region of the visible spectra. Thus, to enrich the palette of colors and widen the scope of high-tech application for the AIEgen systems, it is necessary to introduce some variation in the molecules conformation to produce an emission shift to larger wavelength, known as a red-shift [1, 2].

To accomplish this new objective, it is necessary to incorporate heteroatoms into the luminogen, which can induce electronic perturbation, like the polarization caused by intramolecular charge transfer (ICT) [2]. That can considerably alter the photophysical behaviors of the luminogen, especially the produced

Figure 8 Arylene-vinylene core-based AIEgens with its crystal structures obtained from chem 3D.



colors. Thus, an AIEgen that presents some kind of heteroatom in their structure could be able to emit at longer wavelengths only if it can achieve a polarization charge transfer effect produced by electron donor-acceptor pairs [31, 32]. These pairs are demonstrated in Fig. 9, in which the structures are conformed by a triphenylamine (TPA) group and an acceptor part. The TPA is an excellent electron-donating group, and besides the fact that it is not AIE active, it can be used as a building group to produce AIEgen systems, because of its propeller-shaped structure. On the other hand, the benzaldehyde and the fluorenone parts are electron-accepting groups, which gave the acceptor-donor pair necessary in each molecule to produce a red-shifted emission.

In the same line, other researchers have synthesized a variety of TPA-based luminogens. Obtaining immensely promoted quantum yields in the solid state compared to those obtained in solution. Also, it was found that this compound presents an electrofluorochromic behavior [33]. This was performed by joining together TPA and diOMe-TPA with two well-known AIEgens, the triphenylethylene (TPE) and the benzo[b]thiophene-1,1-dioxide (BTO). Molecules synthesized are shown in Fig. 10 [34].

Recently, the development of various advanced materials which are TPA based is used for optoelectronic applications such as electrochromic, electrofluorochromic and polymeric memory devices.

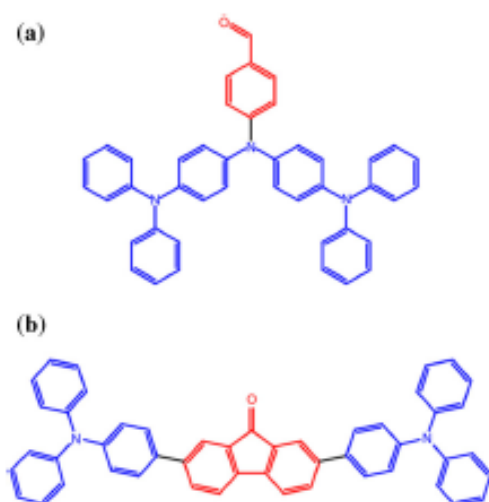


Figure 9 Examples of luminogens containing oxygen and nitrogen heteroatoms. The structures marked with red are the electron-withdrawing blocks, and the ones in blue are the electron-donor groups.

Furthermore, it has been studied as a series of high-performance polymers that will contribute to the design of materials for applications such as data storage, displays and flexible electronics [35].

Cyano-containing AIEgens

One subgroup of the heteroatom-containing AIEgens is the cyano- or nitrile-containing group. This functional group is quite simple; it owns a high polarizable ability and is comparably smaller than other functional groups, making the cyano group a frequently used group for the design of optical materials, which lead to the development of a large variety of AIEgens containing cyano groups [36].

Therefore, the cyano group, besides not being as large as other groups like carboxylic acids or phenylic moieties, still is capable of producing steric effects due to the massive electronic cloud around it, which gives rise to twisted conformations. Another advantage of the cyano group is its capacity to provide electronic effects. Because of its electron-withdrawing nature, it is possible to create a donor-acceptor (D-A)

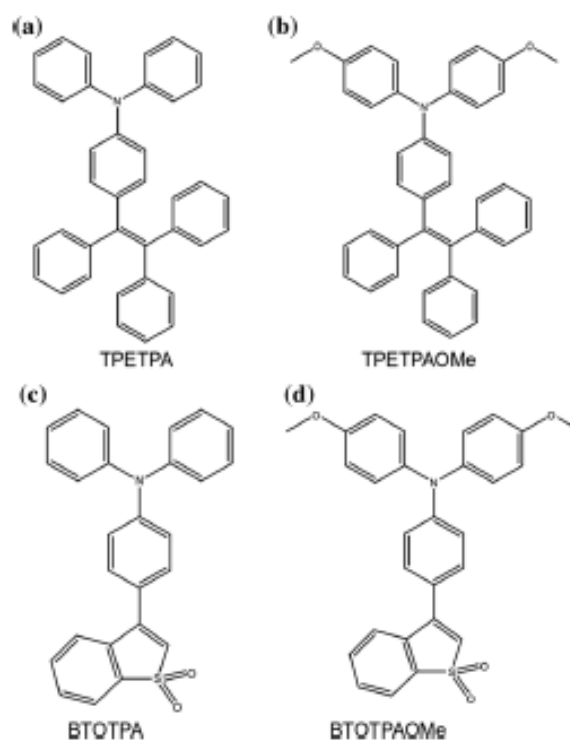


Figure 10 Examples of TPA-luminogens with novel AIE characteristics.

system. Another essential feature of molecules that contain cyano groups is that, under the crystalline state, the cyano groups are capable of interacting with hydrogen atoms of the neighboring molecules to form hydrogen bonds of the following type C–H...N. As it is known, the hydrogen bonds are decisive for biological functions, the conformation of different macromolecular structures, and in regard to our interests, they have been mostly used to model chromophores that increase their dipole moment during electronic excitations [37–42]. This allows the molecule to form a network in its crystalline structure, which increase the rigidity of the crystal and reduce the motion possibility of the free movable groups in the molecule Fig. 13 [43]. Because of these strong supramolecular interactions, the system by itself becomes more rigid, and the planar configuration is avoided preventing the π – π stacking interactions.

Such activity induces, in the crystalline state, a tight packing between molecules, but at the same time avoids the formation of the π – π stacking interaction. These features make the cyano group a fairly used functional group to create AIEgens with donor–acceptor characteristics, H-bonding capabilities and special features such as mechano-responsive aggregation-induced emission [44].

Recent discoveries show that certain cyano-containing molecules could be used for fluorescence imaging in living cells [45]. This is one of the most interesting applications for these kinds of molecules. Molecules shown in Fig. 11 are just some examples of molecules with these characteristics. Furthermore, for a molecule to present such properties it must be stable at pH and light variations, present low toxicity and should be able to penetrate the cell membrane. In addition to bioimaging, it was found that Py–CN–N could be used in the design of ratiometric fluorescent probes [45].

Cyanostilbenes

One of the most common and most studied cyano-containing AIEgens is the cyanostilbene and its derivatives. Generally, there are two variations of the cyanostilbenes; these variations depend on the cyano group position. The 4-cyanostilbene has a stilbene skeleton with a cyano group in the para-position of one aromatic ring, Fig. 12a, and the α -cyanostilbene

with a cyano group located in the α -position of the ethylenic bond, Fig. 12b [46].

4-Cyanostilbene and its derivatives, with the extension of the π -conjugation in the system, are capable of covering the whole visible region, and most of the studies related with these types of cyanostilbenes are focused on the exploitation of the twisted intramolecular charge transfer phenomena (TICT) [47], mainly in those cyanostilbene compounds with a donor–acceptor system where the electron-donor part is located at the opposite side of the cyano group, within the molecule. However, the potential of the 4-cyanostilbene gets reduced due to its lack of chemically reactive sites that prevent further structural modifications from improving the luminescent properties and performing more profound studies. Because of this, the α -cyanostilbene was developed as an alternative to maintain the properties of 4-cyanostilbene and allow the structural tuning of the molecule. Thus, in the following section different α -cyanostilbene and 4-cyanostilbene derivatives will be reviewed in greater depth to understand how all the characteristics mentioned above work synergistically to produce the aggregation-induced enhancement emission.

For instance, one of the examples that shows the importance of the hydrogen bonding capacity in the cyano group in regard to the AIE is the cyano-substituted oligo(para-phenylene vinylene) (CN-DPDSB), sketched in Fig. 13a. This molecule, as expected, barely shows luminescence with a quantum yield around 1% when it is diluted in THF, but in the crystalline state, the luminescence becomes quite strong with an efficiency near to the 80% [43]. The luminescence of this and other organic materials under the solid state can be calculated with the use of an integration sphere [48].

In addition to that, the optimized geometry of CN-DPDSB Fig. 13a shows a non-planar configuration due to the steric hindrance produced by the electronic clouds of the cyano group and the phenyl ring substituents. In solution, these groups are capable of releasing the energy of the excited state via non-radiative pathways like rotation and vibration motions of the substituent groups around the vinyl's double bond; this is the reason for this compound to have a very little luminescence in solution [49]. Furthermore, once the motions of a CN-DPDSB diluted in THF gets restricted by freezing at 77 K, it becomes highly luminescent, and the intensities of the

Figure 11 Confocal fluorescence imaging probes in three different cyanovinyl derivatives. Reprinted (adapted) from Ref. [45], Copyright (2019), with permission from Elsevier.

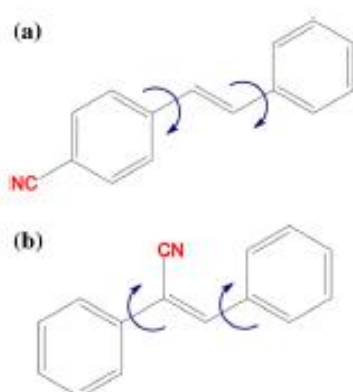
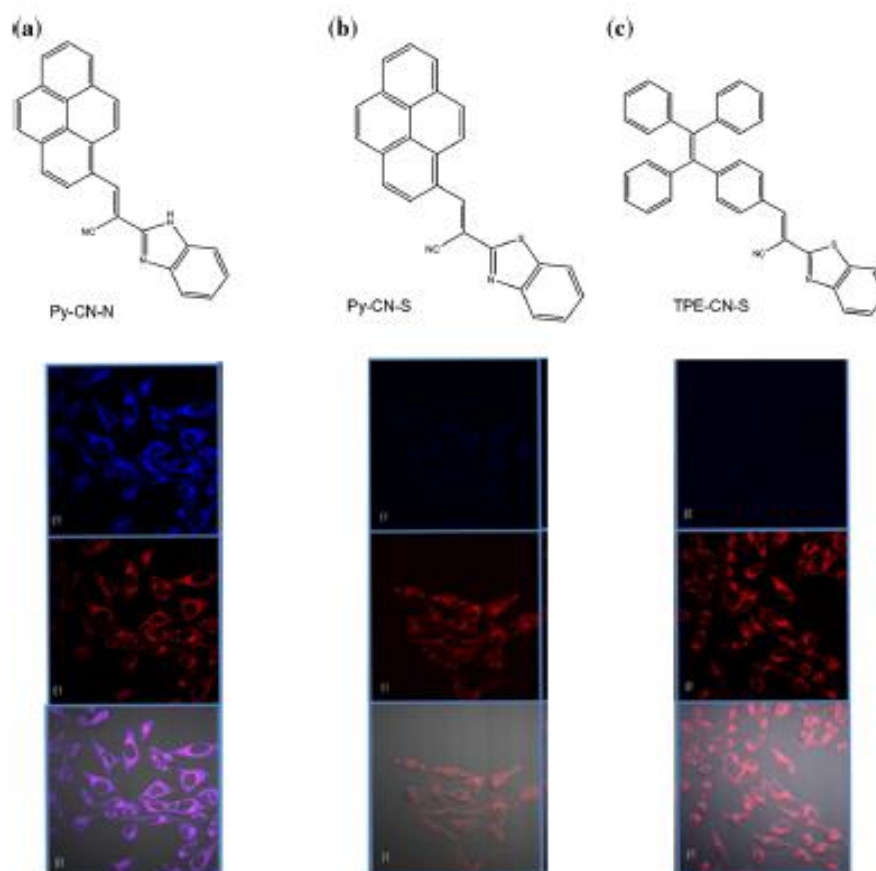


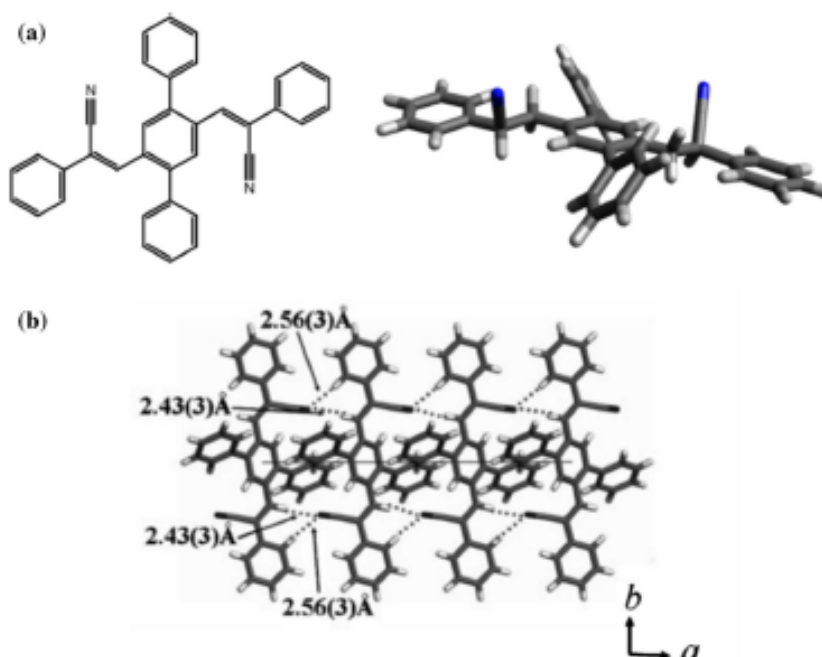
Figure 12 Molecular structure **a** 4-cyanostilbene, and **b** α -cyanostilbene. Blue arrows show the possible rotations on the aromatic rings.

photoluminescence get 100 times higher than those at room temperature [43]. Thus, the observed luminescence enhancement in the crystalline state of CN-

DPDSB has the same origin as the one shown at low temperatures.

The CN-DPDSB molecules are capable of interacting with atoms of the neighboring molecules by two hydrogen bonds of type C-H...N. These hydrogen bonds are formed in two ways: the first one is formed between a nitrogen (N) atom in the cyano group and hydrogen (H) atom in a phenyl substituent, while the other hydrogen bonds occur between the nitrogen in the cyano group with a hydrogen atom in the ethylene moiety of the molecule. The distances of these hydrogen bond interactions are 2.43 and 2.56 Å, respectively Fig. 13b, and their presence is of great importance to fix the double bond and the phenyl rings, preventing their motion [43]. The hydrogen bonds in addition to other supramolecular interactions help to increase the rigidity of the molecule and also avoid a planar conformation, which ensures a high fluorescence of the molecule by the AIE phenomena when it is in the crystalline state.

Figure 13 **a** Molecular structure of CN-DPDSB at the top-left and the geometry of isolated CN-DPDSB at the top-right. **b** Molecular packing of CN-DPDSB and its hydrogen bond interaction viewed in plane *ab*. Reprinted (adapted) from Ref. [43]. Copyright (2007), with permission from Royal Society of Chemistry.



Recently, it has been reported that cyano-functionalized diarylethene derivatives with AIE properties are capable of presenting piezofluorochromic (PFC) behaviors [50]. In general, materials that exhibit the PFC behavior are compounds which are capable of switching their luminescent characteristics in the solid state due to changes generated in the crystalline structure of the material [51]. These changes are mainly produced by an applied mechanical force like the grinding of the crystals and are returned to their natural state by an annealing procedure. The PFC materials have attracted a lot of attention because of their potential applications in data storage, optoelectronic devices, security printing and fluorescent switches [52–54].

Currently, it is not completely clear how the cyano-functionalized diarylethene structure and the PFC characteristics relate to each other. Therefore, a series of *N*-alkyl substituted 3-(4-(10H-phenothiazin-10-yl)phenyl)-2-(1H-indol-3-yl) acrylonitriles (PIA-*n*) were studied Fig. 14 [50].

These molecules present an excellent AIE behavior due to the presence of a suitable donor group, TPA and the acceptor part, which corresponds to the cyano-substituted stilbene. Also, the difference in length of the alkyl chain does not make a significant difference in the absorption spectra of each

compound. However, when the fraction of poor solvent is increased to values above 60, 80 and 40%, the photoluminescence of PIA-8, PIA-12 and PIA-16, respectively, gets gradually reduced [50]. This effect has been widely reported in other AIE systems, and it is not completely clear why it happens, but, as a general idea, it is accepted that high fractions of poor solvents induce a quick aggregation of AIEgens producing an amorphous arrangement rather than a crystalline one, resulting in a reduction in the emission [52, 55, 56]. On the other hand, the PIA-4 did not show a reduction in its luminescence, due to its relative small alkyl chain that makes easier for these PIA-4 molecules to maintain a crystalline structure unlike the other PIA-*n* derivatives with larger alkyl

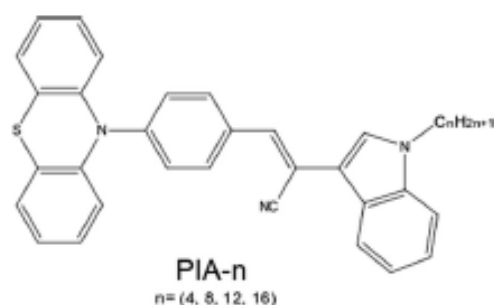


Figure 14 General structure of the cyano-functionalized diarylethene.

chains. Under this consideration, the photoluminescence intensity is dependent on the degree of crystallinity or amorphousness in the material [57, 58].

In regard to the piezofluorochromic properties, all the PIA derivatives displayed a red-shifted behavior after grinding. The bathochromic shift, in the grounded material, was more critical in PIA-4, and according to the increasing length of the alkyl chains, the effect was less and less noticeable [50]. This behavior must be a consequence of the steric hindrance produced by the alkyl chains, as the alkyl chain gets more substantial it is much more difficult for the molecules to adopt a planar conformation and as a consequence to this the intermolecular π - π stacking would be less probable. In general, it is more difficult for the PIA derivative with the largest alkyl chain to change from a crystalline to an amorphous state by grinding [59].

Structurally similar to the previously discussed compounds, two fluorophores illustrate the significant difference in AIE properties that could produce the presence or absence of a functional group like the cyano (Fig. 15). These two compounds present the same main structure. Both have methoxy groups and phenyl moieties, but the critical characteristics in this two molecules are that one fluorophore contains cyano groups, while the other one has hydrogen atoms instead. For ease, the top compound in Fig. 15 will be called as "C1" and the bottom one "C2".

The two compounds luminescent behavior was studied under the solution conditions using zinc phthalocyanine as standard [60]. These results show that the C1 molecules present very strong photoluminescence (PL), while the C2 has a quite poor PL. Moreover, the quantum yield for C1 is nearly twice as the C2's. Contrarily, under aggregation, the completely planar framework of C1 is counterproductive leaving the possibility to form π - π stacking that leads to an ACQ effect, while in C2 the substitution of the cyano groups in the phenylenevinylene skeleton induces a slight torsion in the molecule which is enough to suppress the parallel stacking between neighboring molecules, resulting in excellent photoluminescence under the solid state for C2 (Fig. 15c).

In addition, under the crystalline state the -CN and -NO₂ groups in the C2 compound are responsible for intermolecular interactions of the type C-H...N and C-H...O hydrogen bonds, which are in charge to form layers of co-planar molecules that have their aromatic and aliphatic parts alternated with a minor

slipping in direction of the principal axis in the crystalline system [61, 62].

Another example refers to four different AIEgen systems with highly emissive characteristics which were synthesized from TPA, a strong electron-donor group and the AIE-active α -cyanostilbene and their optical and photoluminescent properties were studied. These compounds vary between each other in two major ways: the presence or absence of dimethoxy and bromine groups in the TPA section of the molecule or the para-position of the α -cyanostilbene phenyl's ring, respectively, Fig. 16.

The optical properties of these compounds present different behaviors depending on whether they have or not the bromide and dimethoxy auxochromes. The compounds that present these auxochromes suffer a bathochromic shift not only on their maximum absorption peak but also on their maximum emission peak. The maximum bathochromic effect presented refers to the diOMe-TPA-CNBr compound followed by diOMe-TPA-CN, then TPA-CNBr and finally TPA-CN. This enhanced red-shift behavior is produced due to the introduction of bromide and dimethoxy groups that induce a stronger acceptor-donor character inside the molecule. In addition to the bathochromic shifts all the TPA-cyanostilbene derivatives present the AIE features, but those that present the dimethoxy group in their structure present a massive enhance of its emission in solid state compared to those compound without the dimethoxy groups. This occurs because of two main reasons: first, the stronger acceptor-donor effect which moves the maximum absorption and emission peaks to longer wavelengths, contributing to color tuning. Second, the crystalline structure in which each of the molecules crystallizes. It is known that the π - π stacking interactions occur between two molecular faces in which their π orbitals overlap. But, for this to happen it is necessary to have a minimum distance between the two faces that will overlap. Thus, in order to have a fluorescence quenching, it is necessary to have the two overlapping planes in a distance that is smaller than 3.5 Å. For molecules shown in Fig. 16, TPA-CN, diOMe-TPA-CN and diOMe-TPA-CNBr have a distance of 6.689, 4.941 and 4.096 Å, respectively, indicating that these three structures are incapable of suffering a π - π stacking interaction. Moreover, these molecules are capable of forming an aromatic hydrogen bond (C-H... π) that helps to restrict the intermolecular motions and brings out the

Author's personal copy

J Mater Sci

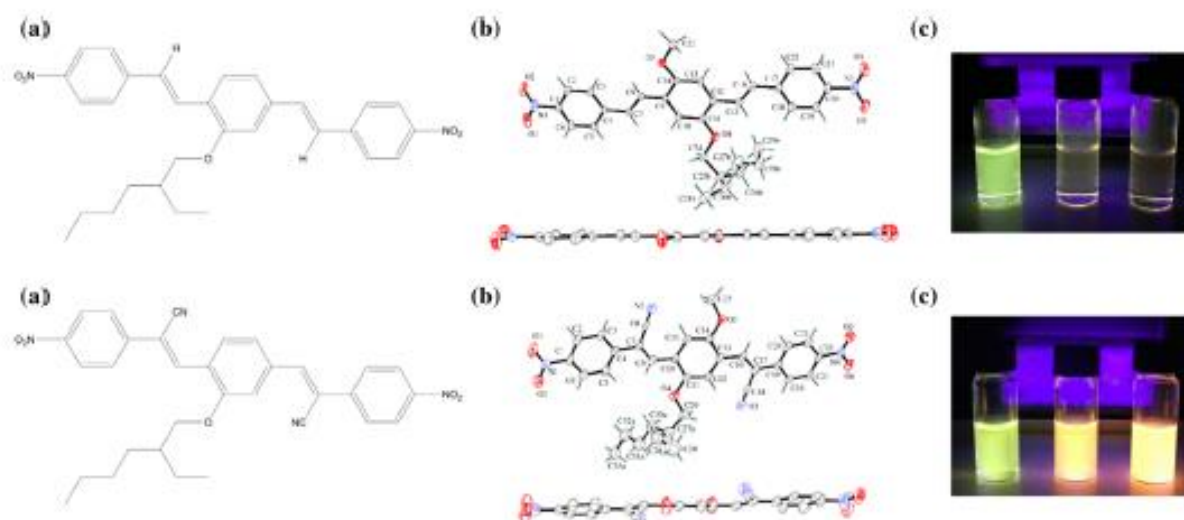


Figure 15 **a** Molecular structure of compounds C1(top) and C2(bottom). **b** molecular model with thermal ellipsoids drawn at 30% probability of C1(top) and C2(bottom). **c** Solution of C1(top) and C2(bottom) in dioxane (10^{-5} M); dioxane/water 50% and

dioxane/water 90% under 375 nm UV light. Reprinted (adapted) with permissions from Refs. [61, 62]. <http://creativecommons.org/licenses/by/4.0/> for CC BY.

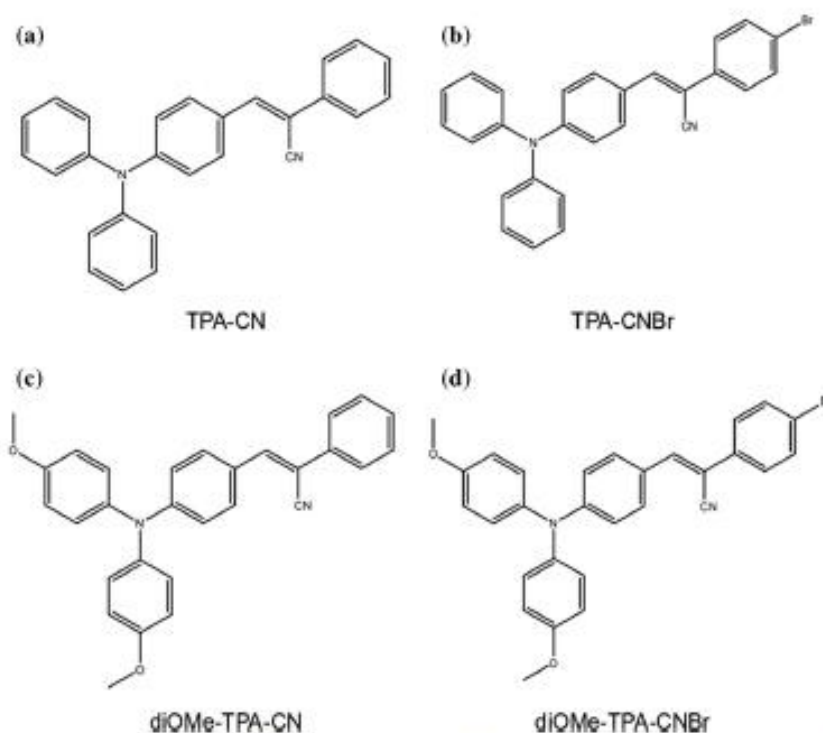


Figure 16 Molecular structures of 2-(phenyl)-3-[4-(N,N)diphenylamino)phenyl]acrylonitrile (TPA-CN), 2-(phenyl)-3-[4-bis(4-methoxyphenylamino)phenyl]acrylonitrile (diOMe-TPA-CN), 2-(4-bromophenyl)-

3-[4-(N,N)diphenylamino)phenyl]acrylonitrile (TPA-CNBr) and 2-(4-bromophenyl)-3-[4-bis(4-methoxyphenylamino)phenyl]acrylonitrile (diOMe-TPA-CNBr).

highest photoluminescent quantum yield at solid state [63].

As mentioned at the beginning of this section, the most used and studied cyanostilbenes are the α -cyanostilbenes due to its great possibilities in structural tunability, unlike the 4-cyanostilbene, which are quite restricted in this aspect. Besides that, there are several studies in 4-cyanostilbenes derivatives. An example of this type of molecules is the di-substituted TPE Fig. 17, one which has the cyano groups at opposite phenyl groups and the other one which has the cyano group at adjacent phenyl moieties. An interesting aspect of these two compounds relies on their ability to present different emission characteristics under their crystalline state [64].

In what refers to their PL behavior, the E and Z isomers can present some luminescence in a THF solution, which is quite rare in a molecule with AIE characteristics. In addition to this, when the fraction of water (f_w) is aggregated and constantly increased to the THF solutions of E and Z compounds, their emission intensity is not strictly increased. However, it fluctuates depending on the value of the f_w . For example, when the f_w is around the 30%, 50% and 60% the emission intensity drops drastically but, when the f_w is at 10%, 20%, 70% and enhancement in the emission intensities is observed. Those solutions with a f_w of 90–95% presented a tenfold emission intensity (Fig. 18) [64].

As expected, both the E and Z isomers present AIE characteristics due to their intermolecular interactions that activate the RIR mechanism, restricting the free rotation of the phenyl moieties and blocking the non-radiative pathways, but it also produces a red-

shift behavior as the E and Z molecules aggregate. This phenomenon is produced by the intermolecular interactions that play a significant role in the electron transition process between neighboring molecules and within the same molecule [65]. In addition to that, these relatively small molecules are capable of producing an AIE effect with red-shift, which is quite rare [66, 67]. On the other hand, the small molecules capable of producing an AIE with blue-shift are much more common and fairly more studied [68–71].

Diaminodicyanoquinodimethanes (DADQS)

One of the systems of interest due to its intrinsic characteristics is the DADQs. The first synthesized DADQs exhibit a strong emission enhancement when the system is in viscous matrices [72] crystals, nanocrystals or colloids [73] and amorphous nanoparticles [74, 75]. This enhancement is attributed to the inhibition of torsional motions when the molecule is in the excited state. The DADQs are molecules generally synthesized from the reaction between 7,7,8,8-tetracyanoquinodimethane (TCNQ) and different kind of amines. Such compounds are of great interest due to the ease by which structural changes can be made, allowing to design and modulate different characteristics in the DADQs, which give rise to possible applications for these compounds. Such applications include the use of these compound in electroluminescent devices [76], sensing applications, determination of environment effect [73, 77, 78], dyes in liquid crystal displays and non-linear optics [79–82].

Like CN-DPDSB, the DADQs fluorescence gets diminished when they are in solutions with a low viscosity coefficient; their photoluminescence quantum yields (PLQYs) generally range between 10^{-2} and 10^{-3} . Whereas the PLQY gets strongly increased when the solution has a high viscosity coefficient, the temperature is reduced, or the aggregation is induced, producing an increase in the fluorescence time from picoseconds to nanoseconds [72, 77].

An example of these molecules is shown below, Fig. 19, which contain certain unique properties [83]. The skeleton of these molecules is confirmed, by the already known, donor-acceptor (D-A) system, where a dicyanomethylene moiety forms the electron-accepting group and the electron-donating group will

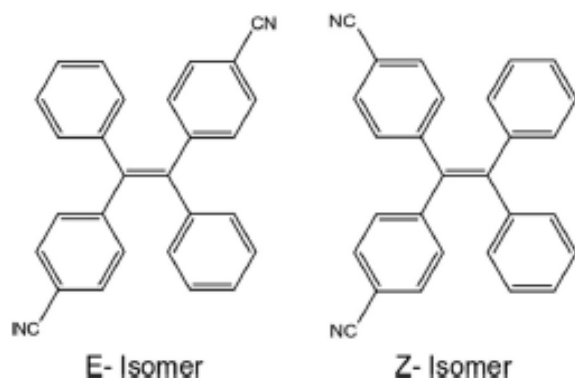


Figure 17 Molecular structure of (E)-4,4'-(1,2-diphenylethene-1,2-diyl)dibenzonitrile, E-1, and (Z)-4,4'-(1,2-diphenylethene-1,2-diyl)dibenzonitrile.

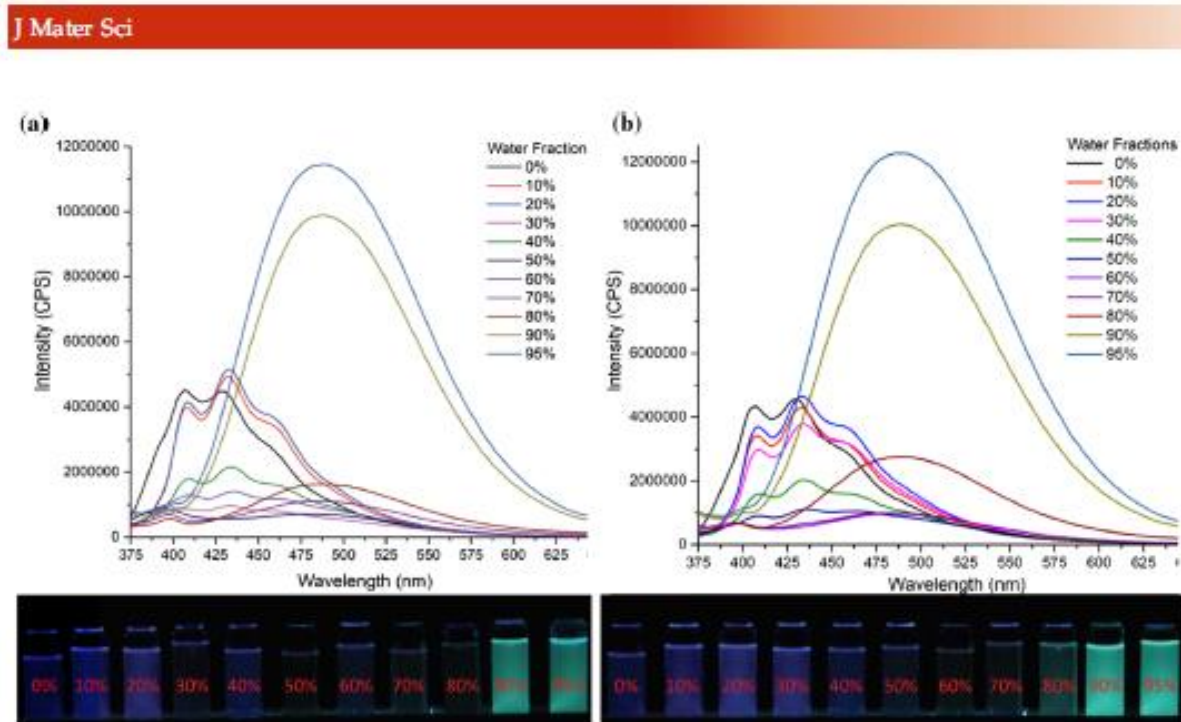


Figure 18 Absorption emission spectra and PL image of water/THF solution **a** corresponds to the E-isomer. **b** Corresponds to the Z-isomer. Reprinted (adapted) with permission from Ref. [64]. Copyright (2018) American Chemical Society.

be each of the amine derivatives located at the top of their respective molecule. In addition to that, the DADQs dipole moments are alterable independent on the excited state of the molecule. In the ground state, the dipole moment (μ_g) can arrive to values around 15–20 D, while in the excited state (μ_e) the value gets highly reduced to less than 0.5 D [72, 84, 85]. At the same time, the differences between the dipole moments of the excited and the ground

states produce a dependence on the DADQs maximum absorption position and the medium polarity, while the maximum of fluorescence position is considerably less dependent to the medium polarity. The small values of μ_e could explain this decrease in the dependence between the fluorescence and the medium polarity.

For DADQs (b) and (c), it has been experimentally determined that the ground-state geometries are not

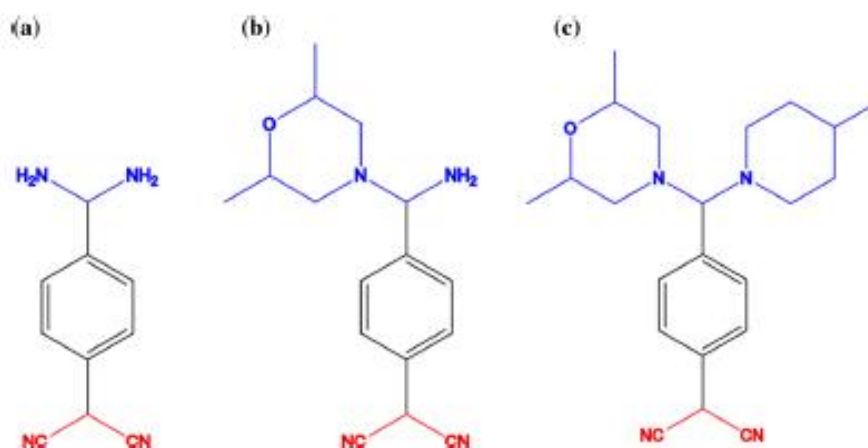


Figure 19 Diaminodicyanoquinodimethanes derivatives. In blue are marked the electron-donor groups and in red are the electron-acceptor groups for each molecule.

completely planar due to a twist in the bond that joins together the benzene and the electron-donating groups. In regard to the DADQ shown in Fig. 19a, it has not been possible to determine its geometry experimentally, but computational calculation implies that its geometry will have similar behavior to those already observed in (b) and (c) but with a dihedral angle slightly smaller. Also, electronic excitations in the ground-state geometries, of the three compounds, produced a partial planarization in the conformation of the molecules. This reduction in the dihedral angles is dependent on the medium viscosity and the hindrance produced by the electron-donor moieties [72, 83, 85]. As a result of this, the excited-state relaxation process is in competition between the radiative pathway and the non-radiative one. In which the most restricted are the intermolecular motions, the most favored the radiative pathway gets. Because of this, the radiative pathway gets reinforced when the medium viscosity increases and the temperature drops, producing enhance in the fluorescence intensity which means a greater PLQY and a slowdown in the fluorescence decay time.

In addition to that, several studies have shown that zwitterionic DADQ molecules, especially those with groups that are not conjugated with the central π -conjugation system of the DADQs (remote groups), present an optical second harmonic generation [79, 86–89]. Also, DADQs with these functionalities are much more likely to aggregate, especially those bearing amino groups as remote functionalities. The presence of these remote groups significantly influences the solubility of these molecules, increasing their solubility, both in water and in organic solvents, facilitating different processes such as doping of water-soluble polymers and enabling their application in other fields such as organic vapor sensing.

Several DADQs molecules with remote functionalities had been studied Fig. 20. As in the other cases, these molecules suffer a fluorescence decay or quenching when they are in solution, but they exhibit a fluorescence enhancement in their crystalline state and doped polymer films. Also, they present a high dipole moment of the ground state, which is congruent with the examples previously seen and with other similar reported molecules [72, 81, 84, 90].

The 8 compounds shown in Fig. 18 display an absorption spectrum for the acetonitrile solution, the polymer film and the solid state that are very similar in height, width and shape. This indicates that

molecular aggregation has little to no impact on the electronic absorption spectra of these compounds [16]. Moreover, it has been found that the emission of these compounds in low polar solvents is slightly stronger than the one produced in more polar solvents. In addition to that, these compounds are capable of producing an emission enhancement in the solid and polymer films that is much more significant than the one produced in the acetonitrile solution.

In the sake of finding further insight into the emission enhancement and the role of the remote functionalities of these molecules, a single-crystal x-ray analysis was performed for compounds (B) and (C) Fig. 20. The results showed that compounds (B) and (C) crystallize in a monoclinic system with space group $P2_1/n$ and orthorhombic with space group $Pbca$, respectively [91]. Furthermore, the dihedral angle between the electron-donor moieties and the benzenoid ring are quite significant, ranging between 50° and 53° . This reduction in planarity is of great importance to avoid the π - π stacking of neighboring molecules. But, it also facilitates non-covalent interactions between the carbon atoms of the remote functionalities and the nitrogen (N) atoms in the negative polarized dicyanomethylene moiety. These interactions, besides of their weakness, are plentiful enough to influence in the organization of the DADQ molecules and contribute to the emission enhancement [16]. Compound (E) [72] and derivatives of compound (D) and G [92] are capable of producing hydrogen bonds. All of these associations together possibly play a significant role in the restriction of the non-radiative relaxation pathway.

In summary, the cyano functionalities are widely used to expand the color palette that these luminogens could provide. This is done by integrating different electron-donating group like carbazoles, TPA or alkylamines with the cyano groups which work as an electron-accepting group and complete the D-A system within the molecule. The cyano group is also responsible for the generation of twisted conformations, which are favorable for the AIE effect [93]. Its steric properties produce a distortion in the neighboring moieties conformation, delaying the π - π stacking interactions that cause the ACQ effect seen in conventional systems. Furthermore, the twisted configuration is responsible for weakening the overall conjugation in the luminogenic molecule. This facilitates the intramolecular motions, by reducing

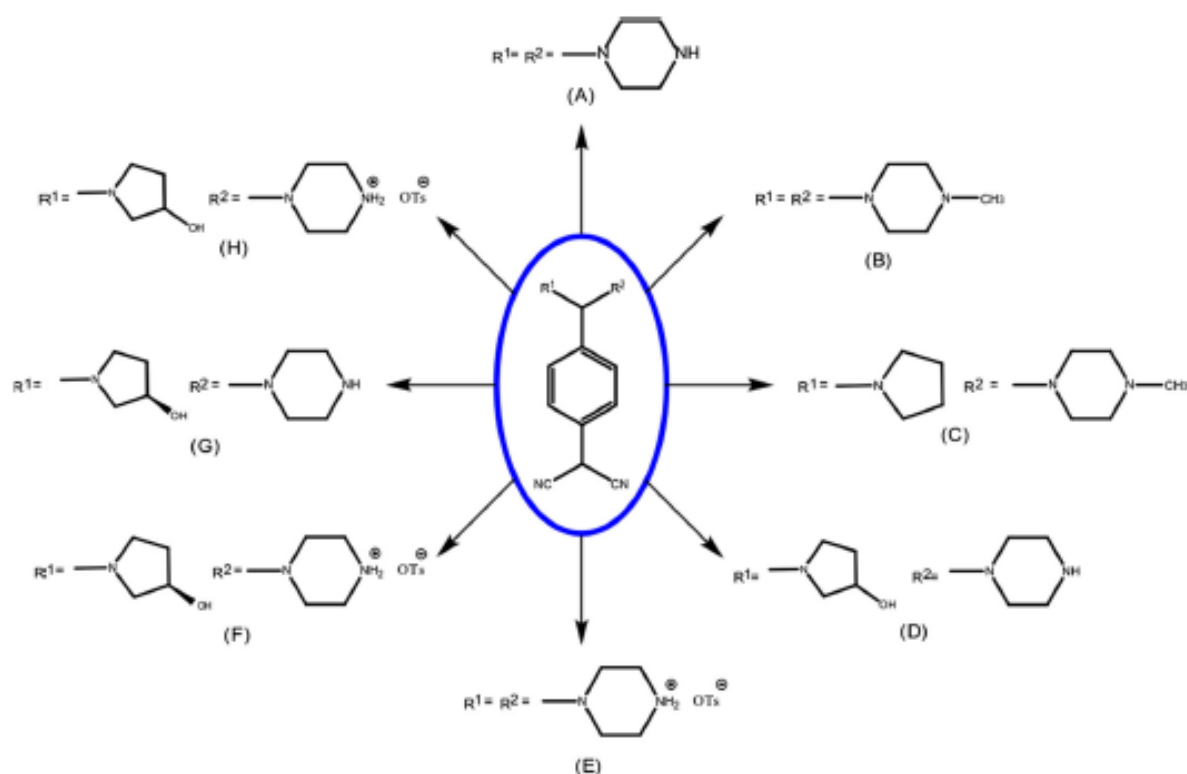


Figure 20 Possible substitutions with remote functionalities in TCNQ molecule.

their energy barriers, and therefore promotes decay of the excited state by non-radiative mechanisms.

Conclusions

The AIE phenomenon is the effect in which the light emission of a luminogen gets enhanced by the formation of aggregates. AIEgens are typically non-planar molecules with π -conjugated systems that are not luminescent as isolated or unconstrained species.

Cyano group is a great building block with unique properties capable of enhancing and red-shift the emissions of a typical hydrocarbon AIEgen. In addition to that, the electronic effect produced by the cyano group in the luminogen induces an electronic polarization produced by the intramolecular charge transfer (ICT) and considerably alter the behavior of the luminogen, especially the color. On the other hand, the steric effect of the cyano group produces a twisted conformation in the luminogen, which in a dilute solution increases the intermolecular rotation but, in the aggregated state, prevents the formation of

a planar structure avoiding the π - π stacking between molecules. Besides, the critical property of the cyano group is its capacity to form hydrogen bonds between the nitrogen atoms in the cyano groups and the hydrogen atoms of neighboring molecules. This interaction enhances the rigidity of the different AIEgen moieties in the aggregate stated and increases the radiative photophysical pathway substantially.

Finally, the AIE study is of significant academic value because it has provided a new platform to decipher the non-radiative processes that lead to the emission quenching in luminogens under solution and to understand the underlying mechanisms that bring about radiative decay in the aggregate state.

Funding

This study was funded by Yachay Tech internal Project "Aggregation-induced emission Effect in Diaminodicynoquinodimethanes derivatives".

Compliance with ethical standards

Conflict of interest The authors declare that they have no conflict of interest.

References

- [1] Mei J, Leung NLC, Kwok RTK, Lam JWY, Tang BZ (2015) Aggregation-induced emission: together we shine, united we soar! *Chem Rev* 115(21):11718–11940. <https://doi.org/10.1021/acs.chemrev.5b00263>
- [2] Hong Y, Lam JWY, Tang BZ (2011) Aggregation-induced emission. *Chem Soc Rev* 40(11):5361–5388. <https://doi.org/10.1039/C1CS15113D>
- [3] Birks JB (1970) *Photophysics of aromatic molecules*. Wiley, London
- [4] Pálsson LO, Wang C, Batsanov AS et al (2010) Efficient intramolecular charge transfer in oligoene-linked donor- π -acceptor molecules. *Chem A Eur J* 16(5):1470–1479. <http://doi.org/10.1002/chem.200902099>
- [5] Bagechi B, Fleming GR, Oxtoby DW (2003) Theory of electronic relaxation in solution in the absence of an activation barrier. *J Chem Phys* 118(12):7375–7385. <https://doi.org/10.1063/1.1444729>
- [6] Ben-Amotz D, Scott TW (1987) Microscopic frictional forces on molecular motion in liquids. Picosecond rotational diffusion in alkanes and alcohols. *J Chem Phys* 87(7):3739–3748. <https://doi.org/10.1063/1.452928>
- [7] Castner EW, Maroncelli M, Fleming GR (1987) Subpicosecond resolution studies of solvation dynamics in polar aprotic and alcohol solvents. *J Chem Phys* 86(3):1090–1097. <https://doi.org/10.1063/1.452249>
- [8] Kramers HA (1940) Brownian motion in a field of force and the diffusion model of chemical reactions. *Physica* 7(4):284–304
- [9] Sun YP, Sahljel J (1989) Application of the Kramers equation to stilbene photoisomerization in n-alkanes using translational diffusion coefficients to define microviscosity. *J Phys Chem* 93(26):8310–8316. <https://doi.org/10.1021/j100363a008>
- [10] Xu Q, Fleming GR (2001) Isomerization dynamics of 1, 1'-diethyl-4, 4'-cyanine (1144C) studied by different third-order nonlinear spectroscopic measurements. *J Phys Chem A* 105:10187–10195
- [11] Yoshihara T, Druzhinin SI, Zachariasse KA (2004) Fast intramolecular charge transfer with a planar rigidized electron donor/acceptor molecule. *J Am Chem Soc* 126:8535–8539
- [12] Mei J, Hong Y, Lam JWY, Qin A, Tang Y, Tang BZ (2014) Aggregation-induced emission: the whole is more brilliant than the parts. *Adv Mater* 26(31):5429–5479. <https://doi.org/10.1002/adma.201401356>
- [13] Luo J, Xie Z, Xie Z et al (2001) Aggregation-induced emission of 1-methyl-1,2,3,4,5-pentaphenylsilole. *Chem Commun* 18:1740–1741. <https://doi.org/10.1039/b105159h>
- [14] Wilson JN, Smith MD, Enkelmann V, Bunz UHF (2004) Cruciform π -systems: effect of aggregation on emission. *Chem Commun* 4(15):1700–1701. <https://doi.org/10.1039/b406495j>
- [15] Hong Y, Lam JWY, Tang BZ (2009) Aggregation-induced emission: phenomenon, mechanism and applications. *Chem Commun* 29:4332–4353. <https://doi.org/10.1039/b904665h>
- [16] Jayanty S, Radhakrishnan TP (2004) Enhanced fluorescence of remote functionalized diaminodicyanoquinodimethanes in the solid state and fluorescence switching in a doped polymer by solvent vapors. *Chem A Eur J* 10(3):791–797. <https://doi.org/10.1002/chem.200305123>
- [17] Davis R, Saleesh Kumar NS, Abraham S et al (2008) Molecular packing and solid-state fluorescence of alkoxy-cyano substituted diphenylbutadienes: structure of the luminescent aggregates. *J Phys Chem C* 112(6):2137–2146. <https://doi.org/10.1021/jp710352m>
- [18] Zhao Z, Lam JWY, Tang BZ (2012) Tetraphenylethene: a versatile AIE building block for the construction of efficient luminescent materials for organic light-emitting diodes. *J Mater Chem* 22(45):23726–23740. <https://doi.org/10.1039/c2jm31949g>
- [19] Turro NJ, Scaiano JC, Ramamurthy V (2010) *Modern molecular photochemistry of organic molecules*, 1st edn. University Science Books, Hemdon
- [20] Peng Q, Yi Y, Shuai Z, Shao J (2007) Supporting information for towards quantitative prediction of molecular fluorescence quantum efficiency: role of Duschinsky rotation. *Sci York* 129(30):1–10. <https://doi.org/10.1021/ja067946e>
- [21] He Z, Ke C, Tang BZ (2018) Journey of aggregation-induced emission research. *ACS Omega* 3(3):3267–3277. <https://doi.org/10.1021/acsomega.8b00062>
- [22] Chen J, Law CCW, Lam JWY et al (2003) Synthesis, light emission, nanoaggregation, and restricted intramolecular rotation of 1,1-substituted 2,3,4,5-tetraphenylsiloles. *Chem Mater* 15(7):1535–1546. <https://doi.org/10.1021/cm021715z>
- [23] Ren Y, Lam JWY, Dong Y, Tang BZ, Wong KS (2005) Enhanced emission efficiency and excited state lifetime due to restricted intramolecular motion in silole aggregates. *J Phys Chem B* 109(3):1135–1140. <https://doi.org/10.1021/jp046659z>
- [24] Leung NLC, Xie N, Yuan W et al (2014) Restriction of intramolecular motions: the general mechanism behind aggregation-induced emission. *Chem A Eur J* 20(47):15349–15353. <https://doi.org/10.1002/chem.201403811>
- [25] Zhao W, He Z, Lam JWY et al (2016) Rational molecular design for achieving persistent and efficient pure organic

- room-temperature phosphorescence. *Chemistry* 1(4): 592–602. <https://doi.org/10.1016/j.chempr.2016.08.010>
- [26] Marian CM (2012) Spin-orbit coupling and intersystem crossing in molecules. *Wiley Interdiscip Rev Comput Mol Sci* 2(2):187–203. <https://doi.org/10.1002/wcms.83>
- [27] Kwon MS, Yu Y, Coburn C et al (2015) Suppressing molecular motions for enhanced room-temperature phosphorescence of metal-free organic materials. *Nat Commun*. <https://doi.org/10.1038/ncomms9947>
- [28] Zhang J, Sclarman E, Yang L, Jiang J, Zhang G (2018) Aggregation-induced enhancement of molecular phosphorescence lifetime: a first-principle study. *J Phys Chem C*. <https://doi.org/10.1021/acs.jpcc.8b07087>
- [29] Shimizu M, Takeda Y, Higashi M, Hiyama T (2009) 1,4-Bis(alkenyl)-2,5-dipiperidinobenzenes: minimal fluorophores exhibiting highly efficient emission in the solid state. *Angew Chem Int Ed* 48(20):3653–3656. <https://doi.org/10.1002/anie.200900963>
- [30] Shimizu M, Tatsumi H, Mochida K, Shimono K, Hiyama T (2009) Synthesis, crystal structure, and photophysical properties of (1E,3E,5E)-1,3,4,6-tetraarylhexa-1,3,5-trienes: a new class of fluorophores exhibiting aggregation-induced emission. *Chem Asian J* 4(8):1289–1297. <https://doi.org/10.1002/asia.200900110>
- [31] Ning Z, Chen Z, Zhang Q et al (2007) Aggregation-induced emission (AIE)-active starburst triarylamine fluorophores as potential non-doped red emitters for organic light-emitting diodes and Cl₂ gas chemodosimeter. *Adv Funct Mater* 17(18):3799–3807. <https://doi.org/10.1002/adfm.200700649>
- [32] Nosova DA, Zarochevtseva EP, Vysotskaya SO, Klemesheva NA, Korotkov VI (2014) The influence of the crystal structure on aggregation-induced luminescence of derivatives of aminobenzoic acid. *Opt Spectrosc* 117(6):880–886. <https://doi.org/10.1134/s0030400x14120170>
- [33] Gouille V, Harriman A, Lehn JM (1993) An electro-photo-switch: redox switching of the luminescence of a bipyridine metal complex. *J Chem Soc Chem Commun* 12:1034–1036. <https://doi.org/10.1039/C39930001034>
- [34] Lin HT, Huang CL, Liou GS (2019) Design, synthesis, and electrochromism of new triphenylamine derivatives with AIE-active pendent groups. *ACS Appl Mater Interfaces* 11(12):11684–11690. <https://doi.org/10.1021/acsami.9b00659>
- [35] Yen HJ, Liou GS (2019) Design and preparation of triphenylamine-based polymeric materials towards emergent optoelectronic applications. *Prog Polym Sci* 89:250–287. <https://doi.org/10.1016/j.progpolymsci.2018.12.001>
- [36] Yeh HC, Wu WC, Wen YS, Dai DC, Wang JK, Chen CT (2004) Derivative of α , β -dicyanostilbene: convenient precursor for the synthesis of diphenylmaleimide compounds, E-Z isomerization, crystal structure, and solid-state fluorescence. *J Org Chem* 69(19):6455–6462. <https://doi.org/10.1021/jo049512c>
- [37] Toh KC, Stojkovic EA, van Stokkum IHM, Moffat K, Kennis JTM (2010) Proton-transfer and hydrogen-bond interactions determine fluorescence quantum yield and photochemical efficiency of bacteriophytochrome. *Proc Natl Acad Sci* 107(20): 9170–9175. <https://doi.org/10.1073/pnas.0911535107>
- [38] Petong P, Pottel R, Kaatz U (2002) Dielectric relaxation of H-bonded liquids. mixtures of ethanol and n-hexanol at different compositions and temperatures. *J Phys Chem A* 103(31):6114–6121. <https://doi.org/10.1021/jp9910461>
- [39] Mondal JA, Ghosh HN, Mukherjee T, Palit DK (2005) S₂ fluorescence and ultrafast relaxation dynamics of the S₂ and S₁ states of a ketocyanine dye. *J Phys Chem A* 109(31):6836–6846. <https://doi.org/10.1021/jp0508498>
- [40] Mondal JA, Samant V, Varne M et al (2009) The role of hydrogen-bonding interactions in the ultrafast relaxation dynamics of the excited states of 3- and 4-aminofluoren-9-ones. *ChemPhysChem* 10(17):2995–3012. <https://doi.org/10.1002/cphc.200900325>
- [41] Fayed TA, El-Morsi MA, El-Nahass MN (2011) Intramolecular charge transfer emission of a new ketocyanine dye: effects of hydrogen bonding and electrolyte. *J Photochem Photobiol A Chem* 224(1):38–45. <https://doi.org/10.1016/j.jphotochem.2011.09.004>
- [42] Benigno AJ, Ahmed E, Berg M (1996) The influence of solvent dynamics on the lifetime of solute-solvent hydrogen bonds. *J Chem Phys* 104(19):7382–7394. <https://doi.org/10.1063/1.471454>
- [43] Li Y, Li F, Zhang H et al (2007) Tight intermolecular packing through supramolecular interactions in crystals of cyano substituted oligo(para-phenylene vinylene): a key factor for aggregation-induced emission. *Chem Commun* 1(3):231–233. <https://doi.org/10.1039/b612732k>
- [44] Kurita M, Momma M, Mizuguchi K, Nakano H (2013) Fluorescence color change of aggregation-induced emission of 4-[bis(4-methylphenyl)amino]benzaldehyde. *ChemPhysChem* 14(17):3898–3901. <https://doi.org/10.1002/cphc.201300781>
- [45] Nie H, Liang Y, Han C, Zhang R, Zhang X, Yan H (2019) Rational design of cyanovinyl-pyrene dual-emission AIE-gens for potential application in dual-channel imaging and ratiometric sensing in living cells. *Dye Pigment* 168:42–48. <https://doi.org/10.1016/j.dyepig.2019.04.034>
- [46] Zhu L, Zhao Y (2013) Cyanostilbene-based intelligent organic optoelectronic materials. *J Mater Chem C* 1(6):1059–1065. <https://doi.org/10.1039/c2tc00593j>
- [47] Grabowski ZR, Rotkiewicz K, Rettig W (2003) Structural changes accompanying intramolecular electron transfer:

- focus on twisted intramolecular charge-transfer states and structures. *Chem Rev* 103(10):3899–4032. <https://doi.org/10.1021/cr940745l>
- [48] Kawamura Y, Sasabe H, Adachi C (2004) Simple accurate system for measuring absolute photoluminescence quantum efficiency in organic solid-state thin films. *Jpn J Appl Phys Part 1 Regul Pap Short Notes Rev Pap* 43(11A):7729–7730. <https://doi.org/10.1143/jjap.43.7729>
- [49] Sharafy S, Muszkat KA (1971) Viscosity dependence of fluorescence quantum yields. *J Am Chem Soc* 93(17):4119–4125. <https://doi.org/10.1021/ja00746a004>
- [50] Liu Y, Cao Y, Li X, Li Y, Wang B (2019) Cyano-functionalized diarylethene derivatives with aggregation-induced emission enhancement and piezofluorochromic behaviours. *Aust J Chem* 72(5):369–374. <https://doi.org/10.1071/CH18450>
- [51] Chen Z, Li Z, Hu F, Yu GA, Yin J, Liu SH (2016) Novel carbazole-based aggregation-induced emission-active gold(I) complexes with various mechanofluorochromic behaviors, vol 125. Elsevier, Amsterdam. <https://doi.org/10.1016/j.dyepig.2015.10.038>
- [52] Han T, Feng X, Chen D, Dong Y (2015) A diethylaminophenol functionalized Schiff base: crystallization-induced emission-enhancement, switchable fluorescence and application for security printing and data storage. *J Mater Chem C* 3(28):7446–7454. <https://doi.org/10.1039/c5tc00891c>
- [53] Sheng O, Jin C, Luo J et al (2018) Mg₂B₂O₅ nanowire enabled multifunctional solid-state electrolytes with high ionic conductivity, excellent mechanical properties, and flame-retardant performance. *Nano Lett*. <https://doi.org/10.1021/acs.nanolett.8b00659>
- [54] Zhang X, Ma Z, Yang Y, Zhang X, Jia X, Wei Y (2014) Fine-tuning the mechanofluorochromic properties of benzothiadiazole-cored cyano-substituted diphenylethene derivatives through D–A effect. *J Mater Chem C* 2(42):8932–8938. <https://doi.org/10.1039/c4tc01457j>
- [55] Luo X, Li J, Li C et al (2011) Reversible switching of the emission of diphenyldibenzofulvenes by thermal and mechanical stimuli. *Adv Mater* 23(29):3261–3265. <https://doi.org/10.1002/adma.201101059>
- [56] Shen XY, Wang YJ, Zhao E et al (2013) Effects of substitution with donor–acceptor groups on the properties of tetraphenylethene trimer: aggregation-induced emission, solvatochromism, and mechanochromism. *J Phys Chem C* 117(14):7334–7347. <https://doi.org/10.1021/jp311360p>
- [57] Cao YQ, Xi Y, Teng XY, Li Y, Yan X, Chen L (2017) Alkoxy substituted D-π-A dimethyl-4-pyrone derivatives: aggregation induced emission enhancement, mechanochromic and solvatochromic properties. *Dye Pigment* 137:75–83. <https://doi.org/10.1016/j.dyepig.2016.09.063>
- [58] Liu Y, Lei Y, Li F et al (2016) Indene-1,3-dione-methylene-4H-pyran derivatives containing alkoxy chains of various lengths: aggregation-induced emission enhancement, mechanofluorochromic properties and solvent-induced emission changes. *J Mater Chem C* 4(14):2862–2870. <http://doi.org/10.1039/c5tc02932e>
- [59] Teng XY, Wu XC, Cao YQ et al (2017) Piezochromic luminescence and aggregation induced emission of 9,10-bis[2-(2-alkoxynaphthalen-1-yl)viny]anthracene derivatives. *Chin Chem Lett* 28(7):1485–1491. <https://doi.org/10.1016/j.ccllet.2017.02.018>
- [60] Vincett PS, Voigt EM, Rieckhoff KE (1971) Phosphorescence and fluorescence of phthalocyanines. *J Chem Phys* 55(8):4131–4140. <https://doi.org/10.1063/1.1676714>
- [61] Caruso U, Panunzi B, Diana R et al (2018) Supplementary materials AIE/ACQ effects in two DR/NIR emitters: a structural and DFT comparative analysis. *Molecules* 23:2–6
- [62] Caruso U, Panunzi B, Diana R et al (2018) AIE/ACQ effects in two DR/NIR emitters: a structural and DFT comparative analysis. *Molecules* 23(8):1947. <https://doi.org/10.3390/molecules23081947>
- [63] Chen SY, Chiu YW, Liou GS (2019) Substituent effects of AIE-active α-cyanostilbene-containing triphenylamine derivatives on electrofluorochromic behavior. *Nanoscale* 11(17):8597–8603. <https://doi.org/10.1039/c9nr02692d>
- [64] Hurlock MJ, Kan Y, LeCrivain T, Lapka J, Nash KL, Zhang Q (2018) Molecular association-induced emission shifts for E/Z isomers and selective sensing of nitroaromatic explosives. *Cryst Growth Des* 18(10):6197–6203. <https://doi.org/10.1021/acs.cgd.8b01065>
- [65] Li Q, Li Z (2017) The strong light-emission materials in the aggregated state: what happens from a single molecule to the collective group. *Adv Sci* 4(7):1–15. <https://doi.org/10.1002/advs.201600484>
- [66] Xie Y, Tu J, Zhang T et al (2017) Mechanoluminescence from pure hydrocarbon AIEgen. *Chem Commun* 53(82):11330–11333. <https://doi.org/10.1039/c7cc04663d>
- [67] Li Y, Lin H, Luo C et al (2017) Aggregation induced red shift emission of phosphorus doped carbon dots. *RSC Adv* 7(51):32225–32228. <https://doi.org/10.1039/c7ra04781a>
- [68] Zhang Q, Su J, Feng D, Wei Z, Zou X, Zhou H (2015) Piezofluorochromic metal-organic framework: a micro-scissor lift. *J Am Chem Soc* 137:2–7
- [69] Wei Z, Gu Z, Arvapally RK et al (2014) Rigidifying fluorescent linkers by MOF formation for fluorescence blue shift and quantum yield enhancement. *J Am Ceram Soc* 136:8269–8276

J Mater Sci

- [70] Shustova NB, McCarthy BD, Dincă M (2011) Turn-on fluorescence in tetraphenylethylene-based metal-organic frameworks: an alternative to aggregation-induced emission. *J Am Chem Soc* 133(50):20126–20129. <https://doi.org/10.1021/ja209327q>
- [71] Yang X, Lu R, Zhou H et al (2009) Aggregation-induced blue shift of fluorescence emission due to suppression of TICT in a phenothiazine-based organogel. *J Colloid Interface Sci* 339(2):527–532. <https://doi.org/10.1016/j.jcis.2009.07.033>
- [72] Bloor D, Kagawa Y, Szablewski M et al (2001) Matrix dependence of light emission from TCNQ adducts. *J Mater Chem* 11(12):3053–3062. <https://doi.org/10.1039/b104992p>
- [73] Chandaluri CG, Patra A, Radhakrishnan TP (2010) Polyelectrolyte-assisted formation of molecular nanoparticles exhibiting strongly enhanced fluorescence. *Chem A Eur J* 16(29):8699–8706. <https://doi.org/10.1002/chem.201000502>
- [74] Patra A, Chandaluri CG, Radhakrishnan TP (2012) Optical materials based on molecular nanoparticles. *Nanoscale* 4(2):343–359. <https://doi.org/10.1039/c1nr11313e>
- [75] Srujana P, Radhakrishnan TP (2015) Extensively reversible thermal transformations of a bistable, fluorescence-switchable molecular solid: entry into functional molecular phase-change materials. *Angew Chem Int Ed* 54(25):7270–7274. <https://doi.org/10.1002/anie.201501032>
- [76] Kagawa Y, Takada N, Matsuda H et al (2016) Photo- and electroluminescence for TCNQ-amino adducts. *Mol Cryst Liq Cryst Sci Technol Sect A* 2000(349):499–502. <https://doi.org/10.1080/10587250008024971>
- [77] Pålsson LO, Vaughan HL, Smith A et al (2006) Guest-host interactions between dichroic dyes and anisotropic hosts. *J Lumin* 117(1):113–122. <https://doi.org/10.1016/j.jlumin.2005.03.017>
- [78] Chandaluri CG, Radhakrishnan TP (2012) Amorphous-to-crystalline transformation with fluorescence enhancement and switching of molecular nanoparticles fixed in a polymer thin film. *Angew Chem Int Ed* 51(47):11849–11852. <https://doi.org/10.1002/anie.201205081>
- [79] Jayanty S, Gangopadhyay P, Radhakrishnan TP (2002) Steering molecular dipoles from centrosymmetric to a non-centrosymmetric and SHG active assembly using remote functionality and complexation. *J Mater Chem* 12(9):2792–2797. <https://doi.org/10.1039/b202804m>
- [80] Patra A, Hebalkar N, Sreedhar B, Radhakrishnan TP (2007) Formation and growth of molecular nanocrystals probed by their optical properties. *J Phys Chem C* 111(44):16184–16191. <https://doi.org/10.1021/jp075103j>
- [81] Cole JM, Copley RC, McIntyre GJ, Howard JA, Szablewski M, Cross GH (2002) Charge-density study of the nonlinear optical precursor DED-TCNQ at 20 K. *Phys Rev B Condens Matter Mater Phys* 65(12):1251071–1251071. <https://doi.org/10.1103/PhysRevB.65.125107>
- [82] Chandaluri CG, Radhakrishnan TP (2013) Hierarchical assembly of a molecular material through the amorphous phase and the evolution of its fluorescence emission. *J Mater Chem C* 1(29):4464–4471. <https://doi.org/10.1039/c3tc30615a>
- [83] Szablewski M, Fox MA, Dias FB et al (2014) Ultrafast dynamics and computational studies on diaminodicyanoquinodimethanes (DADQs). *J Phys Chem B* 118(24):6815–6828. <https://doi.org/10.1021/jp411358d>
- [84] Szablewski M, Bloor D, Kagawa Y et al (2006) Matrix dependence of blue light emission from a novel NH₂-functionalized dicyanoquinodimethane derivative. *J Phys Org Chem* 19(3):206–213. <https://doi.org/10.1002/poc.1020>
- [85] Cross GH, Hackman NA, Thomas PR, Szablewski M, Pålsson LO, Bloor D (2003) Local field and aggregation dependence of the micro- and macroscopic optical non-linearity of zwitterionic molecules. *Opt Mater Amst* 21(1–3):29–37. [https://doi.org/10.1016/S0925-3467\(02\)00108-8](https://doi.org/10.1016/S0925-3467(02)00108-8)
- [86] Ravi M (1998) A simple method for the estimation of hyperpolarisabilities: application to diamino substituted dicyanoquinodimethane molecules. *Proc Indian Acad Sci (Chem Sci)* 110(2):133–141. <https://doi.org/10.1007/BF02871150>
- [87] Jayanty S, Radhakrishnan TP (2001) Solid-state charge transfer promoted by an anchoring agent: a two-component analogue of Kofler's ternary complex. *Chem Mater* 13(6):2072–2077. <https://doi.org/10.1021/cm000884i>
- [88] Jayanty S, Radhakrishnan TP (2001) Modeling molecule-in-a-crystal: the case of push-pull quinonoids structural modifications that molecules undergo when they assemble into the crystalline state are important indicators of the microenvironment in the molecular crystal. *Accurate Appra* 12:2460–2462
- [89] Ravi M, Szablewski M, Hackman NA et al (1999) Crystal structures of amino substituted dicyanoquinodimethanes with potential nonlinear optical applications. *New J Chem* 23(8):841–844. <https://doi.org/10.1039/a903793d>
- [90] Srinivasa Gopalan R, Kulkarni GU, Ravi M, Rao CNR (2001) A charge density study of an intramolecular charge-transfer quinoid compound with strong NLO properties. *New J Chem* 25(9):1108–1110. <https://doi.org/10.1039/b103117c>
- [91] Jayanty S (2004) Enhanced fluorescence of remote functionalized diaminodicyanoquinodimethanes in the solid state and fluorescence switching in a doped polymer by solvent vapors. *Chem A Eur J Wiley Online Libr*. <https://doi.org/10.1002/chem.200305123/full>
- [92] Ravi M, Gangopadhyay P, Rao DN, Cohen S, Agrawal I, Radhakrishnan TP (1998) Dual influence of H-bonding on the solid-state second-harmonic generation of a chiral



Author's personal copy

J Mater Sci

quinonoid compound. Chem Mater 10(9):2371–2377. <https://doi.org/10.1021/cm9800128>

- [93] Srujana P, Gera T, Radhakrishnan TP (2016) Fluorescence enhancement in crystals tuned by a molecular torsion angle: a model to analyze structural impact. J Mater Chem C 4(27):6510–6515. <https://doi.org/10.1039/c6tc01610c>

Publisher's Note Springer Nature remains neutral with regard to jurisdictional claims in published maps and institutional affiliations.



Chapter 2.

Methodology

2.1. General information

2.1.1. Reagents

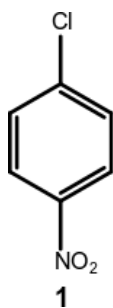
All reagents were purchased from commercial sources and used without further purification. Acetonitrile was purchased from Scharlau with an HPLC purity grade, 2-chloronitrobenzene, pyrrolidine and ethylenediamine were purchased from Sigma Aldrich with a 99% purity, chlorobenzene, Sulfuric acid were purchased from J.T.Baker with a 97.99% purity, nitric acid was purchased from Emsure at 65% purity, TCNQ, dichloromethane, sodium sulfate. TLC silica gel 60 plates by Merck KGaA were used for thin-layer chromatography. Silica 60 0.04-0.063 mm by Marcherey-Nagel were used for Column chromatography.

2.1.2. Equipment

UPLC-MS spectrometry was performed on a Waters instrument comprising a binary system manager (ACQUITY UPLC® I-Class) with a reversed-phase column SunFire™ C18 3.5 μm (2.1 \times 100 mm) and an automatic injector and Waters® SYNAPT® G2-S/Si as mass spectrometer. Linear gradients of MeCN (0.01% formic acid) into H₂O (0.01% formic acid) were run at flow rate of 0.3 mL/min. The solvents for UPLC were H₂O (Type I), and MeCN (HPLC quality) with a gradient 5 to 95% MeCN to H₂O. IR spectrometry was performed on a mid-infrared spectrometer (Agilent FTIR, Cary 630) equipped with a single reflection, diamond attenuated total reflectance (ATR), working in a wavelength range of 5100-600 cm^{-1} . With a 25 mm interferometer permanently working Michelson 45°. UV-Vis spectrometry was performed on a double beam, double monochromator ratio recording UV/Vis/NIR, (PerkinElmer Lambda 1050). Equipped with Tungsten-halogen and deuterium lamps operating from 175-3300 nm with a detector photomultiplier R6872 for high energy in the UV/Vis wavelength range, controlled by PerkinElmer WinLab software. The fluorescence spectrums were measured with a miniature Fiber Optic Spectrometer, 2-MHz analog-to-digital (A/D) converter, 2048-element CCD-array detector, resolution to 0.1 nm (FWHM), (USB2000+, Ocean Optics), connected to a PC via USB 2.0 port controlled by OceanView software. The source used for excitation was a Fabry-Perot laser diode class 3R, 405 nm, bandwidth 1 nm, output power 4.0 mW, vertically polarized and multi-longitudinal mode, collimating lens (Thorlabs, model LDM405). Thermo-scientific Nanodrop UV-Vis spectrophotometer.

2.2. Chemical section – Synthesis

2.2.1. Synthesis of 1-chloro-4-nitrobenzene (1)

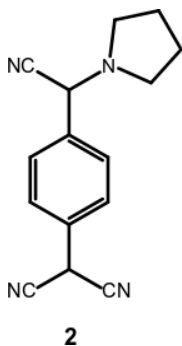


Procedure reported in Ref.¹⁴ was followed with minor modifications. Chlorobenzene (112 g, 1 mol, 1.45 eq) is added to a round-bottom flask and heated on a water bath to 40°C. With a vigorous stirring a mixture of sulfuric acid (60 g, 32.6 ml, 0.95 mol, 1.38 eq) and nitric acid (68 g, 45 ml, 0.69 mol, 1 eq) is added dropwise to the chlorobenzene. Addition of the acid requires around 10 minutes, controlling that the temperature is between 40 – 50 °C.

Stirring is continued for two hours while the temperature is slowly reduced. Then, the mixture gets cooled in an ice-bath, occasionally stirred with a glass rod until the product precipitate. After standing in the ice-bath for some time, precipitate is filtered off and washed with cold water, to yield p-chloronitrobenzene (1). The precipitate has an appearance of light yellow flakes (80 g, yield of 50.77 %).

Mp: 79.9-81 °C (Lit.¹⁵ 80-83 °C)

2.2.2. Synthesis of 7-pyrrolidino-7,8,8-tricyanoquinodimethane (2)



Procedure reported in ref.¹⁶ was followed with minor modifications. Pyrrolidine (69.7 mg, 81µl, 0.98 mmol; 0.8 eq) was added at once to a warm solution (50 °C) of 7,7,8,8-tetracyanoquinodimethane (TCNQ) (251 mg, 1.22 mmol, 1 eq) in 20ml of acetonitrile. Initially the TCNQ solution presents a green color which, after the addition of pyrrolidine, changes to a dark green for a split second and rapidly turned dark purple. The solution was stirred at 60 °C for 4.5 hours. After this, the solution was cooled to

room temperature and then stored in the fridge for three days to allow the crystallization of the product. Finally, the mixture is filtered out to obtain fine purple crystalline needles, which are washed with cool acetonitrile (3x5 ml) and dried over a day under reduced pressure to obtain 2 (199.3 mg, yield of 80.36 %).

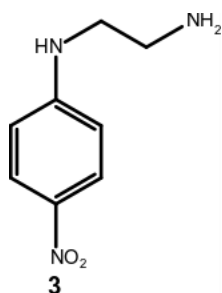
Mp: decompose at 190 °C

FT-IR (ATR) $\tilde{\nu}$ (cm⁻¹): 2192.44(w), 2163.23(w)

UV/Vis (ACN) λ_{max} (nm): 559

ESI-MS (m/z): calculated for C₁₅N₄H₁₂ = 248.3255, found: 249.0986 corresponding to [M-H]⁻

2.2.3. Synthesis of N-(4-nitrophenyl)ethylenediamine (3)

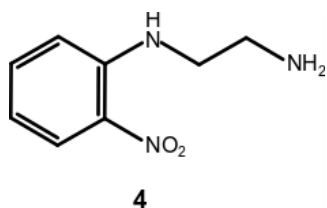


Procedure reported in Ref ¹⁷ was followed with some modifications. Previously synthesized 1-chloro-4-nitrobenzene (1) (0.79 g, 5 mmol, 1 eq) was dissolved in a round bottom flask with ethylenediamine (1.5 g, 1.67 ml, 25 mmol, 5 eq). Then, the reaction temperature was raised to 110 – 120 °C keeping a vigorous stirring for six hours. After that, the mixture cooled at room temperature, and the evaporated under reduced pressure. The crude is dissolved in the minimum amount of ethanol and purified by chromatographic column, using methanol as mobile phase. All fractions were analyzed by TLC and the matching phases were collected and concentrated under reduced pressure to obtain (3) as light orange crystals (0.404 g, yield of 44.64 %)

Mp: 144-145 °C (Lit.¹⁸ 148-150 °C)

UV/Vis (ACN) λ_{max} (nm): 382

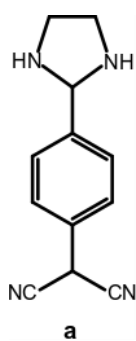
2.2.4. Synthesis of N-(2-nitrophenyl)ethylenediamine (4)



Procedure reported in Ref ¹⁹ was followed with some modifications. Commercial 1-chloro-2-nitrobenzene (1.58g, 10mmol, 1eq) was dissolved in a round bottom flask with ethylenediamine (2.97 g, 3.3 ml, 50 mmol, 5 eq). Then, the reaction temperature was raised to 110 – 120 °C keeping vigorous stirring for five hours. Later, the mixture was cooled to room temperature, and then evaporated under reduced pressure. The crude was re-dissolved in DCM and dried with Na₂SO₄. Finally, the product was filter and concentrated under reduced pressure to obtain (4) as light orange crystals (1.52 g, yield of 83.97 %).

Mp: 256-258 °C (Lit.¹⁹ 260-261 °C)

2.2.5. Synthesis of 2-(4-(imidazolidin-2-yl)phenyl)malononitrile (a)



Procedure reported in Ref ¹⁶ was followed with minor modifications. Ethylenediamine (26.6 mg, 0.44 mmol, 1 eq) was added to a previously warmed solution (at 40 °C) of PTCNQ (110 mg, 0.44 mmol, 1 eq) in acetonitrile (10 ml). The solution changed rapidly from deep purple to an intense green and within the next minutes it changed to yellow. Then, the temperature was raised to 70 °C and the reaction was stirred over the next four hours. The mixture was cooled slowly at room temperature for three hours and let it rest overnight in the fridge to allow the product crystallization. Finally, the mixture was filtered off and washed with cool acetonitrile (3x5 ml) to yield a fine grain yellow powder (66.3 mg, yield of 71.75 %).

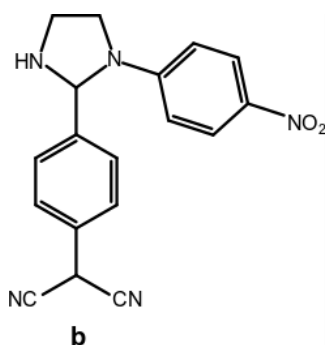
Mp: Decompose at 317 °C (Lit.²⁰ Irreversibly decompose at 280 °C)

FT-IR (ATR) $\tilde{\nu}$ (cm⁻¹): 3178.23(m), 2183.97(m), 2144.11(s), 1578.25(vs), 1503.04(vs), 1325.32(vs)

UV/Vis (ACN) λ_{\max} nm: 408

ESI-MS (m/z): calculated for C₁₂N₄H₁₀ = 210.2332, found: 210.1280 corresponding to [M+H]⁺

2.2.6. Synthesis of 2-(4-(1-(4-nitrophenyl)imidazolidin-2-yl)phenyl)malononitrile (b)



Procedure reported in Ref ¹⁶ was employed as an analogous method for the synthesis of 2-(4-(1-(4-nitrophenyl)imidazolidin-2-yl)phenyl)malononitrile (**b**). Compound (**3**) (0.3 mg, 1.66 mmol, 1 eq) was dissolved in 10 ml of acetonitrile and added to warm solution (at 50 °C) of PTCNQ (**2**) (0.411 g, 1.66 mmol, 1 eq) in 10 ml of acetonitrile. The solution was heated and stirred to reflux for seven hours and then it was allowed to cool down at room temperature and immediately after it was stored in fridge for one day to allow the product crystallization. The obtained precipitate was filtered in vacuum and washed with cool acetonitrile (3x3 ml). Finally, the obtained solid is recrystallized in acetonitrile to get product (**b**) as yellow needles (0.286 g, yield of 52.15 %).

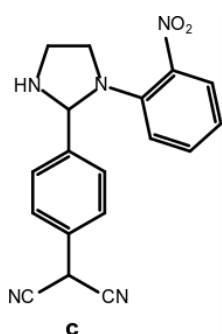
Mp: 161.9 – 163.7 °C

FT-IR (ATR) $\tilde{\nu}$ (cm⁻¹): 3282.74(m), 2175.03(m), 2123.65(s), 1593.89(vs), 1547.23(m), 1448.98(m), 1305.40(vs)

UV/Vis (ACN) λ_{max} (nm): 371

ESI-MS (m/z): calculated for C₁₈O₂N₅H₁₂ = 331.3255, found: 331.1743 corresponding to [M+H]⁺

2.2.7. Synthesis of 2-(4-(1-(2-nitrophenyl)imidazolidin-2-yl)phenyl)malononitrile (c)



Procedure reported in Ref ¹⁶ was employed as an analogous method for the synthesis of 2-(4-(1-(2-nitrophenyl)imidazolidin-2-yl)phenyl)malononitrile (**c**). PTCNQ (**2**) (101.3 mg, 0.4 mmol, 1 eq) was dissolved in 10 ml of acetonitrile at 40 °C. Then, compound (**4**) (73.84 mg, 0.4 mmol, 1 eq) was added to solution. The reaction was heated at 60 °C and let it stir over four days. The reaction was followed by thin layer chromatography, which showed that after four days the reaction does not go further.

2.3. AIE studies

2.3.1. Quantum yield (QY) measurements

Quantum yield measurements (QY) were performed using the comparative method of Williams *et al.*,²¹ which involves the use of characterized standard samples with previously known QY values. With this approach, it can be assumed that standard and test sample solutions with absorbance at similar wavelengths will be absorbing the same number of photons. Therefore, a ratio between the integrated fluorescence intensities of the two solutions (recorded under identical conditions) will yield the ratio of the quantum yield values. Since QY is known for the standard sample, the QY for the test sample can be easily calculated.²²

Hence, for this approach **a** was used as the standard sample and **b** as the test sample. Both were diluted in DMSO at a concentration of 200 µg/ml and placed in scrupulously clean 1cm fluorescence cuvettes. The emission spectra of both, reference and sample were recorded in full and corrected for the blank (solvent only) to perform proper emission intensity integration. The configuration used for data collection was a 180° excitation-fluorescence detection geometry, with a slight deflection of the optical fiber from the

excitation source to avoid any interference signal from the source. Additionally, a careful description of the fluorescence spectrum must be done by the selection of a mathematical function that adequately describes the profile of the spectrum. Due to the considerable asymmetry exhibited by Fluorescence spectra, Log-Normal profiles are most often used.²³ Also, the absorption (optical density) of both samples were recorded under the same conditions as the emission spectrum. Finally, the relative quantum yield (QY) of the sample in the solvent used (DMSO) was calculated according to in equation (1)

$$\Phi_x = \Phi_{st} \frac{Int_x \left(\frac{1-10^{A_{st}}}{1-10^{A_x}} \right) \frac{n_x^2}{n_{st}^2}}{Int_{st}} \quad (1)$$

Where, Φ refers to the quantum yield, Int is the area under the emission peak, A states for the absorbance at the excitation wavelength and n is the refractive index of the used solvent. The subscripts st and x denotes the values of the standard and test samples, respectively.

2.3.2. Theoretical approach

Quantum chemical calculations has been conducted in DADQ derivatives to obtain a further insight into the possible reasons of fluorescence enhancement produced in this molecules. All geometry optimizations were initially optimized using a force field approach with Avogadro and later with the program package Gaussian 16 (revision A.03). The ground and excited state optimizations were carried out at the Cam-B3LYP/def2TZVP level of Density Functional Theory (DFT), adding GD3BJ as the dispersion correction factor.²⁰ In addition, the Polarizable Continuum Model (PCM) using the integral equation formalism variant (IEFPCM) as the SCRF with acetonitrile (ACN) was used as implicit solvent model. The structure optimizations were ensured to be at its minimum through frequency calculation in each structure.

2.4. Antibacterial Activity

2.4.1. Preparation of inoculums

2.4.1.1. Culture media

Prepared by a mixture of Luria-Bertani LB broth base (7.5 g) with agar-agar (10 g), place in a clean 1-liter flask, and add 500ml of distilled water. Note that containers used for media must have vented tops and should be capable of holding 20 % more than the intended volume of medium, to allow for expansion during sterilization. Swirl the flaks to mix the powder mixture into the water as homogenously as possible. Cover the flask

with aluminum foil and put it in the autoclave, set the equipment at 1atm and 120 °C for 30 minutes. Once the sterilization finishes, take the flask out and let it cool down for 40 to 60 minutes.

Set the needed petri dishes in a laminar flow hood and pour the culture media inside the petri dishes until the whole area of the plate is completely covered. Allow the plates to cool and the agar to completely solidifies.

2.4.1.2. *Bacteria strains*

Escherichia coli (DH5-alpha) was chosen for antibacterial activity evaluation. The bacterial stock cultures were incubated for 24 hours at 37 °C on Luria Bertani (LB) broth base, following by refrigeration storage at 4 °C.

2.4.2. Antibacterial tests

Two techniques were used to test the antibacterial activity of synthesized DADQs (**a**, **b**, **2** and **3**). The agar diffusion technique and optical density (OD) measurements were applied in order to study of antibiotic efficacy of the synthesized molecules.

2.4.2.1. *Agar diffusion*

Different dilutions of the selected compounds (**a**, **b**, **2** and **3**) were prepared at different concentrations (1mg/ml; 0,1mg/ml and 0,01mg/ml) each one, using 5:5 water/DMSO system as solvent. Once the solutions are prepared, firstly it is necessary to inoculate the agar plates containing the appropriate medium with the bacteria strains. Then, three μ l of each solution were added onto the agar plates and incubated at 37 °C for 24 hours. After that, the inhibition zones were observed under uv-light. Ampicillin (100 μ g/ml), Kanamycin sulfate (100 μ g/ml) and the solvent system (5:5 water/DMSO) were used as positive controls.

2.4.2.2. *Optical density measurements (OD)*

Optical density measurements were performed on a Thermo-scientific Nanodrop UV-Vis spectrophotometer. Absorbance measurements were taken every 30 minutes at 600 nm wavelength and room temperature. Six different test tubes were prepared with 2.5 ml of Luria Bertani (LB) broth base and 135 μ L of *E. coli* (DH5-alpha) strains to obtain an initial OD₆₀₀ of 0,02. For tube 1 nothing else was added, while for tube 2 it was additionally added 100 μ L of the solvent system (5:5; water/DMSO). For tubes 3, 4, and 5 it was added 100 μ L of 1mg/ml solutions of compounds **2**, **a** and **b** respectively. In addition, another test tube was prepared for **3** under the same conditions but with a



variation on the solvent system. In this case just water was used; due to, the high hydrophilicity of this compounds unlike compounds **(3)**, **(a)** and **(b)** which needed to be previously diluted in DMSO. All test tubes were kept in a shaker incubator at 37 °C for the entire measurement period.



Chapter 3

Results and Discussion

Diaminodicyanoquinodimethanes derivatives (DADQs) have proven over the years strong emission enhancement as crystals,^{24,25} colloids,⁴ thin layer films or even in viscous matrices.²⁶ Furthermore, since 1962 a prototype molecule having an imidazolidine group named 2-(4-(imidazolidin-2-yl)phenyl)malonitrile (Figure 1, Structure a),²⁷ has been used for different studies on linear optics^{28–30} and solar cell application.^{31,32} Despite of this, 2-(4-(imidazolidin-2-yl)phenyl)malonitrile (**a**) had never been isolated or characterized structurally until 2016, when Srujana²⁰ reported a synthetic approach which required the use of a sacrificial pyrrolidine. 2-(4-(imidazolidin-2-yl)phenyl)malononitrile (**a**) with a rigid and compact imidazolidine could be the ideal scaffold to perform structural modifications through substitutions on the nitrogen atoms, with potential impact on the emission enhancement in the solid state. Also it could serve as a model to subsequent develop of more complex systems.

In the present work, we report the synthesis and structural characterization of 2-(4-(imidazolidin-2-yl)phenyl)malonitrile (**a**) and two N-alkylated derivatives **b** and **c** (**Figure 1**). In addition, the systematic variations of the emission enhancement and different biological tests was also studied. Finally, structural and computational analysis were used to explain the obtained results, and provide a general approach to conceptualize the impact of intra- and inter- molecular interactions on the AIE phenomena of organic fluorophores.

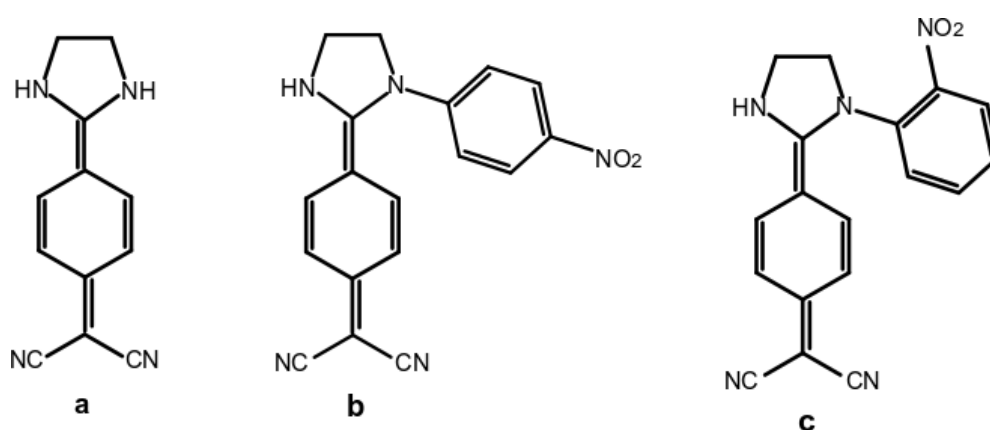
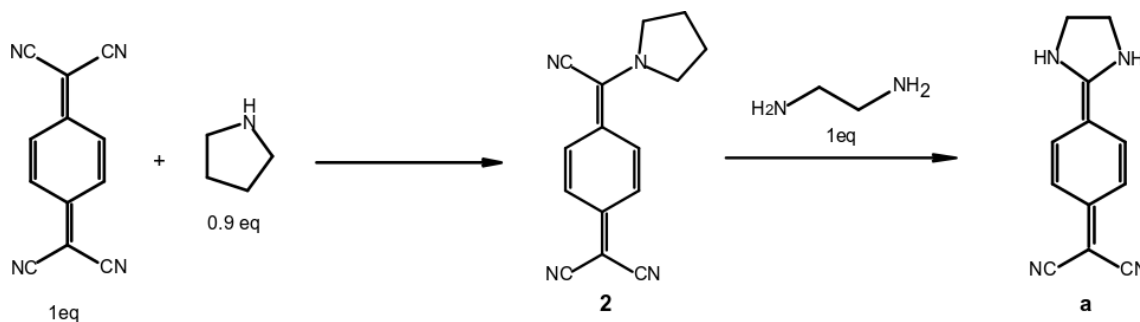


Figure 1. Molecular structure of the target molecules. a) 2-(4-(imidazolidin-2-yl)phenyl)malononitrile. b) 2-(4-(1-(4-nitrophenyl)imidazolidin-2-yl)phenyl)malononitrile. c) 2-(4-(1-(2-nitrophenyl)imidazolidin-2-yl)phenyl)malononitrile.

3.1.Synthesis

3.1.1. Synthesis of 2-(4-(imidazolidin-2-yl)phenyl)malononitrile (**a**)

The synthetic procedure to obtain **a** was followed with minor modification from ref.¹⁶ (**Scheme 1**)



*Scheme1. General approach for the synthesis of 2-(4-(imidazolidin-2-yl)phenyl)malononitrile (**a**).*

At first 7,7,8,8-Tetracyanoquinodimethane (TCNQ) was reacted with a sacrifice pyrrolidine to favor substitution in the germinal cyano group of TCNQ.¹⁶ Also, the use of a pyrrolidine avoids the formation of possible oligomeric or polymeric species once the corresponding diamine gets added to the TCNQ.²⁰ After that, 1 eq of 7-pyrrolidino-7,8,8-tricyanoquinodimethane (PTCNQ) (**2**) reacts with 1 eq of ethylenediamine, as shown in **Scheme1**, to produce 2-(4-(imidazolidin-2-yl)phenyl)malononitrile (**a**).

After 5 minutes of the addition of ethylenediamine to the solution of PTCNQ and acetonitrile the color of the reaction changes from deep purple to light yellow. The progress of reaction was followed by thin layer chromatography (TLC) and once all the PTCNQ is consumed remove the stirrer and let the solution slowly cool down to room temperature. Finally, solution was stored in the fridge for 1 day, filtered off and rinsed three times with cool acetonitrile. Then, store it in the fridge for 3 days at -4°C to ensure that most of the product get crystalized or precipitated and wash with cool acetonitrile. The product precipitates as yellow powder with a yield of reaction of 72%, very similar to those previously reported.¹⁶ The purity of product **a** is proved by TLC, showing that neither any starting reagents nor by-products were present in the final product.

3.1.1.1. Characterization of 2-(4-(imidazolidin-2-yl)phenyl)malononitrile (**a**)

The compound **a** was characterized using UV-Vis, FT-IR and ESI-MS spectrometry, and the results confirmed the structure.

UV-Vis spectra was measured in HPLC grade acetonitrile in a range between 250-850 nm. The absorption spectra show a single peak at 408 nm which could be the result of aromatic π - π^* electronic transition but it may also be due to intramolecular charge transfer that could be produced by the intrinsic zwitterionic characteristics of the DADQ's.³⁵ **(Figure 2)**

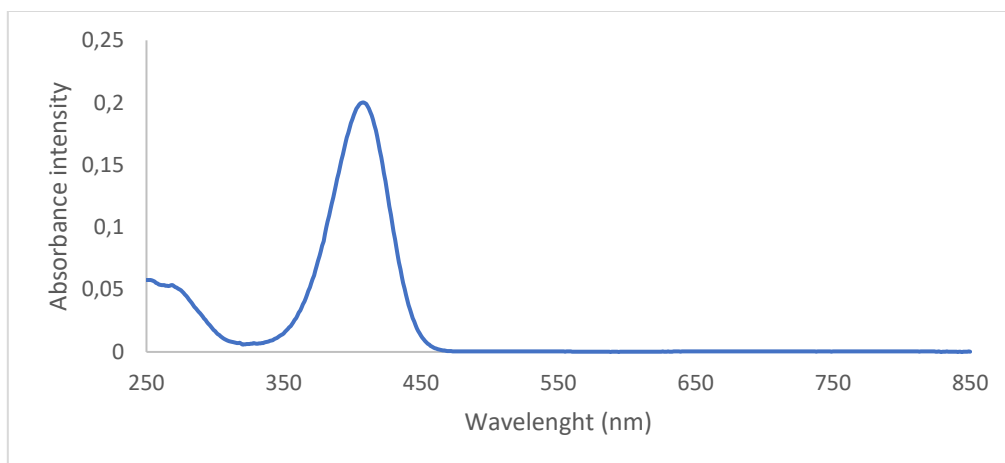


Figure 2. UV-Vis absorption spectra of 2-(4-(imidazolidin-2-yl)phenyl)malononitrile (**a**).

Infrared spectrometry was measured using powder samples with the attenuated reflection method (**Figure 3**). For compound **a** we can observed a signal at 3178.23 cm^{-1} corresponding to the secondary amines N-H stretching (blue) in the molecule, the two signals at 2183 and 2144 cm^{-1} are the expected peaks for asymmetric and symmetric stretching in cyano groups (red). Additionally, there are three other peaks at 1578.25 cm^{-1} (orange), 1503.04 cm^{-1} (green) and 1325.32 cm^{-1} (yellow), which correspond to symmetric stretching between the C=C groups in the Quinone that oscillates between double a single bonds in the molecule³³ (**Figure 3**).

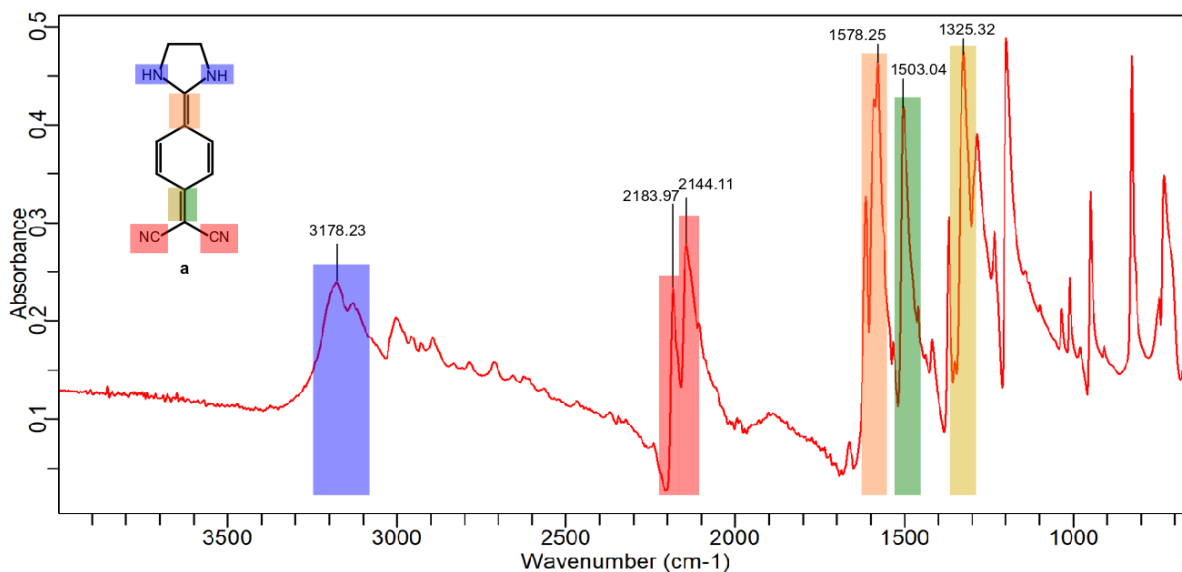


Figure 3. FT-IR absorption spectra of 2-(4-(imidazolidin-2-yl)phenyl)malononitrile (a).

ESI-MS analysis was performed with positive mode and two major peaks were obtained. Firstly, a peak with a m/z of 210.1280 corresponding to the molecular ion, and the second one with mass of 211.1280 corresponding to the protonated ion. The theoretical mass calculated for (a) is 210.2332 (**Figure 4**).

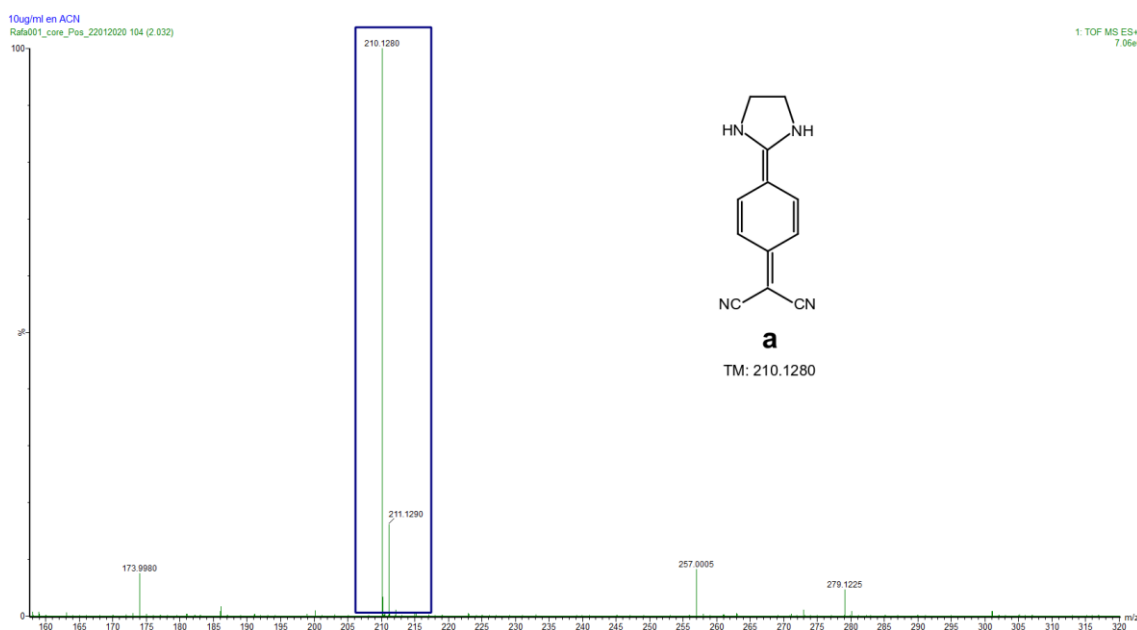
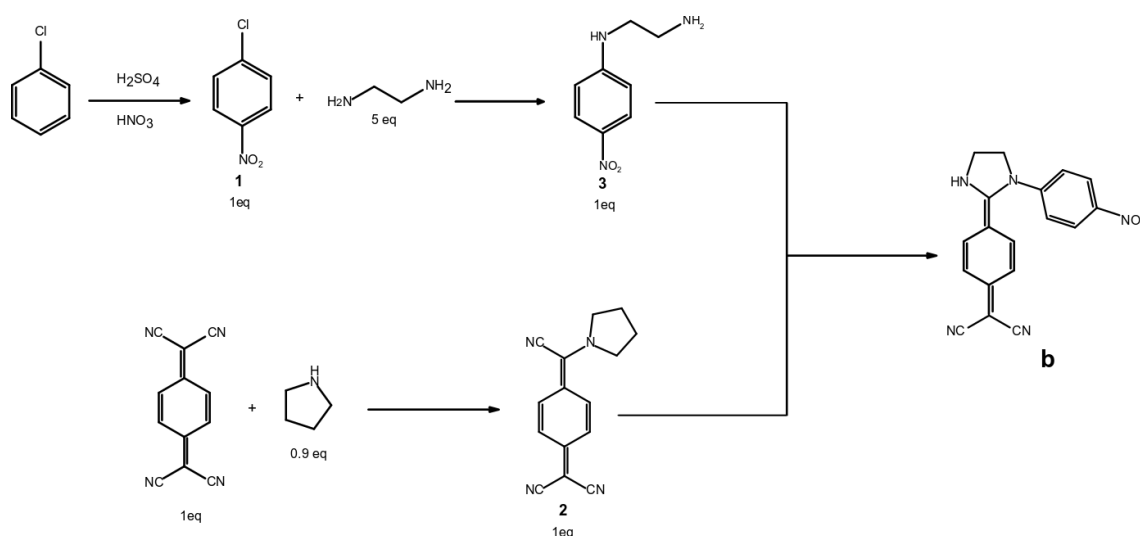


Figure 4. Mass spectrometry of 2-(4-(imidazolidin-2-yl)phenyl)malononitrile (a).

3.1.2. Synthesis of 2-(4-(1-(4-nitrophenyl)imidazolidin-2-yl)phenyl)malononitrile (b).

2-(4-(1-(4-nitrophenyl)imidazolidin-2-yl)phenyl)malononitrile (b) was synthesized by a convergent reaction, as shown in Scheme 2. Firstly, it was necessary to obtain 1 by the nitration of chlorobenzene through an Aromatic Electrophilic Substitution reaction. This reaction was carried out following a reported procedure.³⁴ In general, a nitric/sulfuric acid mixture (1.4:1) was prepared and used as nitration agent. The sulfuric acid acts as a catalyzer for this reaction, because of its nature as a stronger acid than nitric acid, this allows the H₂SO₄ to act as a Bronsted-Lowry acid allowing it to donate a proton to the nitric acid, which acts as a base. Because of this the equilibrium of reaction will be shifted to the formation of nitronium ion species, which are capable to act as an electrophile that will be attacked by a free pair of electrons from the chlorobenzene. In these regards, it is possible that the nucleophilic attack occurs from a para or an ortho position leading to the formation of two isomers as our main products, para-chloronitrobenzene and ortho-chloronitrobenzene. However, it has been reported that the ratio of formation of these two isomers goes in the values of 2/3 for the para specie and 1/3 for the ortho specie.³⁴ Also, it is necessary to add very slowly the acid mixture to the chlorobenzene, set a strong stirring and keep the temperature of reaction under 50°C to avoid the formation of poly-nitrated species.¹⁴ Finally, to obtain pure para-chloronitrobenzene it is necessary to slowly reduce the temperature of the eutectic mixture until it reaches 0°C and filter off the precipitate. This precipitate is washed with cool water to finally obtain pure p-nitrochlorobenzene (1).



Scheme 2. General approach for the synthesis of 2-(4-(1-(4-nitrophenyl)imidazolidin-2-yl)phenyl)malononitrile (b).

Then, it is necessary to perform an aromatic nucleophilic substitution reaction of *p*-nitrochlorobenzene (1, 1 eq) with ethylenediamine (5 eq) (Scheme 2). Such excess of ethylenediamine is used to avoid the formation of the *N,N*-disubstituted product. It is also necessary to keep the reaction temperature under 120°C, because temperatures above this value will produce the formation of an untreatable material that is insoluble in many of tested solvents. After 6 hours of reaction it was necessary to evaporate the solution to dryness under reduced pressure to eliminate the ethylenediamine excess. TLC analysis of final product showed two spots with very different *R_f* values, and it was necessary to use a chromatographic column using methanol as mobile phase in order to purify 3. It is important to highlight that there is few information about reactions to obtain 3, and some of papers that report this reaction claim to use carbonate salts in the reaction, like sodium carbonate or potassium carbonate. After performing our experiments, we can conclude that there is not a reason to use these salts; in fact, the addition of mentioned salts only made more difficult the procedure, because once the reaction is done there is no possible way to separate the product from the carbonate salt in an effective way, due to the high solubility of our product 3 in water.

In parallel, the reaction of TCNQ with pyrrolidine was carried out using the same procedure previously described to (a) to yield PTCNQ (2) as fine purple needle shaped crystals (Scheme 2).

With 2 and 3 in hand, we carried out the final step of this synthesis (Scheme 2). The compound 3 reacts with PTCNQ to give 2-(4-(1-(4-nitrophenyl)imidazolidin-2-yl)phenyl)malononitrile (b). The presence of pyrrolidine in the TCNQ make highly unlikely an intermolecular reaction, avoiding the formation of polymeric species and helping to the intermolecular cycle formation. Thus, equimolecular amounts of 2 and 3 react under reflux using acetonitrile as solvent during seven hours. Five minutes after the addition of 3, the solution started to change from purple color to brown-greenish color, and finally after 30 minutes the mixture became completely yellow. The mixture was stored in fridge for one day, to latter be filtered and washed with cool acetonitrile to obtaining the crude b, which was recrystallized in acetonitrile to finally obtain fine yellow needles of 2-(4-(1-(4-nitrophenyl)imidazolidin-2-yl)phenyl)malononitrile (b).

3.1.2.1. Characterization of 2-(4-(1-(4-nitrophenyl)imidazolidin-2-yl)phenyl)malononitrile (**b**).

The compound **b** was characterized using UV-Vis, FT-IR and ESI-MS spectrometry, and the results confirmed the structure.

UV-Vis spectra was measured in HPLC grade acetonitrile in a range between 200-800 nm. The absorption spectra show a single peak at 371 nm which could be the result of aromatic π - π^* electronic transition but it may also be due to intramolecular charge transfer that could be produced by the presence of the nitro group or by the intrinsic zwitterionic characteristics of the DADQ's.³⁵ (**Figure 5**)

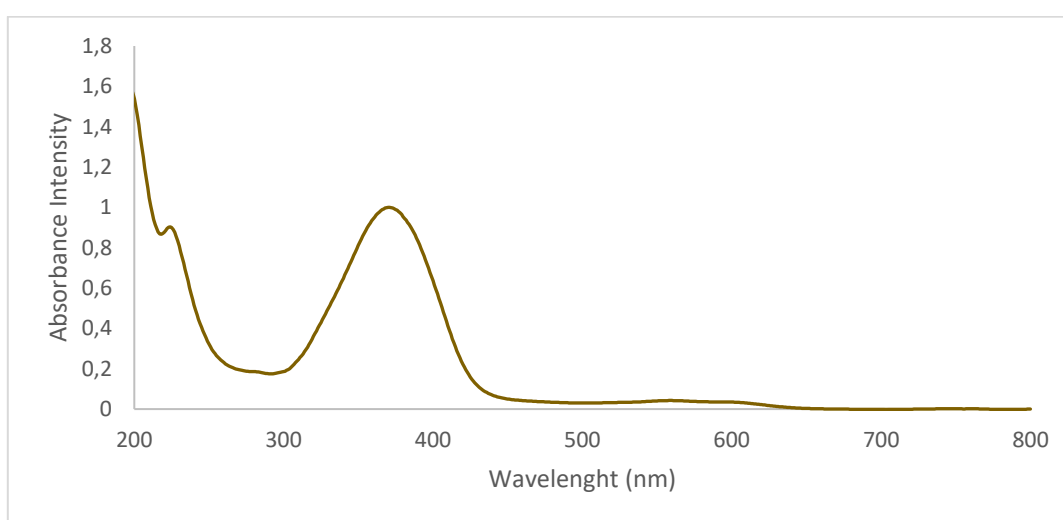


Figure 5. UV-Vis spectra of 2-(4-(1-(4-nitrophenyl)imidazolidin-2-yl)phenyl)malononitrile (**b**).

Infrared spectrometry was measured using powder samples with the attenuated reflection method. For **b** we can observed the expected signal at 3282.74 cm^{-1} with a medium intensity, corresponding to the secondary amine N-H stretching (blue). Also, the two signals at 2175.03 and 2124.65 cm^{-1} which correspond to symmetric and asymmetric $\text{C}\equiv\text{N}$ stretching of the cyano groups (red). Additionally, one strong peak is present at 1593.89 cm^{-1} which by a theoretical calculation approach seems to correspond to a C-N stretching which is behaving partially as a single and a double bond (sky blue). In the same way, another peak with a medium intensity at 1448.98 cm^{-1} corresponding to a C-N stretching seems to present a single and double bond character (purple). Also, the peak at 1547.23 cm^{-1} matches with the expected values for the asymmetric stretching in nitro compounds (green). Unfortunately, the symmetric stretching seems to be hidden due to the other

stronger signals. Finally, a very strong peak appears at 1305.40 cm^{-1} which correspond to both the C=C and N-C stretching (yellow) (**Figure 6**). All detected signals are present in the expected ranges.³³

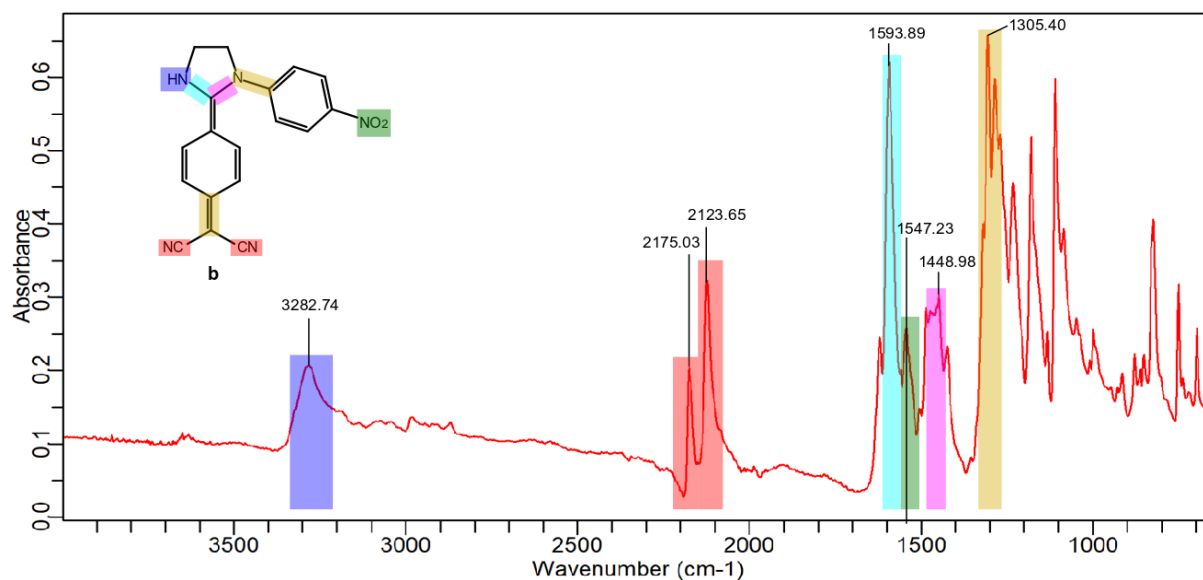


Figure 6. FT-IR absorption spectra of 2-(4-(1-(4-nitrophenyl)imidazolidin-2-yl)phenyl)malononitrile (**b**)

ESI-MS was performed with a positive mode and two major peaks were obtained. Firstly, a peak with a m/z of 330.1735 corresponding to the molecular ion, and the second one with mass of 331.1743 corresponding to the protonated ion. The theoretical mass calculated for (**b**) is 331.3255 (**Figure 7**).

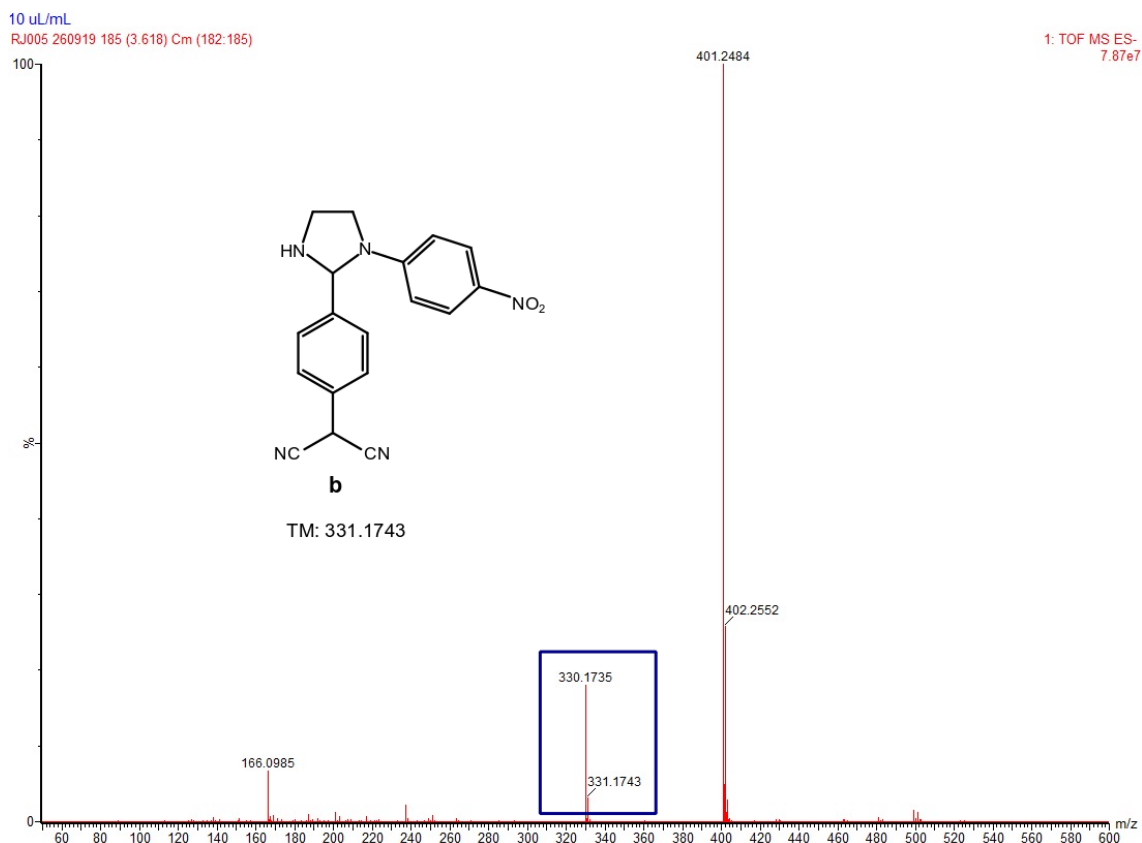
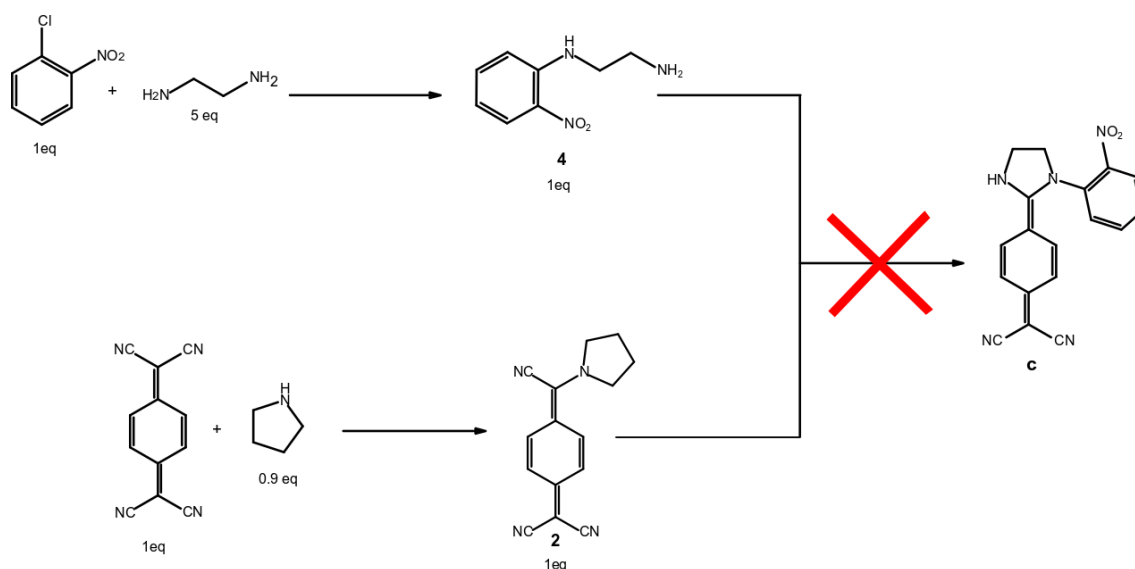


Figure 7. Mass spectrometry of 2-(4-(1-(4-nitrophenyl)imidazolidin-2-yl)phenyl)malononitrile (b)

3.1.3. Synthesis of 2-(4-(1-(2-nitrophenyl)imidazolidin-2-yl)phenyl)malononitrile (c)

The synthesis of 2-(4-(1-(2-nitrophenyl)imidazolidin-2-yl)phenyl)malononitrile (c) was carried out using the similar procedure to previously use to **b** through a convergent synthesis (**Scheme 3**), but using commercial ortho-chloronitrobenzene as starting reagent in place of previously synthesized para-chloronitrobenzene.



Scheme 3. General approach for the synthesis of 2-(4-(1-(2-nitrophenyl)imidazolidin-2-yl)phenyl)malononitrile (*c*)

The aromatic nucleophilic substitution reaction of *o*-chloronitrobenzene and ethylenediamine allowed to obtain **4** as orange crystals. Column chromatography using methanol as solvent was carried out in order to obtain pure **4** (**Scheme 3**).

With **2** and **4** in hand, we performed the similar reaction to obtain *b*. However, not color changes were observed, and TLC showed that initial reagents were present without any formation of other products. Because of this, the reaction was repeated under reflux conditions, and for a longer period (one day). Unfortunately, no positive results were obtained. In order to increase the mobility of the molecules, and with the hope to shift the reaction equilibrium to the product formation, the reaction was also repeated under reflux condition for seven hours, but using an ultrasonic bath as energy source. Unluckily, the TLC test still showed no product formation (**Scheme 3**).

These results could be explained by two hypotheses. Firstly, it is possible for **4** to form an intramolecular hydrogen bond between the oxygen of the nitro group and one of the hydrogens located in any of the amines. This provides **4** a very stable six-member ring that reduces its nucleophilic power, directly influencing the reactivity of N-(2-nitrophenyl)ethylenediamine (**4**) and the equilibrium of reaction. Nevertheless, it is still possible to argue that some product should form if enough mobility (energy) is provided to the system, but experimentally it does not happen therefore, there must be another reason contribution to the no formation of *c*. It could be due to the instability of the

product due to the high steric hindrance produced by the presence of the nitro group in the ortho-position. This steric hindrance could induce the loss of planarity in the molecule, which generally indicates the loss of electronic conjugation and by consequence the reduction of stability. This point will be further discussed in the “theoretical studies” with the use of different computational tools to obtain additional information about this problem. In spite of this further research need to be performed to fully understand the reasons that explain the no formation of **c**.

4.1.1.1. Theoretical approach for the synthesis of 2-(4-(1-(2-nitrophenyl)imidazolidin-2-yl)phenyl)malononitrile (c).

In regards to the synthesis of **c** there could be several reasons for the no reaction of N-(2-nitrophenyl)ethylenediamine (**4**) with 7-pyrrolidino-7,8,8-tricyanoquinodimethane (**2**). One of the hypothesis refers to the possible formation of an intramolecular six-member ring stabilized by a hydrogen bond of the type (N–H···O) between an oxygen (O) in the nitro group and the hydrogen (H) of the secondary amine present in the molecule.

A hydrogen bond distance and energy is quite variable in dependence with the chemical environment of the atoms conforming the bond, in general a hydrogen bond distance goes between 1.6 to 2.3 Å.³⁶ While the energy associated with these interaction could vary from a weak (1–2 kJ mol⁻¹) to strong (161.5 kJ mol⁻¹ in the ion HF₂⁻).^{37,38} Additionally, it is expected to obtain for a six-member ring an angle around 120°. In section 1) of (**Figure 7**) it is possible to form a hydrogen bond that accomplishes the previous mentioned characteristics. The possible hydrogen bond is marked in yellow, it has a distances of 1,82Å and forms an angle of 110°. Additionally, in the side view of the molecule it is possible to see that the molecules remain mainly planar showing that no electronic delocalization is produced stabilizing this configuration over the configuration 2) in **Figure 7**.

Finally, in **Table 1** are shown the two energies associated with each configuration and the difference in energy between the two. As expected configuration 1) is more stable than 2) by 37,56 KJ/mol which is an important energetic difference for two conformations. This benefits the first conformation over the second one, increasing its stability and reducing the reactive capacity of the molecule.

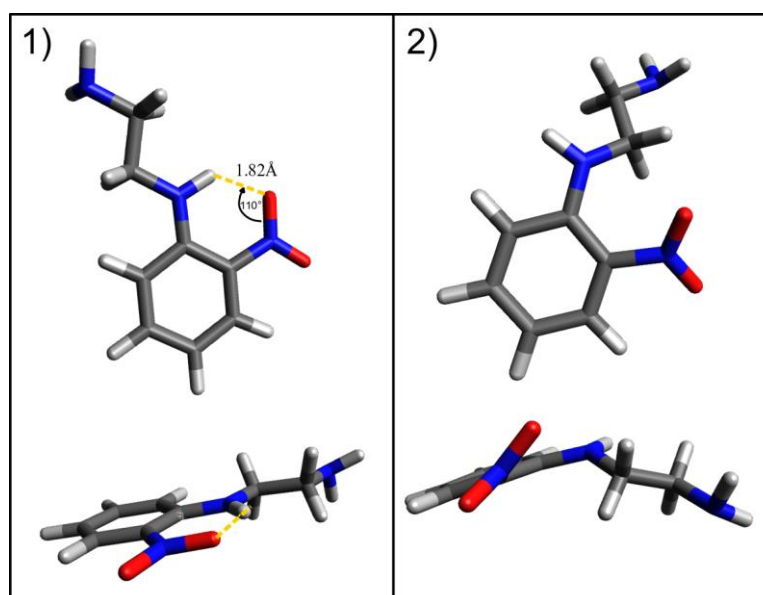


Figure 7. Perspectives from the front and side of the geometrical optimization in two possible configurations for *N*-(2-nitrophenyl)ethylenediamine (**4**). **1**) allows the formation of a six-member ring with a hydrogen bond, marked with a yellow dotted line. **2**) Implies a 180° rotation of the “ethylenediamine” moiety, No possible stabilization by hydrogen bond formation in this configuration.

Energy (hartree)		Energy change (KJ/mol)
1	2	ΔE
-626,052190489569	-626,037897376696	37,56

Table 1. Energetic differences between configuration 1) and 2).

4.2. AIE studies

4.2.1. Quantum yield (QY) measurement

The fluorescence spectra of organic dyes are commonly broad and asymmetric. The source of asymmetry is the participation of electronic and vibrational transitions.⁷ Fluorescence spectra are usually specular images of the absorption spectra, with acute blue and slow red slopes. Additionally, they can be distorted by relaxation processes in the excited state resulting in Stokes shifts and further spectral broadening.³⁹

For a careful description of a complex fluorescence spectrum, it must be deconvolute into individual components. Of key importance for a right deconvolution is the selection of

the mathematical function that adequately describe the profile(s) of individual bands. Due to the considerable asymmetry exhibited by Fluorescence spectra, Log-Normal profiles are most often used, as mentioned in the methodology section.²³

Thus, Fityk⁴⁰ was used for the non-linear fitting of the emission spectra data and to calculate the peak areas associated with the identified peaks. A complex model was created as a sum, $F = \sum_i f_i$, of Log-normal functions. (equation 2)

$$f(x) = \frac{1}{x} \frac{1}{\sigma\sqrt{2\pi}} \exp\left\{-\frac{(\ln x - \mu)^2}{2\sigma^2}\right\} \quad (2)$$

where μ and σ are, the expected value (or mean) and standard deviation of the variable's natural logarithm, (not the expectation and standard deviation of x itself).

The Levenberg-Marquardt method was chosen as the nonlinear least-squares routine. This algorithm involves computing the first derivatives of functions, and is robust and efficient with strong convergence properties. The function of merit used was the weighted sum of squared residuals, WSSR, (χ -square).

The emission spectra of reference and sample were recorded in all visible range, and corrected for the blank (solvent) to perform proper emission intensity integration. The emission spectra and their deconvolution at 405 nm excitation are given in **Figure 8**.

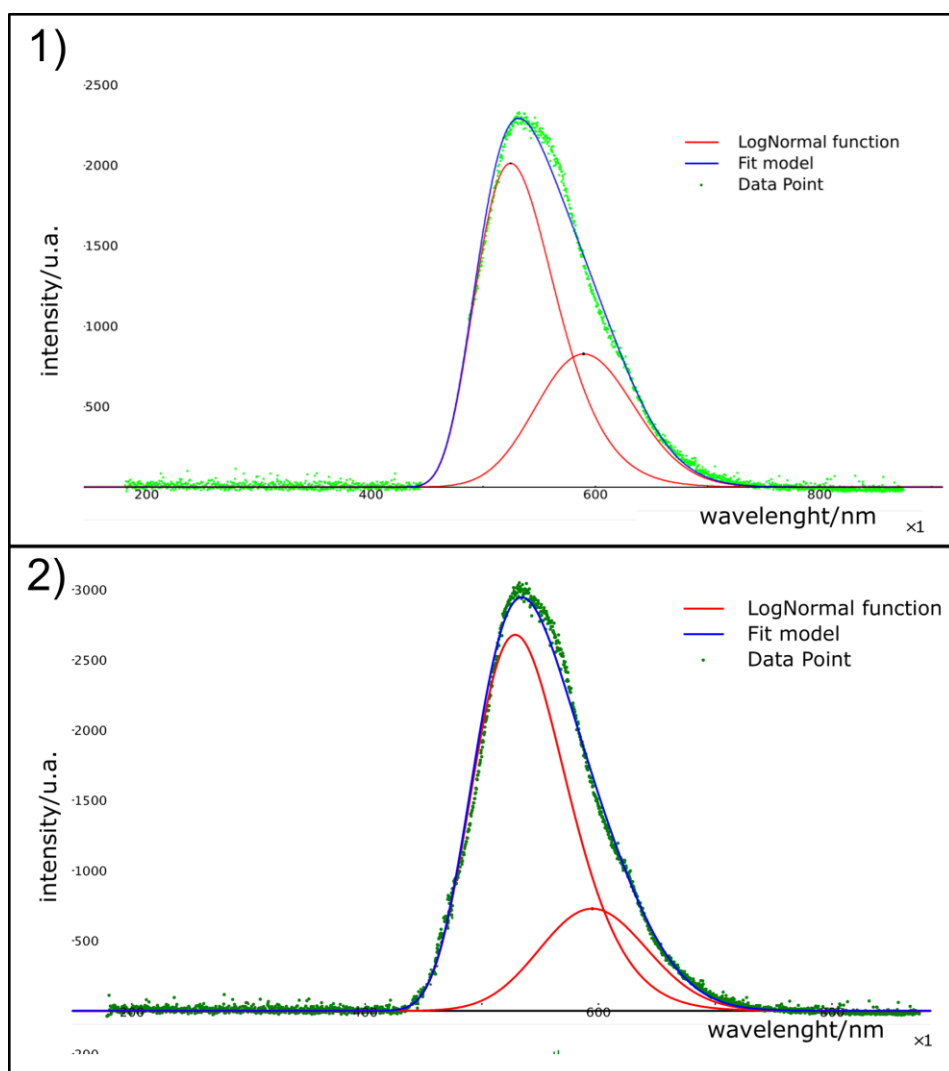


Figure 8. Emission spectra of: 1) 2-(4-(imidazolidin-2-yl)phenyl)malononitrile (a) and 2) 2-(4-(1-(4-nitrophenyl)imidazolidin-2-yl)phenyl)malononitrile (b)

Additionally, the relative quantum yield (QY) of **b** with DMSO as the solvent system was calculated according to equation (1), previously mentioned in methodology section. Additionally, the QY of **a** in DMSO is 10.1%¹⁶ and the refractive index will cancel between each other because the same solvent system was used for both compounds measurements.

	Absorbance at 405 nm	Area under the curve	R-squared
Reference sample: Compound (a)	0,6958	91200.1 + 182323 = 273523.1	0.998345

Test	Sample:	0,5428	83691.1 + 182323 =	0.993176
Compound (b)			266014.1	

Table 2. Areas under the curve and coefficient of determinations for the emission spectrum of 2-(4-(imidazolidin-2-yl)phenyl)malononitrile (a) and 2-(4-(1-(4-nitrophenyl)imidazolidin-2-yl)phenyl)malononitrile (b).

Where, Φ refers to the quantum yield, Int is the area under the emission peak, A states for the absorbance at the excitation wavelength and n is the refractive index of the used solvent. The subscripts st and x denotes the values of the standard and test samples, respectively. Replacing the values shown in **Table 2** into equation (1) we can obtain a QY value of 15.64%, which is slightly higher than the reference sample. This calculation was performed as follow:

$$\Phi_x = \Phi_{st} \frac{Int_x}{Int_{st}} \left(\frac{1 - 10^{A_{st}}}{1 - 10^{A_x}} \right) \frac{n_x^2}{n_{st}^2}$$

$$\Phi_x = 10.1 \frac{266014.1}{273523.1} \left(\frac{1 - 10^{0.6985}}{1 - 10^{0.5428}} \right)$$

$$\Phi_x = 15.64\%$$

Relative quantum yield measurements show that N-substitutions could exert important changes in the quantum yield values of DADQ's systems without significantly modifying the positions of the emission and absorption peaks.

4.2.2. Theoretical Research

Computational calculations have been conducted to study the cause of fluorescence enhancement in DADQ derivatives. For this purpose, ground state geometry optimizations were carried out at the CAM-B3LYP/def2-TZVP level of density functional theory (DFT).⁴¹ Additionally, calculations with the implicit solvent model (SCRF) were incorporated with acetonitrile as the solvent. This was because acetonitrile is not a protic solvent that could induce fluorescence quenching by hydrogen bonding or a too viscous solvent which enhances the fluorescence due to its viscosity.⁴²

CAM-B3LYP was used for this type of calculations because it has shown a very accurate perform for excited states and species displaying a strong charge-transfer character.⁴³ In all cases as specified in the methodology section the genuine minima of each structure

were proved by showing no negative (imaginary) frequencies in the frequency calculations.

4.2.2.1. Geometry in Ground & Excited states

All DADQ's are molecules which maintain an equilibrium between a benzenoid form and a quinonoid zwitterion (**Figure 9**), this allows this molecules to present different behaviors than a normal double bonded molecule. Therefore, all geometry calculations will be performed taking in account the quinonoid form of the DADQ's.

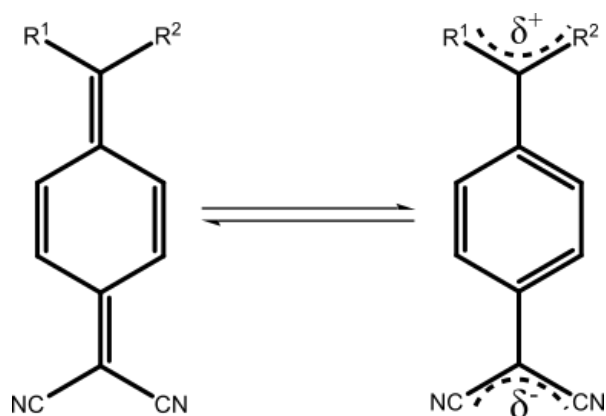
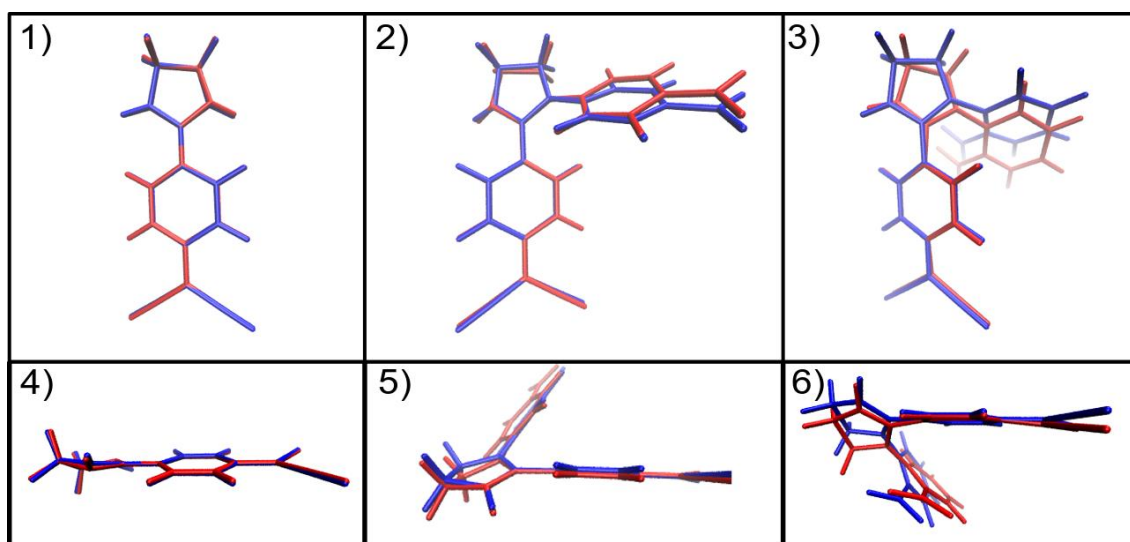


Figure 9. Benzenoid and quinonoid resonance forms for any DADQ derivative.

For a molecule to have high quantum yields (QY), firstly; it is necessary that the molecule presents a very similar geometry between the excited and the ground state when they are optimized (at their minimum of energy). Differences between excited state and ground state geometries of all the studied compounds are shown in **Figure 10**.

In the case of **a** most of the geometry changes are negligible, leaving the excited and ground states of **a**, with just a little twist produced in the “imidazolidine” like moiety and at the benzene part of the molecule. For **b** we can see that the “malonitrile” moiety of the molecule presents barely any difference between the excited and the ground state. The major differences produced for this molecules occurs at the nitrobenzene moiety, here we can immediately recognize that there is a difference between the excited and the ground states. While, in the ground state the nitrobenzene part of the molecule is much more perpendicular in respect to the rest of the molecule; the excited state rotates a little trying to get a more planar configuration. Despite this, the molecule still is not planar avoiding the possible loss of the AIE behavior by π - π stacking interactions. Finally, the geometric variations between states for **c** are much more important. It is noticeable the great

differences at the imidazolidine and nitrobenzene parts of the molecule, the nitrobenzene moiety differs a lot from the excited to the ground state. Additionally, the imidazolidine moiety gets highly twisted in the excited state due to the steric hindrance that produce the presence of the nitro group at the orto-position of the benzene. Furthermore, this important steric hindrance induces in the excited state a noticeable bend in the core of the molecule, this indicates a possible loss of aromaticity in the molecule.



*Figure 10. Comparison between the ground state (blue) and excited state (red) structures calculated at the CAM-B3LYP/def2-TZVP level of DFT and TD-DFT, respectively. Where 1), 2) and 3) illustrates a front perspective of molecules **a**, **b**, and **c**. while 4), 5) and 6) show a lateral view of the same respective molecules.*

Each of these geometry changes were checked by measuring the most important dihedral angles of each specie. The possible torsions at each dihedral angles are represented in **Figure 11** by arrows. It is important to remark that either the quenching or enhancement of the DADQs fluorescence is directly related and mainly controlled by the photoinduced intramolecular torsions produced at each of the dihedral angles D_γ , D_δ for **a** and D_α , D_β , D_γ , D_δ for **b** and **c**.

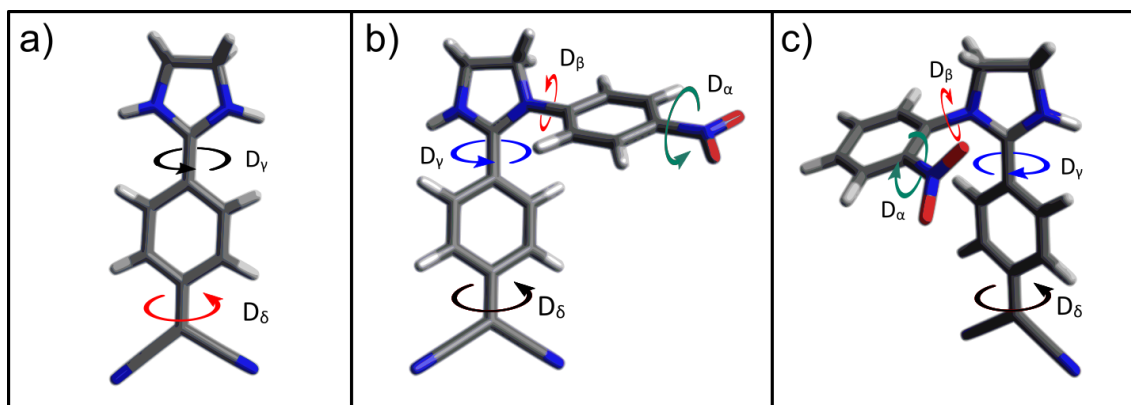


Figure 11. Kinds of intramolecular torsion angles that affect the fluorescence deactivation mechanism in DADQs: a) 2-(4-(imidazolidin-2-yl)phenyl)malononitrile (**a**) with the two types of dihedral angles D_γ , D_δ . b) 2-(4-(1-(4-nitrophenyl)imidazolidin-2-yl)phenyl)malononitrile (**b**) with the four types of dihedral angles D_α , D_β , D_γ , D_δ . c) 2-(4-(1-(2-nitrophenyl)imidazolidin-2-yl)phenyl)malononitrile (**c**) with the four types of dihedral angles D_α , D_β , D_γ , D_δ

A further insight into these geometrical changes is required. Thus, it is necessary to measure the dihedral angles at each of the possible torsion sites indicated in **Figure 11**. The measurements on each of the molecules are shown in **Table 3**, as we can see these values are quite variable in some cases and remain mostly the same in other cases. The D_δ dihedral angle remains mostly unchanged not only between excited and ground states but also between all 3 compounds, this tells that the bottom section of the molecule remains mainly unaltered by conformational or configurational changes produced in the upper section of the molecule.

In the case of D_γ a complete different behavior is observed (**Table 3**), there is a variation of around 10° between the excited and the ground state in all three compounds. Additionally, it is a great variation between **a** and **b** and **c** derivatives, this shows that substitutions in the imidazolidine like moiety induces a change in this dihedral angles.

For D_β there are important rotations produced either by the different substitutions in each compound and by the change of the electron disposition in the S_1 and S_0 states. Furthermore, it seems to produce a loss in electrons delocalization around the Quinone section of **c** due to a loss of planarity in the molecules excited state.

Finally, as we can see in **Table 3** for D_α the rotation is mainly negligible for **b**, which changes only $0,4^\circ$ between the excited and the ground states, showing that the electrons remain mostly delocalized between the aromatic ring and the nitro group. On the other

hand, in **c** there is a complete different story. The nitro group is strongly deviated from the aromatic ring either in the ground state and excited state, this may be due to the strong steric hindrance produced by the presence of the nitro group in the orto-position. Because of this, the electronic conjugation between the benzene ring and the nitro group gets highly reduced.

Dihedral angles	a (S_0)	a (S_1)	b (S_0)	b (S_1)	c (S_0)	c (S_1)
D_α	-	-	1,5°	1,9°	34,4°	22,9°
D_β	-	-	-40,4°	-20,7°	53,3°	43,3°
D_γ	16°	5,8°	-33,7°	-20,5°	31,4°	38,5°
D_δ	-0,3°	0,4°	0,2°	0,3°	-0,4°	0,4°

Table 3. Dihedral angles of compounds (a), (b) and (c) at the ground (S_0) and excited (S_1) states.

4.2.2.2. Oscillator strength and dipole moments

In regards to the oscillator strength, when molecules capable of absorption and emission of photons are studied, it is necessary to take into account the oscillator strength of such molecules. The oscillator strength is a dimensionless value that expresses the probability of absorption or emission of electromagnetic radiation in transitions between energy levels of an atom or a molecule.⁴⁴ For example, a transition that is quantum mechanically fully allowed need to have an oscillator strength around 1.0.⁴⁵ In these regards, the calculated oscillator strengths for each of the studied compounds would provide a good idea on which of them will have good quantum yields and which do not. Thus, for **a** there are oscillator strength values of 1.232 and 1.2889 for the ground and excited states respectively, indicating that absorption and emission of photons are quantum mechanically allowed. For **b** there are values of 0.785 and 1.0087 for the S_0 and the S_1 states respectively, indicating in the same manner as **a** that the electronic transitions are quantum chemically allowed. Finally, for **c** we have oscillator strength of less than 0.01 indicating that the transition in this compound are forbidden, therefore it should not be expected to find any kind of fluorescence in **c** (**Table 4**).

For the dipole moment, the presence of a donor-acceptor system in our molecules will produce an electron shift from the dicyanomethane to the amine groups upon photoexcitation. This electronic transitions gives rise to a reduction of the dipole moment in the excited state of around 2,5 D for **a** and **b**, while the dipole moment for **c** increases in 1.5 D (**Table 4**). When a fluorophore gets excited an electron is induced to move from one orbital to another. If the initial and the final orbitals are separated in space, the

electronic transition is accompanied by an instantaneous change in the dipole moment.⁴⁶ When this change produces an increase in the dipole moment the excited state (also known as Frank-Condon state) (**Figure 12**) is not in equilibrium with the solvent molecules in the solvation shell. Therefore, in this scenario it is expected to have a positive solvatochromism (red-shift) in the fluorescence spectrum as the solvents polarity gets increased. On the other hand, when the change produced by the electronic transitions diminishes the dipole moment value; it is expected to observe an opposite behavior. In our case the fluorescence spectrum will present a negative solvatochromism (blue-shift) when the solvents polarity is increased.¹⁶

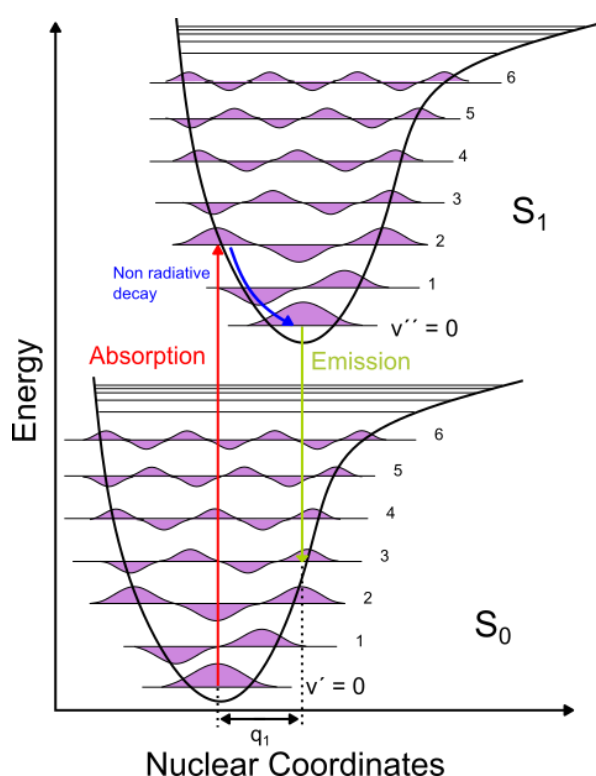


Figure 12. Energy diagram for Franck–Condon principle. Because vibrational motions are comparably faster than nuclear motions, the vibrational levels that requires a minimal change in the nuclear coordinates are strongly favored. Thus $v'=0$ to $v''=2$ is favored in this example.

Thus, theoretically it is expected to see negative solvatochromism for **a** and **b** while for **c** it would be expected to see a positive solvatochromism.

		a	b	c
Oscillator Strength	S ₀	1,2520	0,7850	0,0030
	S ₁	1,2889	1,0087	0,0005
Dipole moment (Debye)	S ₀	29,3167	31,0528	30,5951
	S ₁	27,1140	28,5555	31,0556

Table 4. Oscillator strength and dipole moments of compounds (**a**), (**b**) and (**c**) in the ground and excited state.

4.2.2.3. Energies associated with the optimized geometries

With respect to the energies associated to the optimized ground and excited states, in (Table 5) are specified the calculated energies for each of the compounds and the energy variation between S₀ and S₁ states. Additionally, in (Table 6) are presented the energies associated with compounds **b** and **c** and the difference in energy between those two compounds. The calculated energies show that compounds **a** and **b** slightly change from the ground to the excited state, whereas for **c** the change of energy between the two states is 4 and 3 times larger than compounds **a** and **b**, respectively. This high differences in energy between the states S₀ and S₁ in compound **c** shows a very different excited state that may cause a lack of fluorescence in this molecule.

		a	b	c
Energy (hartree)	S ₀	-682,215573965	-1117,75295526	-1117,74682374
	S ₁	-682,210919905	-1117,74558489	-1117,72531889
Energy change (KJ/mol)	ΔE	12,2169075	19,34722125	56,45023125

Table 5. Energies and their variation in the optimized geometries of 2-(4-(imidazolidin-2-yl)phenyl)malononitrile (**a**), 2-(4-(1-(4-nitrophenyl)imidazolidin-2-yl)phenyl)malononitrile (**b**) and 2-(4-(1-(2-nitrophenyl)imidazolidin-2-yl)phenyl)malononitrile (**c**) in their ground (S₀) and excited state (S₁).

In addition, the difference between the energies of **b** and **c** indicates that **b** is more stable than **c** in ground state, but this stability is much more noticeable between the excited states of both compounds. (Table 6)

	Energy (hartree)		Energy change (KJ/mol)
	b	c	ΔE
S₀	-1117,75295526	-1117,74682374	16,15962096
S₁	-1117,74558489	-1117,72531889	53,411043

Table 6. difference of energies between the ground and excited states of 2-(4-(1-(4-nitrophenyl)imidazolidin-2-yl)phenyl)malononitrile (**b**) and 2-(4-(1-(2-nitrophenyl)imidazolidin-2-yl)phenyl)malononitrile (**c**).

4.2.2.4. Mulliken Charges

About the distribution of charges in **a**, **b** and **c** we can see that the conformation and the configuration of the molecules does not affect the bottom part of the molecule (dicyanomethane and quinone moieties). However, in nitrogen atom N4 shown in **Figure 13**, the charge strongly decreases from **a** in comparison with **b** and **c** (**Annex 1**). The increase of negative charge value in **a** is due to the absence of nitrobenzene moiety, present as *N*-substituent for **b** and **c** derivatives. The nitrobenzene scaffold promotes the mentioned behavior due to the electron withdrawing effect of nitro group.

Regarding **b** and **c** derivatives, it is noticeable that the carbon atom directly bonded to the nitro group will be strongly affected by its presence. In the case of **b**, C18 showed a positive charge of +0,11 while for **c** the charge in C18 was the opposite -0,11. The same behavior is expected for C14, which for **b** showed a charge of -0,14, while for **c** it has a +0,08 charge (**Annex 1**).

Additionally, the same calculations were performed for *p*-nitrotoluene and *o*-nitrotoluene to compare the effect of the different nitro substitutions in the aromatic ring. Whereas, we can observe that the *orto*-substitution has a slightly higher negative charge located into the oxygens of the nitro group than the one's in *para*-substitution. In **b** and **c** there is an opposite behavior, showing that *para*-substitution has a higher negative charge at the oxygens of the nitro group than the *orto*-substitution. This results could be explained by the loss of planarity between the nitro group and the aromatic ring in **c**. This loss of planarity reduces the inductive capacity of the nitro group, preventing the adequate attraction of the electronic density from the aromatic ring to the nitro group.

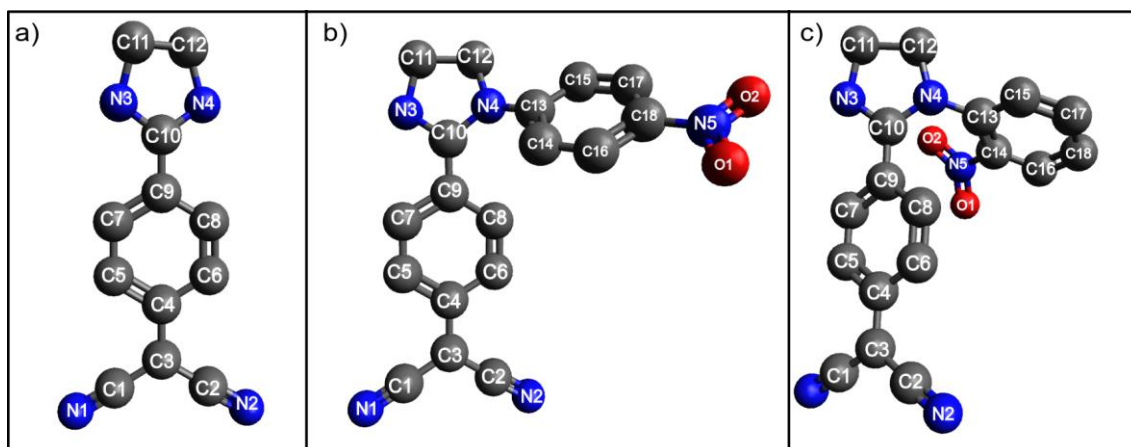


Figure 13. Labeled atoms on 2-(4-(imidazolidin-2-yl)phenyl)malononitrile (a), 2-(4-(1-(4-nitrophenyl)imidazolidin-2-yl)phenyl)malononitrile (b) and 2-(4-(1-(2-nitrophenyl)imidazolidin-2-yl)phenyl)malononitrile (c).

4.3. Antibacterial Activity

Antibacterial activity was tested for compounds (**a**, **b**, **2** and **3**). For this sake two techniques were used, the agar diffusion technique and the optical density (OD) measurements to study of antibiotic efficacy of the synthesized molecules.

4.3.1. Agar diffusion method

The results obtained for the agar diffusion technique, exhibited inhibition zones for all the tested molecules. Also, it is important to remark that the solvent system by itself shows some sort of antibacterial activity but it is not as important as the ones observed for the studied compounds. For this test the labels R11, R12, R13 corresponds to dilutions of **2** (1000 $\mu\text{g/ml}$; 100 $\mu\text{g/ml}$ and 10 $\mu\text{g/ml}$), respectively. In the same way the labels R21, R22, R23 correspond to the same dilutions of **3**, R31, R32, R33 correspond to the respective dilutions of **a** and R41, R42, R43 correspond to the respective dilutions of **b**. Also, the letters K, S and A states for kanamycin, the solvent system and ampicillin, respectively (**Figure 14**).

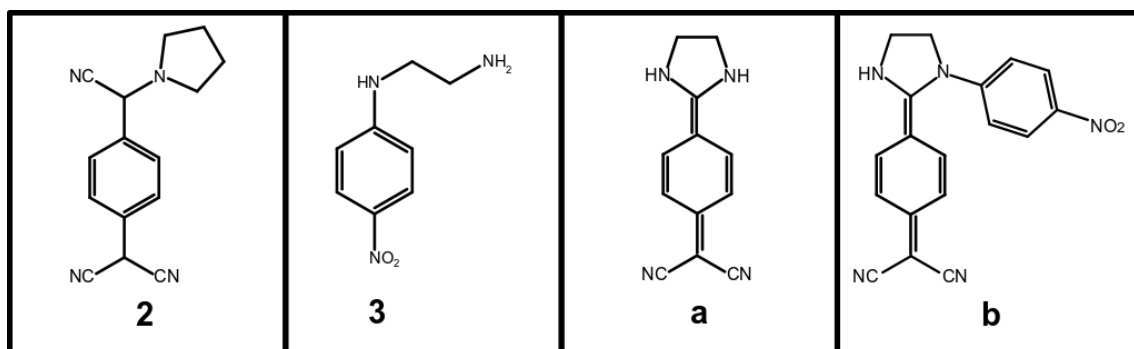


Figure 14. Chemical structure of the four studied molecules.

We can see that the antibacterial activity is appreciable for the 1000 $\mu\text{g/ml}$ and the 100 $\mu\text{g/ml}$ dilutions in all samples, while for the 10 $\mu\text{g/ml}$ dilution the inhibition zones are barely perceptible and could be mostly because of the solvent system rather than the compound itself (**Figure 15**). Additionally, the antibacterial activity is considerably more significant for **2** and **3** than for **a** and **b**. Also, the obtained results indicate that all the tested compounds exhibited a weaker antimicrobial activity on the *E. coli* strains than the control antibiotics. Finally, it is important to remark that this technique is mostly used as a qualitative test; besides, the hydrophobicity of the compounds will interfere with the diffusion of the component to the culture medium. Due to the above, although the determination of the antibacterial activity can be obtained by this technique, other methods would give better results.^{47,48}

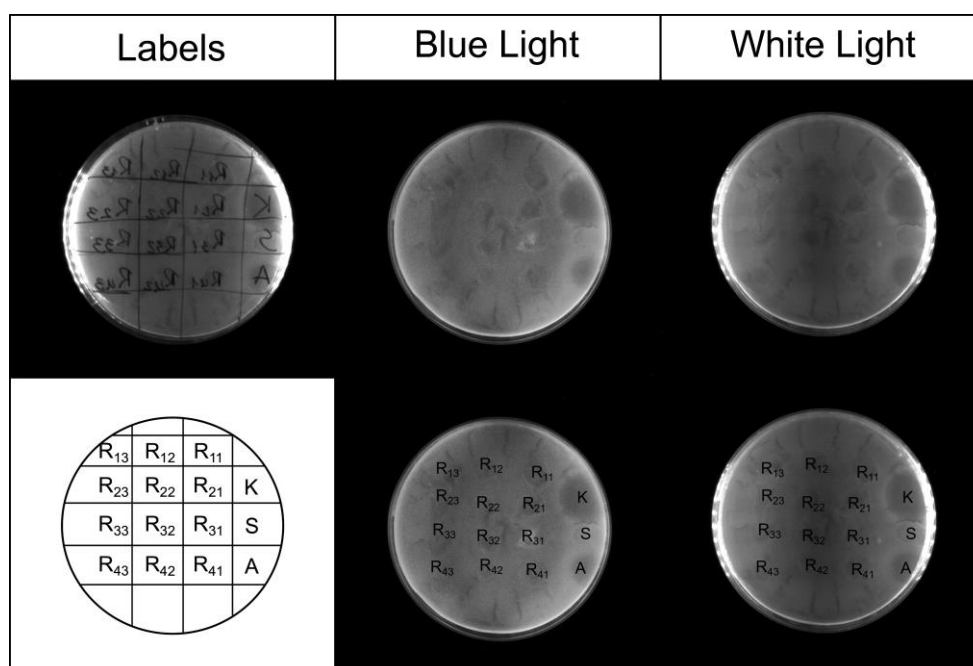


Figure 15. Antibacterial activity test performed in E. coli strains for compounds (a, b, 2 and 3). Revealed under blue light and white light.

4.3.2. Optical density measurements (OD₆₀₀)

The results for the OD₆₀₀ studies showed that all the compound presents some sort of antibacterial activity. Initially, the OD₆₀₀ measurements were performed just with test tubes 1 and 6 (**Table 7**) for a period of 10 hours and a half, until the steady-state in the growth curve was reached (**Figure 16**). For Test tube 6 it is appreciable that it presents an antibacterial activity if it is compared with the strains that grew in normal conditions (T. tube1). After that, the other test tubes were measured in the same manner. Thus, as expected T. tube 2 showed that the solvent by itself presented some sort of antibacterial activity; but, over that T. tubes 3, 4 and 5 exhibited a much important activity against the E. coli strains (**Figure 17**).

T. tube	1	2	3	4	5	6
LB Broth	2,5 ml	2,5ml	2,5ml	2,5ml	2,5ml	2,5ml
E. coli strain	135 ul					
Water	-	50 ul	50 ul	50 ul	50 ul	100 ul
DMSO	-	50 ul	50 ul	50 ul	50 ul	-
Compound 2	-	-	100 ug	-	-	-
Compound a	-	-	-	100 ug	-	-
Compound b	-	-	-	-	100 ug	-
Compound 3						100 ug

Table 7. Content of each test tube for the OD₆₀₀ measurements.

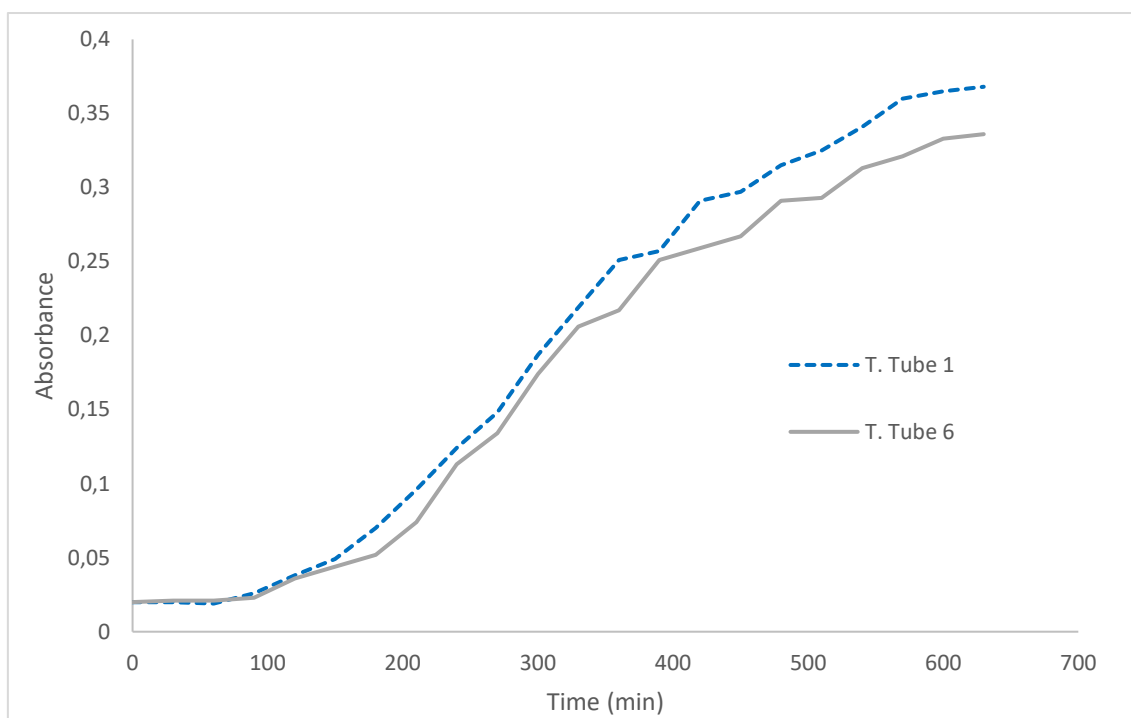


Figure 16. Growth curve for test tube 1 and 6 with the log phase, the exponential phase and the beginning of the steady-state phase.
Detailed data provided in Annex 2.

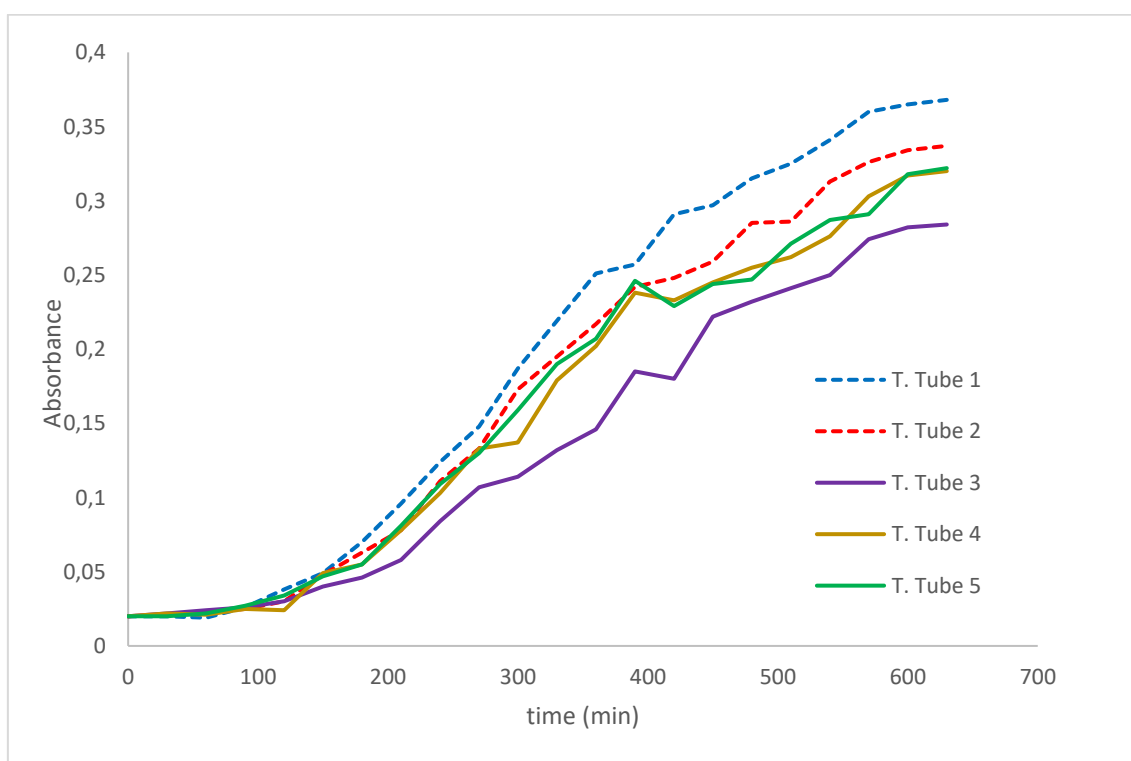


Figure 17. Growth curve for test tube 1 to 5 with the log phase, the exponential phase and the beginning of the steady-state phase.
Detailed data provided in Annex 2.

Additionally, it has been demonstrated that *E. coli* cultures with an OD₆₀₀ of 0,1 and incubated in a LB Broth present a concentration around 8×10^8 cells/ml.^{49,50} With this value it is possible to estimate the amount of cell per ml that correspond to the different obtained OD₆₀₀ values as shown in **Table 8**. In these regards, it is possible to have some quantitative approximations about the efficiency of each compound antibacterial activity. Therefore, the solvent system by itself (T. Tube2) is capable to inhibit the *E. coli* growth around 8,5% in comparison with the normal conditions of growth (T. Tube1); henceforth, the other test tubes must take in account the solvent's activity and will be directly compared with the inhibition capacity of the latter one, with the exception of T. Tube 6. Thus, **2** (T. Tube 3) showed the major inhibition capacity, reducing the bacteria growth by a 14,3%; while, **a** and **b** showed a reduction of 4,7 and 4,4 %, respectively. For **3** (T. Tube 6) the inhibition will be compared directly with the values obtained for normal growth conditions (T. tube 1) and reaches a value of 8,7% of inhibition.

	OD ₆₀₀	cells/ml	% of inhibition	Δ % of inhibition
Standard	0,1	8×10^8	-	-
T. Tube 1	0,365	$2,92 \times 10^9$	100	0
T. Tube 2	0,334	$2,672 \times 10^9$	91,50684932	8,5
T. Tube 3	0,282	$2,256 \times 10^9$	77,26027397	14,3
T. Tube 4	0,317	$2,536 \times 10^9$	86,84931507	4,7
T. Tube 5	0,318	$2,544 \times 10^9$	87,12328767	4,4
T. Tube 6	0,333	$2,664 \times 10^9$	91,23287671	8,77

Table 8. Final OD₆₀₀ values and the estimated number of cells per ml for each growth curve performed.

Finally, taking into account the chemical structures for each of the studied compounds and their respect inhibition capacity it is possible that the cyano the primary and secondary amine groups played an important role for the antibacterial capacity in each of the molecules. This is because the inhibition activity reduces with the number of cyano groups present in each of the molecules, like **3** that has the most important inhibition activity of all the compounds but it strongly reduces for **a** and **b**. Also, the primary and secondary amines seem to play an important role because as the primary or secondary amines get oxidized to secondary or tertiary amines respectively the antibacterial activity also reduces, like in the case of **3**, **a** and **b**. Finally, comparing the antibacterial activities of **a** and **b** it seems that the presence of the nitro-benzene moiety does not contribute to biological activity. However, it is necessary to perform more investigations to obtain a

further insight into the possible conformational changes that could affect the antibacterial activity of the DADQs derivative.

Conclusions

Two potential aggregation-induced emission diaminodicyanoquinodimethanes (DADQs) systems (**a** and **b**) were designed and synthesized using 7-pyrrolidino-7,8,8-tricyanoquinodimethan (PTCNQ) as precursor. These compounds were characterized with UV-Vis, FTIR, and ESI-MS spectroscopy. Additionally, the fluorescence quantum yield of **b** was obtained using a comparative method with **a** as the reference sample, giving an approximate quantum yield of 15.63%, which is mainly attributed to restricted internal rotations and non-planar configurations present in the molecule. These behaviors avoid the non-radiative decays and π - π stacking interactions that a common chromophore may present. However, other effects, such as molecular aggregation, may contribute as well with this phenomenon. Additionally, computational calculations provide dipole moments and oscillator strengths values that support the found quantum yields and propose a negative solvatochromic effect in both molecules. The biological activity test of these molecules reveals an inhibition capacity to E. coli strains, which could be directly related to the presence of cyano groups present in the molecular structure of the studied molecules. In summary, synthesized diaminodicyanoquinones (DADQ's) are valuable customizable fluorescent systems with potential photophysical and bio-luminescent applications.

Recommendations

- For the synthesis of **c** it would be necessary to try other approaches for the reaction. For instance, using different solvents to try to reach higher temperatures or try the reaction on inert atmosphere to discard the possibility that moisture or oxygen are the responsible for the no-reaction. Also, it would be a great idea to try the same reaction conditions in a microwave reaction system to obtain a higher molecular mobility and force the formation of **c**.
- It is necessary to perform more research on the AIE characteristics of **b**. For this, it will be necessary to record the quantum yields with different conditions like changing the temperature, solvent's viscosity or level of aggregation. Additionally, it will be important to measure the quantum yield (QY) with

different concentrations to further understand the mechanisms behind the AIE characteristics of **b**.

- For further insight into the relationship between the antimicrobial activity and the molecular structure of each compound, it would be necessary to perform the same proves with TCNQ and with 7,7-dipyrrolidino-8,8-tricyanoquinodimethane to understand the role of cyano and pyrrolidine groups for the antimicrobial activity.

References

1. Mei J, Leung NLC, Kwok RTK, Lam JWY, Tang BZ. Aggregation-Induced Emission: Together We Shine, United We Soar! *Chem Rev.* 2015;115(21):11718-11940. doi:10.1021/acs.chemrev.5b00263
2. Hong Y, Lam JWY, Tang BZ. Aggregation-induced emission: Phenomenon, mechanism and applications. *Chem Commun.* 2009;(29):4332-4353. doi:10.1039/b904665h
3. Kagawa Y, Takada N, Matsuda H, et al. Photo-and electroluminescence for TCNQ-amino adducts. *Mol Cryst Liq Cryst Sci Technol Sect A Mol Cryst Liq Cryst.* 2000;349(June 2016):499-502. doi:10.1080/10587250008024971
4. Chandaluri CG, Patra A, Radhakrishnan TP. Polyelectrolyte-assisted formation of molecular nanoparticles exhibiting strongly enhanced fluorescence. *Chem - A Eur J.* 2010;16(29):8699-8706. doi:10.1002/chem.201000502
5. Pålsson LO, Vaughan HL, Smith A, et al. Guest-host interactions between dichroic dyes and anisotropic hosts. *J Lumin.* 2006;117(1):113-122. doi:10.1016/j.jlumin.2005.03.017
6. Chandaluri CG, Radhakrishnan TP. Amorphous-to-crystalline transformation with fluorescence enhancement and switching of molecular nanoparticles fixed in a polymer thin film. *Angew Chemie - Int Ed.* 2012;51(47):11849-11852. doi:10.1002/anie.201205081
7. Birks JB. *Photophysics of Aromatic Molecules.* (Wiley-Interscience, ed.). London; new york; 1970.
8. Thomas SW, Joly GD, Swager TM. Chemical sensors based on amplifying fluorescent conjugated polymers. *Chem Rev.* 2007;107(4):1339-1386. doi:10.1021/cr0501339
9. Gaylord BS, Wang S, Heeger AJ, Bazan GC. Water-soluble conjugated oligomers: Effect of chain length and aggregation on photoluminescence-quenching efficiencies. *J Am Chem Soc.* 2001;123(26):6417-6418. doi:10.1021/ja010373f
10. Wang J, Zhao Y, Dou C, et al. Alkyl and dendron substituted quinacridones: Synthesis, structures, and luminescent properties. *J Phys Chem B.* 2007;111(19):5082-5089. doi:10.1021/jp068646m

11. Fan C, Wang S, Hong JW, Bazan GC, Plaxco KW, Heeger AJ. Heeger-Gold-Nano-Quench. 2003;100(11):1-5. [papers2://publication/uuiid/7C12473C-1ECD-4360-B423-E33740A56AA8](https://pubs.aip.org/publication/uuiid/7C12473C-1ECD-4360-B423-E33740A56AA8).
12. Hong Y, Lam JWY, Tang BZ. Aggregation-induced emission. *Chem Soc Rev*. 2011;40(11):5361-5388. doi:10.1039/PhysRevE.70.016603
13. Luo J, Xie Z, Xie Z, et al. Aggregation-induced emission of 1-methyl-1,2,3,4,5-pentaphenylsilole. *Chem Commun*. 2001;18:1740-1741. doi:10.1039/b105159h
14. Fierz-david Hans Eduard BL. *Fundamental Processes of Dye Chemistry*. Preface to. London: Interscience publishers; 1949.
15. <https://www.sigmaaldrich.com/catalog/product/aldrich/c59122?lang=en®ion=EC>.
16. Rietsch P, Witte F, Sobottka S, et al. Diaminodicyanoquinones: Fluorescent Dyes with High Dipole Moments and Electron-Acceptor Properties. *Angew Chemie - Int Ed*. 2019;58(24):8235-8239. doi:10.1002/anie.201903204
17. Glotz G, Lebl R, Dallinger D, Kappe CO. Integration of Bromine and Cyanogen Bromide Generators for the Continuous-Flow Synthesis of Cyclic Guanidines. *Angew Chemie - Int Ed*. 2017;56(44):13786-13789. doi:10.1002/anie.201708533
18. Wróbel TM, Kosikowska U, Kaczor AA, et al. Synthesis, structural studies and molecular modelling of a novel imidazoline derivative with antifungal activity. *Molecules*. 2015;20(8):14761-14776. doi:10.3390/molecules200814761
19. Allali M, Benoist E, Habbadi N, Gressier M, Souizi A, Dartiguenave M. Design and synthesis of new ethylenediamine or propylenediamine diacetic acid derivatives for Re(I) organometallic chemistry. *Tetrahedron*. 2004;60(5):1167-1174. doi:10.1016/j.tet.2003.11.058
20. Srujana P, Gera T, Radhakrishnan TP. Fluorescence enhancement in crystals tuned by a molecular torsion angle: A model to analyze structural impact. *J Mater Chem C*. 2016;4(27):6510-6515. doi:10.1039/c6tc01610c
21. Rhys Williams AT, Winfield SA, Miller JN. Relative fluorescence quantum yields using a Computer-controlled luminescence spectrometer. *Analyst*. 1983;108(1290):1067-1071. doi:10.1039/an9830801067
22. Horiba. A Guide to Recording Fluorescence Quantum Yields Introduction: https://static.horiba.com/fileadmin/Horiba/Application/Materials/Material_Research/Quantum_Dots/quantumyieldstrad.pdf.
23. Siano DB, Metzler DE. Band shapes of the electronic spectra of complex molecules. *J Chem Phys*. 1969;51(5):1856-1861. doi:10.1063/1.1672270
24. Jayanty S, Radhakrishnan TP. Enhanced Fluorescence of Remote Functionalized Diaminodicyanoquinodimethanes in the Solid State and Fluorescence Switching in a Doped Polymer by Solvent Vapors. *Chem - A Eur J*. 2004;10(3):791-797. doi:10.1002/chem.200305123
25. Radhakrishnan APCGCTP. Optical materials based on molecular nanoparticles. *R Soc Chem*. 2011. doi:DOI: 10.1039/c1nr11313e

26. Bloor D, Kagawa Y, Szablewski M, et al. Matrix dependence of light emission from TCNQ adducts. *J Mater Chem.* 2001;11(12):3053-3062. doi:10.1039/b104992p
27. Hertler. Substituted Quinodimethans. 111. Displacement Reactions of 7,7,8,8-Tetracyanoquinodimetha. 1962;2806(Vi):3387-3393.
28. Frediani L, Ågren H, Ferrighi L, Ruud K. Second-harmonic generation of solvated molecules using multiconfigurational self-consistent-field quadratic response theory and the polarizable continuum model Second-harmonic generation of solvated molecules using multiconfigurational self-consistent-fi. 2013;144117(2005). doi:10.1063/1.2055180
29. Radhakrishnan TP. Molecular Structure , Symmetry , and Shape as Design Elements in the Fabrication of Molecular Crystals for Second Harmonic Generation and the Role of Molecules-in-Materials. 2008;41(3):367-376.
30. Lalama SJ, Singer KD, Garito AF, Desai KN. Exceptional secondorder nonlinear optical susceptibilities of quinoid systems Exceptional second-order nonlinear optical susceptibilities of quinoid systems. 2006;940(1981):62-65. doi:10.1063/1.92619
31. Greyson EC, Stepp BR, Chen X, et al. Singlet Exciton Fission for Solar Cell Applications : Energy Aspects of Interchromophore. 2010:14223-14232.
32. Paci I, Johnson JC, Chen X, et al. Singlet Fission for Dye-Sensitized Solar Cells : Can a Suitable Sensitizer Be Found ? 2006;(2):16546-16553.
33. Pretsch E, Bühlmann P, Badertscher M. Structure determination of organic compounds: Tables of spectral data. *Struct Determ Org Compd Tables Spectr Data.* 2009:1-433. doi:10.1007/978-3-540-93810-1
34. HARRIS GFP. Isomer Control in the Mononitration of Toluene. 1976:300-312. doi:10.1021/bk-1976-0022.ch020
35. Panja SK, Dwivedi N, Saha S. Tuning the intramolecular charge transfer (ICT) process in push-pull systems: Effect of nitro groups. *RSC Adv.* 2016;6(107):105786-105794. doi:10.1039/c6ra17521j
36. Legon AC, Millen DJ. Angular geometries and other properties of hydrogen-bonded dimers: A simple electrostatic interpretation of the success of the electron-pair model. *Chem Soc Rev.* 1987;16:467-498. doi:10.1039/CS9871600467
37. Larson JW, McMahon TB. Gas-Phase Bihalide and Pseudobihalide Ions. An Ion Cyclotron Resonance Determination of Hydrogen Bond Energies in XHY - Species (X, Y = F, Cl, Br, CN). *Inorg Chem.* 1984;23(14):2029-2033. doi:10.1021/ic00182a010
38. Emsley BJ, Bonds SH. Very Strong Hydrogen Bonding. *Chem Soc Rev.* 1968;9:91-124.
39. Axelrod D, Hellen E, Fulbright R. Topics in Fluorescence Spectroscopy (eds. Lakowicz, J., Geddes, C. D. & Lakowicz, J. R.). 2002;3, 289-343:289-343. doi:10.1007/b112907

40. Wojdyr M, Fityk: A general-purpose peak fitting program. *J Appl Crystallogr.* 2010;43(5 PART 1):1126-1128. doi:10.1107/S0021889810030499
41. Neese F, Hansen A, Liakos DG. Efficient and accurate approximations to the local coupled cluster singles doubles method using a truncated pair natural orbital basis. *J Chem Phys.* 2009;131(6). doi:10.1063/1.3173827
42. Scholz N, Jadhav A, Shreykar M, et al. Coumarin-Rhodamine Hybrids—Novel Probes for the Optical Measurement of Viscosity and Polarity. *J Fluoresc.* 2017;27(6):1949-1956. doi:10.1007/s10895-017-2165-4
43. Karasulu B, Philipp J, Thiel W. Assessment of Franck – Condon Methods for Computing Vibrationally Broadened UV – vis Absorption Spectra of Flavin Derivatives : Ribo fl avin , Roseo fl avin , and 5 - Thio fl avin. 2014.
44. Wolfgang, Demtröder; goleman, daniel; boyatzis, Richard; Mckee A. *Laser Spectroscopy Basic Concepts and Instrumentation.* Vol 53. Second. Berlin: Springer-Verlag; 1996. doi:10.1017/CBO9781107415324.004
45. Kable S. Basic Principles of Fluorescence. *Fundam Fluoresc Imaging.* 2019:1-34. doi:10.1201/9781351129404-1
46. Lakowicz JR. *Principles of Fluorescence Spectroscopy.*; 2006. doi:10.1007/978-0-387-46312-4
47. Vigil ALM, Palou E, Parish ME, Davidson PM. *Methods for Activity Assay and Evaluation of Results.* 3rd ed. CRC Press; 2005. doi:10.1201/9781420028737.ch21
48. Reyes-Tirado F, Palou E, López-Malo A. Métodos de evaluación de la actividad antimicrobiana y determinación de los componentes químicos de los aceites esenciales. *Temas Sel Ing Aliment.* 2014;8:68-78. <http://web.udlap.mx/tsia/files/2015/05/TSIA-81-Reyes-Jurado-et-al-2014.pdf>.
49. Sezonov G, Joseleau-Petit D, D’Ari R. Escherichia coli Physiology in Luria-Bertani Broth. *J Bacteriol.* 2007;189(23):8746-8749. doi:10.1128/JB.01368-07
50. Ausubel FM, Brent R, Kingston RE, et al. *Current Protocols in Molecular Biology: Preface.*; 2010. doi:10.1002/0471142727.mbprefs66

Annexes

	a		b		c	
Mulliken charges So	C1	-0,257120	C1	-0,257330	C1	-0,257592
	C2	-0,257144	C2	-0,256311	C2	-0,256042
	C3	-0,030085	C3	-0,030837	C3	-0,030362
	C4	0,163865	C4	0,165590	C4	0,172198
	C5	-0,277889	C5	-0,274670	C5	-0,276205
	C6	-0,277888	C6	-0,247164	C6	-0,257993
	C7	-0,156695	C7	-0,177319	C7	-0,166580
	C8	-0,156692	C8	-0,157413	C8	-0,145802
	C9	0,072561	C9	-0,038441	C9	0,011632

	C10	0,315050	C10	0,328847	C10	0,250020
	C11	-0,104363	C11	-0,074427	C11	-0,092019
	C12	-0,104365	C12	-0,165474	C12	-0,126682
	N1	-0,085514	N1	-0,084316	N1	-0,084446
	N2	-0,085515	N2	-0,084114	N2	-0,084824
	N3	-0,251769	N3	-0,243675	N3	-0,235722
	N4	-0,251790	N4	-0,016930	N4	-0,028158
	-	-	C13	0,084517	C13	-0,016391
	-	-	C14	-0,144001	C14	0,081983
	-	-	C15	-0,177967	C15	-0,155742
	-	-	C16	-0,162385	C16	-0,145272
	-	-	C17	-0,151828	C17	-0,093599
	-	-	C18	0,112023	C18	-0,110852
	-	-	N5	0,431526	N5	0,459160
	-	-	O1	-0,331159	O1	-0,310155
	-	-	O2	-0,332019	O2	-0,328836
	C1	-0,253786	C1	-0,255387	C1	-0,271823
	C2	-0,253784	C2	-0,253121	C2	-0,270732
	C3	-0,008101	C3	0,001927	C3	-0,012610
	C4	0,168252	C4	0,168825	C4	0,154072
	C5	-0,270494	C5	-0,264203	C5	-0,271031
	C6	-0,270499	C6	-0,242855	C6	-0,243517
	C7	-0,139605	C7	-0,169386	C7	-0,139308
	C8	-0,139608	C8	-0,150902	C8	-0,172797
	C9	-0,018191	C9	-0,092319	C9	-0,050879
	C10	0,372496	C10	0,392713	C10	0,249880
	C11	-0,115644	C11	-0,093056	C11	-0,093354
	C12	-0,115645	C12	-0,186209	C12	-0,124176
Mulliken charges S₁	N1	-0,077932	N1	-0,068803	N1	-0,065991
	N2	-0,077932	N2	-0,068996	N2	-0,066460
	N3	-0,267869	N3	-0,283525	N3	-0,224826
	N4	-0,267870	N4	-0,022575	N4	-0,019521
	-	-	C13	0,134177	C13	0,114862
	-	-	C14	-0,211818	C14	-0,020288
	-	-	C15	-0,189405	C15	-0,172045
	-	-	C16	-0,146036	C16	-0,111060
	-	-	C17	-0,157772	C17	-0,074768
	-	-	C18	0,088741	C18	-0,127476
	-	-	N5	0,430141	N5	0,486281
	-	-	O1	-0,344815	O1	-0,334921
	-	-	O2	-0,346138	O2	-0,354944

Annex 1. Charges for each of the atoms in compounds (a), (b) and (c), in their excited S₁ and ground S₀ states.



OD600						
Time	T. Tube 1	T. Tube 2	T. Tube 3	T. Tube 4	T. Tube 5	T. Tube 6
0	0,02	0,02	0,02	0,02	0,02	0,02
30	0,02	0,021	0,022	0,022	0,02	0,021
60	0,019	0,023	0,024	0,021	0,022	0,021
90	0,026	0,025	0,026	0,025	0,027	0,023
120	0,038	0,03	0,03	0,024	0,034	0,036
150	0,049	0,048	0,04	0,049	0,047	0,044
180	0,07	0,063	0,046	0,055	0,055	0,052
210	0,096	0,078	0,058	0,078	0,081	0,074
240	0,124	0,111	0,084	0,103	0,109	0,113
270	0,148	0,133	0,107	0,133	0,13	0,134
300	0,187	0,173	0,114	0,137	0,159	0,174
330	0,219	0,195	0,132	0,179	0,19	0,206
360	0,251	0,217	0,146	0,202	0,207	0,217
390	0,257	0,242	0,185	0,238	0,246	0,251
420	0,291	0,248	0,18	0,233	0,229	0,259
450	0,297	0,259	0,222	0,245	0,244	0,267
480	0,315	0,285	0,232	0,255	0,247	0,291
510	0,325	0,286	0,241	0,262	0,271	0,293
540	0,341	0,313	0,25	0,276	0,287	0,313
570	0,36	0,326	0,274	0,303	0,291	0,321
600	0,365	0,334	0,282	0,317	0,318	0,333
630	0,368	0,337	0,284	0,32	0,322	0,336

Annex 2. Detailed data of all the OD₆₀₀ values taken for each test tube.